TEXAS INSTRUMENTS INCORPORATED
Apparatus Division
13500 North Central Expressway
P.O Box 6015
Dallas, Texas 75222

Code 1 cat.

FINAL ENGINEERING REPORT
JPL LOW-FIELD MAGNETOMETER

1-76208-1

26 May 1964

This work was performed for the Jet Propulsion Laboratory, California Institute of Technology, sponsored by the National Aeronautics and Space Administration under Contract NAS7-100.

JPL Contract No. 950355

Prepared for
Jet Propulsion Laboratory
California Institute of Technology
Pasadena, California

TABLE OF CONTENTS

Section	Title	Page
I	INTRODUCTION	1
II	INSTRUMENT CHARACTERISTICS	1
	A. Description and Operating Instructions	1
	B. Chassis 33A1—Sensor	4
	1. General	4
	2. Sensor Electrical Setup Procedure	5
	a. Igniter Circuit	5
	b. RF Matching Networks	6
	3. Sensor Assembly Procedure	6
	C. Chassis 33A2—Power Supply	8
	1. Detector Bias Supply	8
	2. +28-Volt RF Supply	8
	3. Igniter Power Supply	8
	4. ±12-Volt Supplies	9
	5. A/PW Converters	9
	6. Ignition Logic Circuit	9
	7. Calibrate Circuit	9
	8. RF Exciter	10
	9. Unit Test Procedure	10
	D. Chassis 33A3—Electronics	11
	1. Wideband Amplifier and Wideband Amplifier Filter	11
	2. Bandpass Amplifiers	11
	3. Demodulators and DC Amplifiers	12
	4. 50-CPS Oscillator and Twin Tee Filter	12
	5. Flip-Flop and Clock-Pulse Generator	12
	6. Phase Shifters and Demodulator Drivers	13
	7. X- and Y-Axis Sweep Driver	13
	8. Z-Axis Sweep Driver	13
	9. Unit Test Procedure	13
III	GENERAL DISCUSSION OF EQUIPMENT	15
	A. Theory of Operation	15
	B. Signal Analysis	18
IV	SYSTEM ANALYSIS	24
	A. Circuit Transfer Functions	24
	B Instrument Transfer Functions	31

TABLE OF CONTENTS (Continued)

Section	Title	Page
V	SYSTEM ERRORS	33
	A. Error Producing Mechanisms	33
	B. Signal Processing in the Carrier Section Electronics	33
	C Phase Shift Analysis	42
	D. System Errors Resulting From DC Amplifier Drift	43
	E. Instrument Noise	45
	APPENDIX— Drawings	47

LIST OF ILLUSTRATIONS

Figure	Title	Page
1	Low-Field Magnetometer	2
2	Magnetometer Block Diagram	16
3	Sensor Diagram	16
4	Two-Axis Block Diagram	17
5	Geometry of Signal Generating Process	19
6	AGC Characteristics	26
7	Wideband Amplifier Filter Phase and Amplitude Characteristics	28
8	Phase-Gain Characteristics of Bandpass Amplifiers	29
9	Low Pass Equivalent Phase and Amplitude Characteristics of Bandpass Amplifier	30
10	Positive Integrator Diagram	31
11	Equivalent Single-Axis Diagram	32
12	Model of Three-Axis Sensor	34
13	Commutated Waveforms	36
14	Two-Axis Model Illustrating Crosstalk Mechanism	44

3

TEXAS INSTRUMENTS INCORPORATED
Apparatus Division
13500 North Central Expressway
P.O Box 6015
Dallas, Texas 75222

26 May 1964

FINAL ENGINEERING REPORT
JPL LOW-FIELD MAGNETOMETER

1-76208-1

I. INTRODUCTION

Texas Instruments Incorporated was engaged by Jet Propulsion Laboratory to design and construct flight and test model low-field magnetometers in accordance with JPL Contract No. 950355, dated 19 November 1962. Representing a culmination of a series of programs by JPL and Texas Instruments, this activity has brought the instrument from a study of the physical phenomena involved to the flight stage reported herein. Results of the earlier programs have been reported in Final Engineering Report, Low-Field Helium Magnetometer Evaluation Program 1-51165-1, dated 25 July 1961; Final Engineering Report, Prototype Low-Field Magnetometer 8-71401-8, dated 25 June 1962, and an addendum thereto, dated 15 November 1962; and in a paper by Reilly and Slocum *

The intent of this report is to present the theoretical basis for the flight model magnetometer, to show the practical implementation of this theory and the results obtained, and to provide the information necessary to operate the device properly. To aid in realizing these objectives, a selection of drawings produced under the contract is included.

II. INSTRUMENT CHARACTERISTICS

A. Description and Operating Instructions

The low-field helium magnetometer developed and fabricated for the Mariner C spacecraft is composed of three basic assemblies: 33A1, the sensor; 33A2, the power supply; and 33A3, the electronics. The instrument is illustrated in Figure 1. The characteristics of the instrument are documented

*R. E. Slocum and F. N. Reilly, "Low-Field Helium Magnetometer for Space Application," IRE Transactions on Nuclear Electronics, Vol. NS-10, No. 1 (January 1963), p. 165.

4

Figure 1. Low-Field Magnetometer

in Table 1; the electronics, power supply and sensor are discussed in the following paragraphs. Circuit diagrams of the instrument are included as an appendix

Table I. Low-Field Magnetometer Characteristics

Weight	
Instrument	6.15 lb
Electronics	2.30 lb
Power supply	2.55 lb
Sensor	1.3 lb
Size	
Electronics	6 × 6 × 2 in. (approximately)
Power supply	6 × 6 × 2 in. (approximately)
Sensor	Appendix, Ref Dr No. 484703
Input Power	
Steady-state input power	7.0 watts (approximately)
Power breakdown:	
Electronics	1.6 watts (approximately)
RF oscillator	2.5 watts (approximately)
Power supply, regulators, and a-to-d converters	2.9 watts (approximately)
Igniter	2.5 watts (for 10 seconds)
Input voltage	2400 cps square wave 50 volts rms

Environmental Specifications, Type Approval		
Vibration		
14g rms noise		18 sec
5.0g rms noise plus 2.0g rms sine 15—40 cps plus 9.0g rms sine 40—2000 cps		600 sec
14g rms noise		18 sec
Shock	5,200g 0.5—1.5 millisecond pulses 3-axis	
Thermal—vacuum (type approval)		
Electronics	−10°C	4 hours
Sensor	+75°C (sensor 65°C)	12 days
	10^{-4} mm Hg	

6

Table I. Low-Field Magnetometer Characteristics (Continued)

Temperature	
Electronics	−20° to +65°C
Sensor	−55° to +55°C

Operational Characteristics

Sensitivity	0 5 gamma peak to peak
Bandwidth	1 cps (approximately)
Zero offset	2 gamma (approximately)
Dynamic range	±364 gamma

The instrument should be visually inspected for foreign material and damage, and the electronics (33A3) and the power supply (33A2) chassis should be mounted in the spacecraft orientation. All connections should be made and checked before applying power. Specific caution must be exercised on the sensor where the preamplifier connector 33A1-P4 and the igniter connector 33A1-P1, or the rf connector 33A1-P2 and the rf connector 33A1-P3, can be interchanged. Crossing P1 and P4 will damage (open) the output transistor in the preamplifier. Crossing the rf connectors makes the system inoperative but does no permanent damage. Operating the system with 33A3-P2 open can damage the coupling capacitors in the sweep drivers.

Input power: 50 volts rms square wave, 2400 cps, 0 dc.

The sensor must be placed in a magnetic field of less than ±400 gamma for operational testing. The ac fields should be much less than 400 gamma.

After completing the above, apply the 2400-cps power; the unit will ignite and begin operating. The X, Y, and Z analog outputs can be monitored on Pins 9, 25, and 42, respectively, of connectors 33A2-P1.

B. Chassis 33A1 — Sensor

1. General

The sensor contains several circuits used in generating an analog signal under application of an external magnetic field. They are listed below with a brief description of the function of each.

Ignition oscillator circuit—initiates gas discharge in the helium lamp and absorption cell

Matching networks—couple rf power into lamp and cell for sustaining the gas discharges

Helmholtz coil system—provides a circularly polarized magnetic sweep field in two orthogonal planes about the absorption cell as well as dc bucking of the external magnetic field

Infrared detector—monitors changes in the transmissivity of the absorption cell to 1.08-micron radiation from the helium lamp

Preamplifier—boosts the detector signal by about 20 db before sending it along the cable to the electronics chassis (This circuit has a differential output in order to reduce common mode pickup in the cabling between the sensor and the electronics chassis.)

The ignition oscillator and rf matching networks will be discussed in detail in the setup procedure section (also Appendix, Ref Dr No. 456469)

The Helmholtz coil system is wired to give a right-handed coordinate system coincident with the spacecraft coordinate axes. The leads coming from the coils are twisted, each with its respective returns, and the three resultant pairs are also twisted together to minimize stray current loops near the absorption cell. The coil returns are brought to a common point at terminals E28 and E29 from which a single return lead is brought to the connector J1. The leads from each coil are routed with their returns to the common point and then twisted with the single return up to J1. The coil system is not referenced to any ground in the sensor.

The infrared detector and the preamplifier are housed in separate modular units. The detector housing forms part of the chassis rf shield. The preamplifier housing is electrically isolated from the rest of the sensor and is grounded to the ±12-volt preamplifier power common inside the module. The detector leads are brought through the chassis rf shield into the preamplifier housing by two 1000-pf feedthrough capacitors.

The four transistors of the preamplifier are mounted on top of the potted preamplifier module for easy access if it becomes necessary to test circuitry or replace transistors.

The preamplifier and detector housing are bonded after installation of the detector and lens. From that point, the two are, mechanically, a single sealed unit.

2. Sensor Electrical Setup Procedure

a. Igniter Circuit

This circuit is set up electrically following mechanical assembly of the sensor. The tuning capacitors across the ignition transformer primary (C12) and secondary (C10, C11) are selected at this time as well as the coupling capacitor (C9) for lamp ignition. Values are selected that give reliable ignition of lamp and cell at the lowest possible supply voltage but permit the igniter circuit to draw no more than 80 ma at 32 volts dc. The primary

side capacitor (C12) is typically 6800 pf, while the series secondary capacitors (C10, C11) are near 27 to 33 pf. To permit a better derating factor on the 1-kc ceramic capacitors used in the secondary, the series arrangement is used. A typical value for C9 is 5 pf

The igniter circuit secondary is referenced to rf ground at the chassis lug on J3, while the oscillator return is not referenced at the sensor.

b. RF Matching Networks

After the ignition circuit is set up, the rf matching networks are fabricated in the sensor and component values are selected. Optimum performance of these circuits gives maximum excitation of the discharge elements with minimum standing wave ratio in each rf channel. The networks are set up using the rf oscillator that will be used with that particular sensor in the finished system.

Each matching network is a simple pi-section with a 1.7- to 11-pf variable capacitor across the load. The series inductors are handwound of No. 26 Polythermaleze-coated magnet wire on a 0.25-inch od fiber glass dowel. Typically, 36 turns were used on the lamp inductor and about 27 turns on the cell side. Both channels require about 150 pf across the inputs.

The cell rf return is referenced to chassis ground on the sensor igniter subassembly No. 1 circuit board. The lamp rf return is referenced to the sensor chassis through its holding fixture and has no separate ground wire returning to the matching network board.

3. Sensor Assembly Procedure

The magnetometer sensor 33A1 is assembled in the following sequence:

Cell support, tube, and ball

Install lens; bond with Epoxylite 295.

Install circular polarizer; bond with Eccogel 1265.

Install prewired absorption cell with Teflon retainer No. 1 in cell support.

Install completed subassembly in sensor housing No. 1 with Teflon retainer No. 2; cell support should project about 0.005 inch beyond tube end.

Insert tube into prewired coil subassembly using indium foil washers on inner flange face and on tube end having the 5-hole bolt circle.

9

Igniter-sensor housing subassembly

Install prewired helium lamp subassembly and bond to housing with Eccobond 56C epoxy solder.

Install connectors J2 and J3, capacitors C14, C15, and C16, insulated terminals E28 and E29; bond with Eccobond solder 56C.

Install 0.010-inch fiber glass insulation board in bottom of housing and bond with Eccobond 55; install Microquartz reflecting material and bond with Stycast 1090.

Install two supports for sensor igniter subassembly No. 1.

Install sensor igniter subassembly No. 2 and bond board and alumina heatsink with Eccobond 55.

Pigtail wires to C14, C15, C16, and J2 and J3; install shrinkable tubing over solder joints on J2 and J3.

Feed wires from lamp and absorption cell through insulator board in bottom of igniter housing; assemble the ball-cell subassembly to the igniter housing subassembly using an indium washer between the contacting metal surfaces. The ball is held to the igniter housing with six brass No. 2/56 panhead machine screws.

Install ignition transformer in igniter housing and bond with Eccobond 55; use the sensor-igniter subassembly No. 1 terminal board as a jig to properly position the ignition transformer.

Install two No. 10/24 spacers on pedestals in igniter housing to support sensor igniter subassembly No. 1; bond with Eccobond 55.

Install 1.7- to 11-pf trimmer capacitors to sensor igniter subassembly No. 1 board.

Feed all wires through sensor-igniter subassembly No. 1 circuit board and install this board. Secure with No. 4/40 and No. 10/24 screws in the appropriate places with lockwashers; the No. 10/24 screws engage a special tubular nut that is inserted from the outside of the sensor housing.

Install the preamplifier-detector module on the end of the ball; electrical setup can now be performed.

After electrical setup of the igniter circuit and rf matching network, install rf gasket and covers.

10

C. Chassis 33A2—Power Supply

The various voltages necessary to operate the magnetometer are generated in this chassis. In addition, a number of other system functions fit logically into the packaging arrangement of unit 33A2. The primary source of power for this chassis is the 50-volt 2400-cps spacecraft power supply. A brief description of the individual functions is given here. (Refer to Appendix, Dr Nos. 508352, 456462 and 484777.)

1. Detector Bias Supply

A conventional voltage doubler and half-wave rectifier are used to obtain the desired dc output voltage of this supply. Ripple reduction is accomplished with a pi-section filter Because of the low current levels of the supply, surge limiting has not been included. The detector network is provided with about 105 volts dc.

2. +28-Volt RF Supply

The rf exciter requires about 100 ma at +28 volts dc. The output of a second secondary winding on T-1 is full-wave rectified and filtered with an L-section to produce 32 volts of raw dc power. A series regulator is employed to stabilize the voltage to the exciter. The level of the regulated output voltage is adjusted by selecting resistors R24 and R25, which establish the base level of the error amplifier. In addition to voltage regulation, it has been necessary to include protection against both short- and long-term excessive current drain on the spacecraft supply. This protection is provided by the surge limiting transistor Q1, which under normal load conditions runs saturated. As the load current increases, the voltage drop across R2 and diodes CR14 and CR17 increases until limited by the forward breakdown of the FD306's Beyond this the Q1 collector current cannot increase, and the transistor comes out of saturation. As the load continues to increase V_{ce} of Q1 increases and maintains the load current constant The current value at which limiting occurs is adjusted by selecting the value of R3. This is normally set to occur at about 150 ma of load current

3 Igniter Power Supply

This supply uses the same transformer secondary and rectifier as the rf supply to develop about 32 volts dc for the igniter circuit. In this case, however, the regulation requirement is not severe and a regulator is not used. Overload protection is necessary and the same type limiter as described above is used. In this case the current limiting level is set to about 150 ma by selecting R5. Note that the return for this supply is not common with the system ground used for the other power supplies. This is necessary to prevent interaction between the two current limiters.

4 ±12-Volt Supplies

These are unregulated supplies which operate from transformer T-2 and a full-wave rectifier. Each supply uses an L-section filter. Overload protection is accomplished in a manner different from that previously discussed. The base of transistor Q3 monitors the +12-volt output level Under normal conditions, Q3 is saturated and reflects a low impedance through the rectifier (composed of CR4, CR5, CR6, and CR8) and back to the primary of transformer T-3. Since this primary is in series with the primary of T-2, any increase in its input impedance will be manifested as a reduced current in the primary of T-2, the ±12-volt transformer. Hence, the +12-volt level will regulate as the load becomes excessive, thereby reducing the base level of Q3 and bringing Q3 out of saturation. The increased output impedance of Q3 is reflected through T-3 and limits the current in T-2. The level at which limiting occurs is adjusted by selecting R14. Voltage dividers with zener diodes in one leg are used on the ±12-volt supplies to establish a reference level for the calibrate circuits.

5. A/PW Converters

The analog-to-pulsewidth converters supplied by JPL are mounted in chassis 33A2. There are two converters per axis converting positive and negative analog values. Upon command, the pulsewidth outputs are provided to the DAS.

6. Ignition Logic Circuit

The function of this circuit is to close the relay which supplies power to the igniter circuit when the instrument is turned on and to hold it closed for a period of about ten seconds. If the lamp or cell fail to ignite or are later extinguished, this ignition sequence repeats when initiated periodically by a backup pulse from the spacecraft. When power is turned on, capacitor C10 holds the monostable multivibrator transistors Q6 and Q7 in the on or quasi-stable state. This gates the relay driver transistors Q4 and Q5 on for about ten seconds. Application of the backup pulse produces the same result. When the magnetometer is locked on, however, it is undesirable for the igniter to function. The ignition logic circuit therefore monitors the 100-cps output of the wideband amplifier. The presence of a 100-cps signal inhibits operation of the igniter relay through diodes CR3 and CR5. As a result, ignition occurs upon application of power to the instrument or in the presence of a backup pulse when the instrument has been turned on but is not locked on to a signal. Once ignition has commenced, diode CR4 holds the igniter on until the monostable drops into its stable state. This is to prevent ignition noise from being confused as a 100-cps signal and turning the igniter off prematurely.

7. Calibrate Circuit

This consists of a series of relays which, when closed on command, sum currents into the sensor Helmholtz coils. Combinations of

currents corresponding to ±40 gamma or ±80 gamma are available. In addition, provisions are available for installing on the carrier board resistors which will permanently sum desired currents into the Helmholtz coils. Currents applied with the relays go to each of the three axes simultaneously, but the permanent currents may be selected individually.

8. RF Exciter

The rf exciter is a three-stage circuit containing a crystal-controlled oscillator and two stages of amplification. The oscillator drives a buffer amplifier that provides an rf output to the sensor absorption cell and drive to the power amplifier. The power amplifier is transformer coupled to the lamp output of the exciter.

Setup procedure for rf exciter:

Connect in-line wattmeter and 50-ohm load to lamp output; total cable length should be about 8 feet.

Connect 50-ohm load to absorption cell output.

Connect to variable voltage supply. Slowly increase voltage to 28 volts while monitoring current. Do not allow current to exceed 120 ma.

Peak oscillators by tuning C8, and then decrease capacitor C8 by one turn.

Peak Q2 stage by tuning C12.

Peak Q3 stage by tuning C18.

Select C15 to give a 130-milliwatt output on J13.

Select C20 to give a maximum output on J-2.

Repeat the tuning operation on each stage.

Check oscillator starting by turning power supply on and off. Rotate C8 one-half turn in both directions; repeat oscillator starting test. Return to original position.

Monitor frequency and short crystal; frequency should shift downward a few kilocycles.

Current after tuning should not exceed 100 ma.

Run unit test.

9. Unit Test Procedure

After visual inspection, a check for electrical continuity is made on the chassis to detect wiring errors. Appropriate dc voltages are applied next to the rectifier outputs of the various unloaded supplies. This permits checking of the filters and the 28-volt dc regulator. At this time the

voltages on the ignition logic circuit and the A/PW converters are checked for polarity. With the supplies still unloaded, the 2400-cps power is applied next. For this test the A/PW converters are disconnected. The peak-to-peak 2400-cps current, which is monitored with a Tektronix current probe, should be about 40 ma. The output voltages of all supplies are checked in the chassis and at the various connector pins where these voltages should appear. Then the various current limiters are checked and adjusted to function at the proper current levels. At the same time, the 28-volt regulator is adjusted to its proper output level. This is done by selecting R24 and R25 to make V_{ce} on Q5 equal to or slightly greater than 2.5 volts dc. The reference voltages for the calibrate circuits are measured and proper operation of the calibrate and ignition logic relays are checked. In checking the ignition logic relay, it is important that the positive voltage be applied to terminal E50. Reversing this polarity will put the voltage in the forward direction across a protective diode in the module. This completes the setup of chassis 33A2.

D. Chassis 33A3—Electronics

The circuits of this chassis may be considered in two groups: those which appear directly in the control loop and those which perform auxiliary functions. The first group consists of the wideband amplifier with its filter, the bandpass amplifiers, and the demodulators and dc amplifiers. Briefly, the function of this segment of the loop is to amplify the sensor error signal, to separate the X- and Y-axis error signals by commutation, to separate and rectify the three error signals by synchronous demodulation, and to use the resulting signal to produce a field-nulling current in the sensor Helmholtz coils. A brief discussion of these circuits follows.

1. Wideband Amplifier and Wideband Amplifier Filter

The function of this circuitry is to amplify with automatic gain control the differential output of the sensor preamplifier and to convert it to a single-ended signal. The large 100-cps component of the signal is then filtered by a bridged tee notch filter. The input stage of the amplifier is differential. The output of this stage is single ended and feeds two cascaded gain stages which have an agc loop closed around them. The agc control signal is developed by rectifying the 100-cps output of these stages. When the system is locked on, the other frequency components in the output are insignificant to the agc action. The circuit will maintain the 100-cps component of its output in the range 3 to 8 volts p-p over the temperature range −20°C to +65°C with an input range of 50 to 1000 mv p-p. In this way the open loop gain of the system remains relatively constant despite considerable variation in the sensor gain. The amplifier proper is followed by the bridged tee notch filter and finally an emitter follower output.

2. Bandpass Amplifiers

The filtered output goes next to the three bandpass amplifiers. These are two-stage amplifiers with twin tee notch filters in their feedback loops.

The three filters are located in a separate module. This configuration provides the necessary bandpass characteristic to prevent saturation by frequencies arising from incomplete filtering and distortion in the wideband amplifier. Commutation is accomplished at the input of the X- and Y-axis amplifiers by shunting the signal to ground through a 2N2432 transistor used in the inverted mode. Gain of the amplifiers is adjusted with an external resistor mounted on the carrier board.

3. Demodulators and DC Amplifiers

The bandpass amplifier outputs are detected with shunt demodulators which also employ 2N2432's in the inverted mode. The first two stages of the amplifier are differential and use 2N2060 transistors, which are dual devices mounted in one TO-5 case. This aids in achieving the necessary temperature stability. The amplifiers are unit tested to have an input voltage change of less than 40 millivolts over the temperature range −20°C to +65°C. In most cases the units show less than half of this change. The dc voltage gain is 60 db or greater. The circuit is balanced initially by selecting an external resistor. Capacitive feedback is used to produce an approximate $1/S$ frequency response. An additional lag and one additional lead break occur in the vicinity of the amplifier crossover frequency; this has the effect of slightly decreasing the system bandwidth. The initial amplifier balance is accomplished by connecting the output to the negative input and measuring the offset at the output. This offset is then matched at the negative input by selecting the external resistor.

The remaining circuits in chassis 33A3 perform auxiliary functions in support of the control loop circuitry. A discussion of these circuits follows.

4. 50-CPS Oscillator and Twin Tee Filter

The oscillator employs a three-stage amplifier section providing about 54 db of voltage gain. The twin tee filter in the negative feedback path gives the amplifier a relatively sharp bandpass characteristic. With the positive feedback loop closed, the circuit oscillates at the bandpass frequency. A saturating push-pull stage is included in the positive loop to ensure sufficient loop gain for oscillation over the temperature range. The sinusoidal output of the oscillator exhibits some amplitude variation with temperature This variation is compensated with the thermistor network at the input of the emitter follower output stage. The output amplitude is set by selecting an external resistor. The circuit maintains its room temperature frequency within ±0.3 cps over the specified temperature range. The oscillator is used to drive the commutator drivers, the demodulator drivers, and the sweep drivers.

5. Flip-Flop and Clock-Pulse Generator

This circuit generates a 25-cps square wave synchronous with the 50-cps reference which drives the commutators in the bandpass

amplifiers and the sweep drivers. The circuit consists of a saturating amplifier section which produces a negative pulse at each negative-going zero crossing of the 50-cps sine wave. The pulse is used to flip a bistable multivibrator, which in turn drives the commutators. The time delay between the sine wave zero crossing and the square wave leading edge is unit tested to be less than 0.5 milliseconds under all temperature conditions. Testing shows this delay to be less than 0.2 milliseconds on all modules.

6. Phase Shifters and Demodulator Drivers

This circuit provides a 50-cps synchronous square wave to drive the associated demodulator. It includes a phase shift network to permit proper phasing of the demodulator. This adjustment is made by selecting an external resistor. The signal is squared in a stage of which the base is clamped to ground during the positive portion of the sine wave. The emitter follower output provides sufficient drive to properly shunt the error signal to ground during the demodulator clamp period. The on and off periods of the square wave are unit tested to be within 2 percent of the desired 10 milliseconds under all environmental conditions.

7. X- and Y-Axis Sweep Drivers

The function of this circuit is to provide commutated 50-cps sinusoidal sweep currents to the X- and Y-axis Helmholtz coils in the sensor. Commutation is accomplished by splitting the output and shunting the two outputs to ground on alternate cycles with inverted 2N2432's. The commutator drive is obtained from the flip-flop and clock-pulse generator. Lead 9 in the module is brought out for test purposes only and should be removed after testing.

8. Z-Axis Sweep Driver

This circuit provides a noncommutated 50-cps sweep current to the Z-axis Helmholtz coils. Phase of the output with respect to the input is continuously adjustable over the range 45 to 135 degrees. Since the X-, Y-, and Z-axis sweep drivers share a common source, this permits the Z sweep current to be 90 degrees out of phase with the X and Y sweep currents. This is necessary to obtain a circular rotating magnetic sweep in the sensor. The adjustment is made by selecting an external resistor. Provision is made also for 180-degree reversal of the output. This is done by connecting terminals 5 and 6 or 6 and 7 of the module.

9. Unit Test Procedure

After assembly the chassis is checked to ensure proper operation and to perform the necessary alignment procedure. A brief description of this is given to aid in system operation and in realignment, should this become necessary. The unit is first inspected visually for assembly errors, and a check for electrical continuity is made. This is followed by application

of power to the chassis. It is extremely important that the sensor coils be simulated by 30-ohm resistors at connector J2 before application of power. This prevents possible back biasing of tantalum capacitors in the sweep drivers. Both power supply currents are monitored and power is removed immediately if either current appreciably exceeds 70 ma. The 50-cps monitor point should have a peak-to-peak amplitude of 80 to 110 mv. The remaining checks are made at various terminals on the carrier boards in the chassis. These points may be located by reference to the Appendix, Dr Nos. 484752 and 484796, and to Figure 1. The following points are checked on side Dr No. 484796.

Terminal No.	Function
E5 and E6	Flip-flop output—about 9 volts p-p, square wave
E26, E27, E30	Demodulator driver outputs—about +0.6 volts, −3 square wave
E59	Z-axis sweep driver output—about 6 volts p-p, 50-cps sine wave
X- and Y-axis sweep driver test lead	X and Y sweep—about 6 volts p-p, 50-cps sine wave
E62 and E63	X and Y axis commutated sweeps—check for proper commutation

A 3-k resistor is tacked to the Z-axis sweep driver output to load the circuit properly. The phase of this point is monitored with respect to the phase at the X and Y sweep driver test point. This phase difference is set to 90 degrees by selecting R5. The peak-to-peak amplitudes at these two points are then measured accurately. The sweep summing resistors for the X and Y axes are internal to the module and have known values. Since the sweep currents on all axes should have equal amplitudes and the voltages before the summing resistors are known, the precise value of the external Z sweep summing resistor R6 can be obtained. The phases of the X- and Y-axis demodulator drivers are set up by running the Z-axis sweep driver output through an attenuator and phase splitter into the wideband amplifier. The amplitude is adjusted so that saturation does not occur at any point in the control loop. By selecting resistors R3 and R4 (located adjacent to the demodulator drivers), the demodulator driver phases are set to yield no dc input to the respective dc amplifiers. A similar procedure is used to select R2 for the Z-axis with the test point of the X- and Y-axis sweep driver used as a signal source.

17

III. GENERAL DISCUSSION OF EQUIPMENT

A. Theory of Operation

The low-field helium magnetometer uses an absorption phenomena in metastable helium to generate a signal which is proportional to the vector values of the magnetic field. The signal is processed to provide analog outputs proportional to the X, Y, and Z components of the magnetic field over a dynamic range of ±400 gamma. The block diagram in Figure 2 illustrates the basic functions in the magnetometer electronics; Figure 3 illustrates the essential sensor components.

The helium lamp and the helium absorption cell are excited by an electrodeless rf discharge. The lamp is excited to generate resonant 1.083-micron radiation; the cell generates a population of 2^3S_1 metastable states. The energy from the lamp is circularly polarized and directed through the absorption cell to an infrared detector. A signal proportional to the vector components of the magnetic field in a plane can be generated by rotating a modulation magnetic field in the plane. Refer to Figure 5 for a schematic of the geometry of the sweep or modulation field. The rotating magnetic field vector, modulates the light beam by varying the degree of absorption of the absorption cell. The signal has the character described by the following equation.

$$s(t) = H(s) \sin (2wt) + h_x(t) \sin wt + h_z(t) \cos wt$$

where

$s(t)$ = signal

$H(s)$ = amplitude proportional to sensor constants such as lamp brightness, infrared detector characteristics, and pressure in the lamp and cell

w = angular frequency in radians

$h_x(t)$ = amplitude proportional to the X component of the field

$h_z(t)$ = amplitude proportional to the Z component of the field

The signal components are expressed in terms of their dependence on the magnetic field. Other factors (e.g., light intensity, metastable density, and lamp and cell pressures) affect the absolute magnitudes but not the relative amplitude of the signal components. In the following paragraphs of this discussion, only the factors affecting relative amplitude will be considered.

The fundamental components of the signal proportional to $h_x(t)$ and $h_z(t)$ contain all the information needed to determine the X and Z components of the magnetic field. The second harmonic component contains little useful information and can become a problem because it is approximately 40 db larger than the information carrying components. The practical problems resulting from the high-level second harmonic will be discussed in a subsequent section.

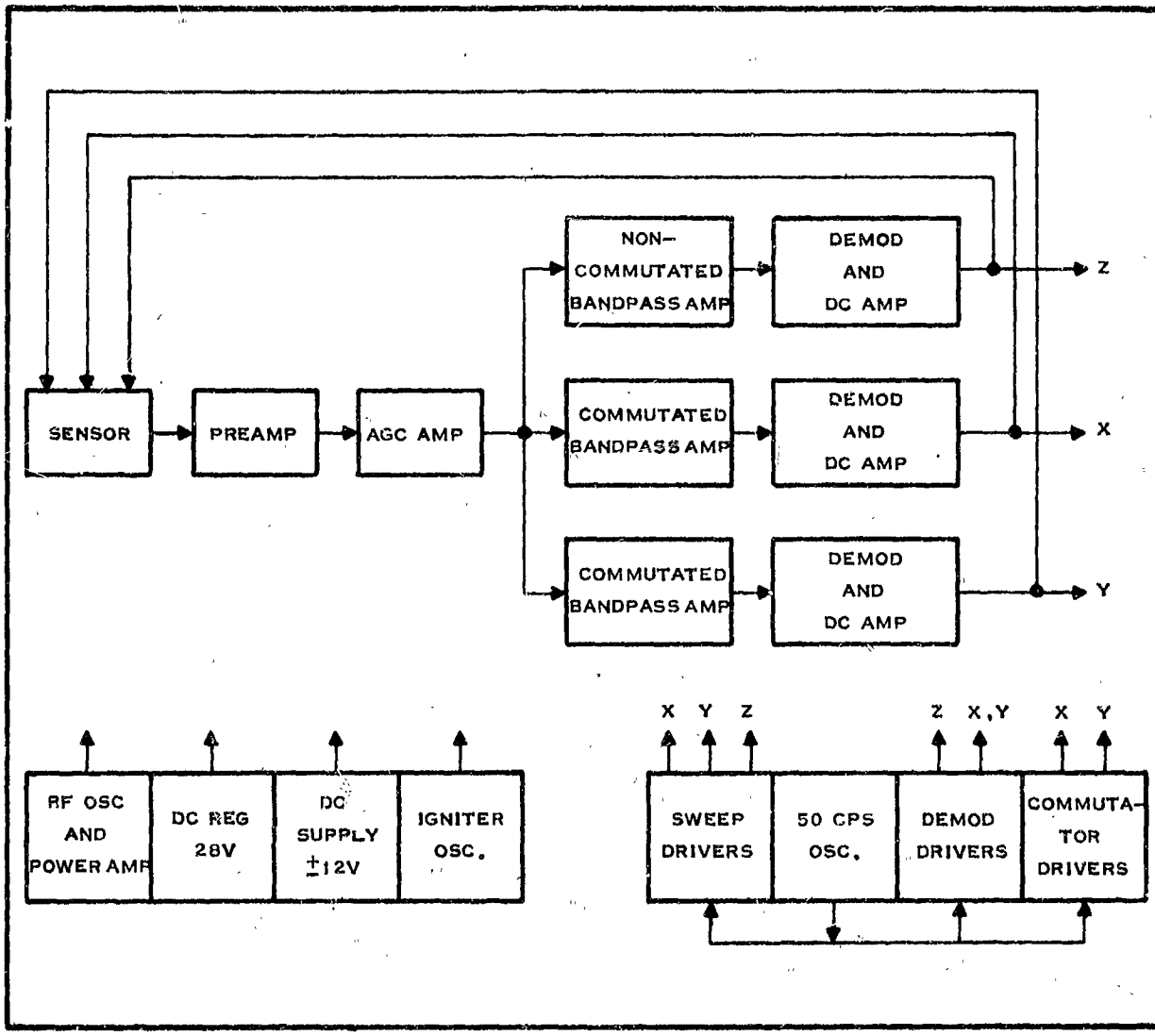

Figure 2. Magnetometer Block Diagram

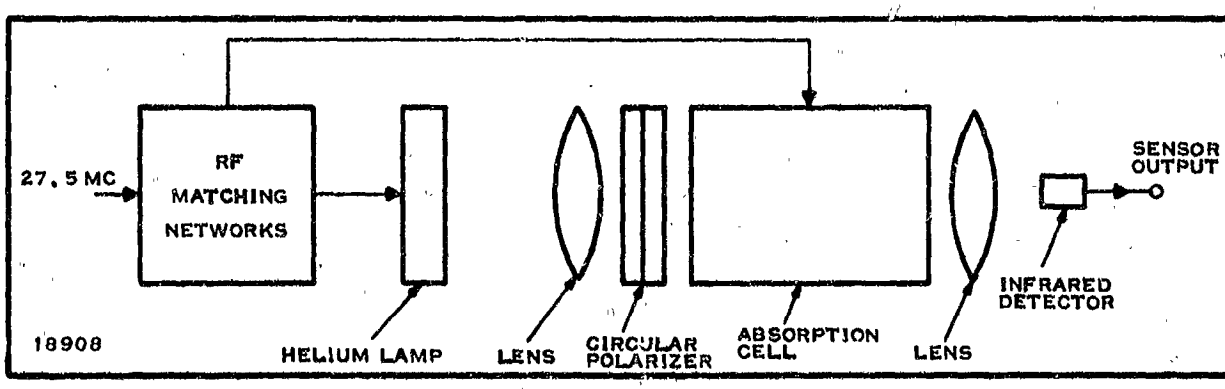

Figure 3. Sensor Diagram

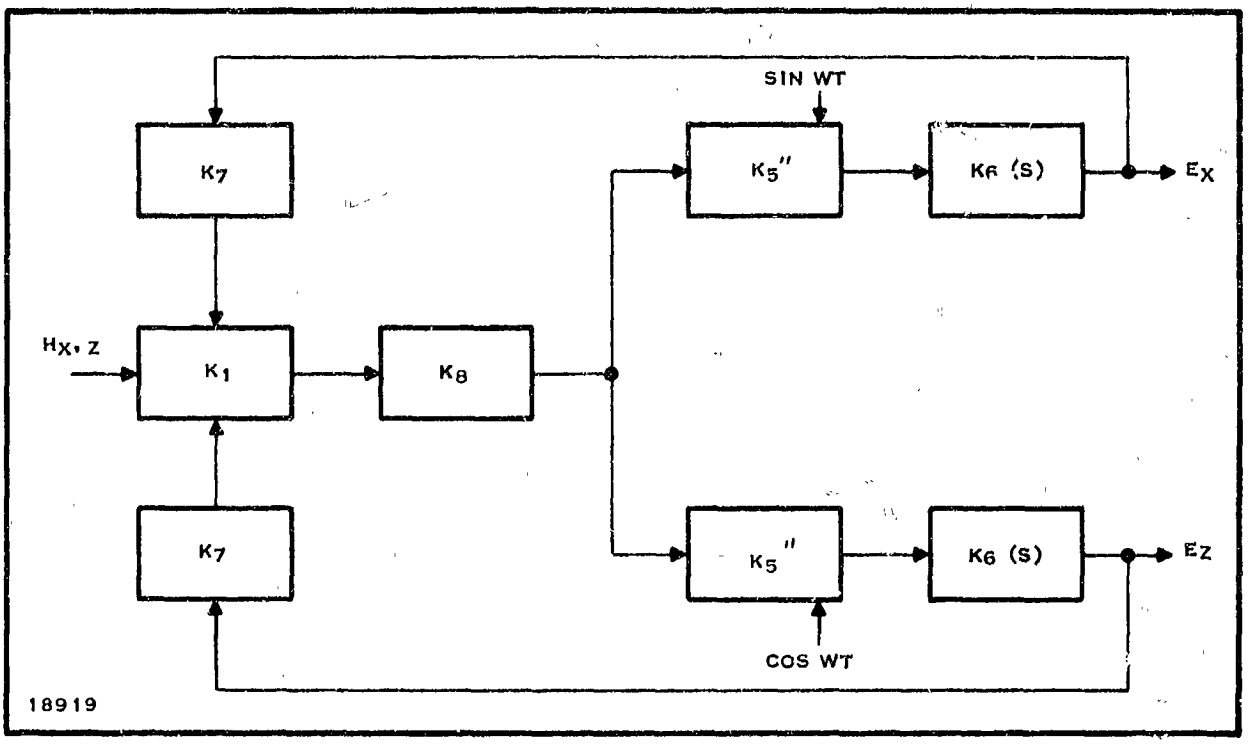

Figure 4. Two-Axis Block Diagram

1. Electronics

A feedback system is employed to process the X and Z signal components and to feed back a magnetic field at the sensor to cancel the respective field components. The absolute values of the signal are not critical when the feedback system is used to provide a reliable calibration. A simplified block diagram in Figure 4 illustrates the basic functions of the servosystem. The X and Z signal components are synchronously demodulated after amplifying and filtering to provide a phase-sensitive dc input to the integrator, which is a dc amplifier with capacitive feedback. The output of the dc amplifier drives a feedback coil on the sensor through a resistor. The current through the feedback coil generates a magnetic field opposite and approximately equal to the magnetic field component on that axis.

$$H_X = KI_X$$

The magnetic field produced by the current in the coil H_X is approximately equal to the input magnetic field h_X. The voltage generated by passing I_X through a signal-developing resistor is proportional to the magnetic field.

The rotating modulation vector is generated by driving the X-bucking coil with I sin wt and the Z-bucking coil with I cos wt. The magnetic fields produced by the two currents will add to produce a rotating magnetic vector.

To this point, two field components (h_X and h_Z) and a rotating modulation field (X-Z plane) have been discussed. To expand to a three-axis instrument, the modulation and signal component must include the X, Y, and Z axes. All three vectors can be covered by time sharing the X-Z and the Y-Z planes in the modulation and signal processing circuit.

The three-axis system is illustrated in Figure 2. The system is identical to the two-axis system with the added gating or commutating circuits and the Y-axis electronics. The supporting circuits such as power supplies, sweep drivers, phase shifter commutators and demodulators are shown.

2. Sensor

The sensor contains the helium lamp, helium absorption cell, optics, polarizers, Helmholtz coils, and the infrared detector. In addition, matching networks, a preamplifier, and an igniter circuit are located in the sensor to improve performance and reliability. The lamp is excited from a 27.5-mc rf exciter at a power level of approximately 1 watt. The lamp emits the usual helium spectrum including the 1.083-micron lines used in the magnetometer to optically pump the metastable states in the absorption cell. The energy from the lamp is collimated and passed through a circular polarizer and the helium absorption cell; then it is focused onto the infrared detector. The transmission of the absorption cell is a function of the angle between the total component of the magnetic field and the optical axis.

The basic optical pumping phenomena can be shown to be

$$s(t) = V \cos^2 \Phi(t)$$

where

V = a constant relating lamp, cell, and infrared detector constants to voltage

Φ = angle between the composite magnetic field and the optical axis.

A Fourier analysis of the signal will produce the expression discussed in the first part of the section.

$$s(t) = V \sin(2wt) + h_X(t) \sin wt + h_Z(t) \cos wt$$

B. Signal Analysis

The signal analysis will begin with the $\cos^2$ dependence and will relate the sensor output to the input magnetic fields. The effects of modulation field unbalance on the sensor output will be computed.

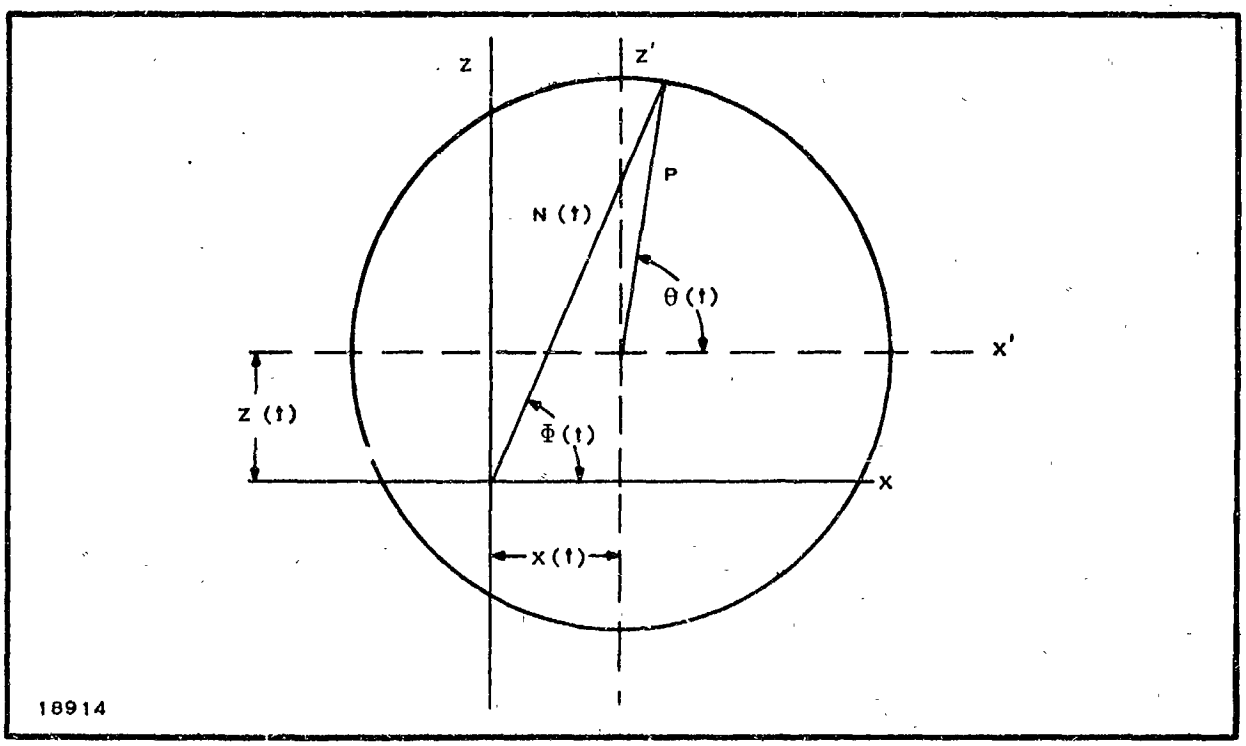

Figure 5. Geometry of Signal Generating Process

Figure 5 illustrates the geometry of the signal generating process with the rotating modulation vector P and the dc magnetic field components X and Z. The X, Z coordinate system represents the absolute reference, and the dashed lines X', Z' represent the coordinate system of the rotating magnetic vector P. From this sketch it can be seen that the instantaneous magnetic field N has a locus on the circle generated by the rotating sweep. Φ is the angle between the vector N and X, Z coordinate system.

$$p = B \sin wt + jC \cos wt$$

w = rotational rate of p

B = amplitude of sin wt component of p

C = amplitude of cos wt component of p

Let $B = C$; then $P = B = C$. Rewriting the preceding equation, we have

$$p = P(\sin wt + j \cos wt) .$$

Note: The sin wt component of p is applied along the X-axis and the cos wt component is applied along the Z-axis.

$$N(t) = jZ(t) + X(t) + P(\sin wt + j \cos wt)$$
$$= X(t) + P \sin wt + j[P \cos wt + Z(t)]$$

For this part of the analysis, X(t) and Z(t) will be defined as dc magnetic field components.

$$X(t) = H_X$$

and

$$Z(t) = H_Z$$

$Z(t)$ = Z component of the magnetic field to be measured

$X(t)$ = X component of the magnetic field to be measured

$\theta(t)$ = angle between the rotating magnetic vector P and its coordinate system X', Z'

$\Phi(t)$ = angle between the composite magnetic field N and the absolute coordinate system X, Z

$N(t)$ = sum of all impinging magnetic fields

Then

$$N(t) = H_X + P \sin wt + j(P \cos wt + H_Z)$$

$$\cos \Phi(t) = \frac{H_X + P \sin wt}{|N(t)|}$$

$$= \frac{H_X + P \sin wt}{\sqrt{(H_X + P \sin wt)^2 + (H_Z + P \cos wt)^2}}$$

Therefore, the result is

$$\cos^2 \Phi(t) = \frac{(H_x + P \sin wt)^2}{(H_x + P \sin wt)^2 + (H_z + P \cos wt)^2}$$

and

$$s(t) = V\left[\frac{(H_x + P \sin wt)^2}{(H_x + P \sin wt)^2 + (H_z + P \cos wt)^2}\right]$$

Conduct Fourier analysis on the above waveform s(t) for dc input fields and perfectly circular sweeps.

Signal Analysis:

$$A_n = \frac{2}{T_1} \int_{-T/2}^{+T/2} s(t) \cos nwt \, d(wt)$$

$$B_n = \frac{2}{T_1} \int_{-T/2}^{+T/2} s(t) \sin nwt \, d(wt)$$

$$s(t) = V \sum_{n=1}^{n=\infty} (A_n \cos nwt + B_n \sin nwt)$$

The expressions for the Fourier coefficients will be converted into the summation form for easy handling on the digital computer. Rewriting the above equations, we have

$$A_n = \frac{1}{\pi} \sum_{-\pi}^{+\pi} s(t) \cos nx\Delta x$$

$$B_n = \frac{1}{\pi} \sum_{-\pi}^{+\pi} s(t) \sin nx\Delta x .$$

Calculate the Fourier coefficient a_1 and b_1 for the condition specified in Table II. (The computations were performed on an IBM 1620 digital computer.)

Given:

$P = 200$ gamma

$V = 1$

θ is varied from 0° to 360° in 10° steps

24

Table II

Variables (γ)	B_{lz}	A_{lx}
$H_x = 0$ $H_z = 0$	5.799×10^{-9}	-2.2×10^{-8}
$H_x = 100$ $H_z = 0$	-5.425×10^{-6}	-0.2500
$H_x = -100$ $H_z = 0$	-4.389×10^{-9}	$+0.25$
$H_x = 0.1$ $H_z = 0$	-1.476×10^{-8}	$-.247 \times 10^{-6}$

$$s(t) = A_{lx} \cos w_1 t + B_{lz} \sin w_1 t + A_o + \frac{1}{\pi} \sum_{n=2}^{n=\infty} (A_n \cos nwt + B_n \sin nwt)$$

The A_o and high harmonic terms are not very significant in the magnetometer because the synchronous demodulator accepts only the fundamental and odd harmonics. It can be shown that all odd harmonics are zero when H_x and H_z field components equal zero. The even harmonic terms are nuisance signals that can cause saturation problems in signal amplifiers but do not enter linear system analysis. Neglecting the harmonics, s(t) can be rewritten

$$s(t) = A_{lx} \cos w_1 t + B_{lz} \sin w_1 t \ .$$

Note: The odd harmonics can be neglected because they are smaller than the fundamental components and the demodulation gain at odd harmonic frequencies is inversely proportional to the harmonic.

The magnetometer produces signals that can be processed effectively by an electronic servosystem of the type discussed in Section IV. The X and Z signal components can be separated by synchronous demodulation. The gain of the model magnetometer sensor analyzed in the preceding computations with a second harmonic output of 0.020 volt will be 48×10^{-6} volt per gamma. The magnetometer sensors delivered as part of this program had a gain of about 30×10^{-6} volt peak with a second harmonic level of about 20 millivolts peak.

Effects of Sweep Unbalance on Sensor Output Signal:

To demonstrate the effects of sweep unbalance on the performance of the three-axis magnetometer, the signal components will be derived as a

function of sweep balance. The steady-state, the second harmonic, and the fourth harmonic terms will be computed.

$$s(t) = \frac{B^2 \sin^2 wt}{B^2 \sin^2 wt + C^2 \cos^2 wt}$$

The error components H_x and H_z can be neglected in this computation because the magnetometer control loop maintains these signals at less than 0.1 percent of the sweep amplitude.

We may rewrite s(t) in a simplified form:

$$s(t) = \frac{B^2(1 - \cos 2wt)}{(B^2 + C^2) + (C^2 - B^2) \cos 2wt} .$$

The Fourier coefficients of s(t) are given by

$$A_o = \frac{V}{T}\int_0^T s(t)\,dt$$

$$A_n = \frac{2V}{T}\int_0^T s(t) \cos nwt\, d(wt)$$

$$B_n = \frac{2V}{T}\int_0^T s(t) \sin nwt\, d(wt) .$$

Let $x = 2wt$:

$$A_o = \frac{V}{2\pi}\int_0^{2\pi} \frac{B^2 dx}{(B^2 + C^2) + (C^2 - B^2) \cos x} - \frac{V}{2\pi}\int_0^{2\pi} \frac{B^2 \cos x dx}{(B^2 + C^2) + (C^2 - B^2) \cos x}$$

$$A_o = \frac{BV}{B + C}$$

$$A_2 = \frac{V}{\pi}\int_0^{2\pi} \frac{B^2 \cos x dx}{(B^2 + C^2) + (C^2 - B^2) \cos x} - \frac{V}{2\pi}\int_0^{2\pi} \frac{B^2 dx}{(B^2 + C^2) + (C^2 - B^2) \cos x}$$

$$- \frac{V}{2\pi}\int_0^{2\pi} \frac{B^2 \cos 2x dx}{(B^2 + C^2) + (C^2 - B^2) \cos x}$$

$$A_2 = \frac{2BCV}{(C+B)^2}$$

$$A_4 = \frac{VB^2}{\pi}\left[\int_0^{2\pi} \frac{\cos 2x\,dx}{(B^2+C^2)+(C^2-B^2)\cos x} - \frac{1}{2}\int_0^{2\pi} \frac{(\cos 3x + \cos x)dx}{(B^2+C^2)+(C^2-B^2)\cos x}\right]$$

$$= -\frac{2BC(B-C)V}{(B+C)^3}$$

B_n terms = 0 because s(t) is an even function.

IV. SYSTEM ANALYSIS

The system performance will be studied with the aid of the functional block diagram and transfer functions. The actual transfer functions of the carrier section circuits will be translated into effective low pass transfer functions. Significant nonlinearities will be specified and their effects on system performance described. Errors resulting from drift, commutations, and crosstalk will be evaluated in Section V. The constants for the block diagram will be determined from a discussion of each circuit in the servoloop. The sensor transfer function will be taken from the signal generation section. The preamplifiers, wideband amplifier, wideband amplifier filter, bandpass amplifier and dc amplifier will be discussed in this section. To support the simplifications of the carrier transfer functions, the equations will be derived for full-wave suppressed carrier signals with arbitrary phase shift and attenuation of the sideband.

A. Circuit Transfer Function

In the derivation, a sinusoid is used as the demodulation function for suppressed carrier amplitude-modulated signals. Use of a sinusoid in place of the usual square wave produces valid results when the input waveform is sinusoidal and when the higher product terms do not affect system operation. The sinusoid is a very good approximation, even when the input waveform is complex because of lower demodulator gain at harmonic frequencies. The equation for f(t) illustrates the demodulator output for an arbitrary phase shift and attenuation of the sidebands.

$F(t)$ = modulated carrier signal

W_c = carrier frequency

W_m = modulation frequency

t = time

27

K_1 = system gain at the upper sideband frequency w_1

K_2 = system gain at the lower sideband frequency w_2

ϕ = upper sideband phase

θ = lower sideband phase

$$F(t) = -K_1 \cos [(W_c + W_m)t + \Phi] + K_2 \cos [(W_c - W_m)t + \theta]$$

G(t) = demodulator reference
= $\sin W_c t$

f(t) = demodulator output

$$f(t) = F(t)G(t)$$

$$= \frac{1}{2}\left\{\sin W_m t\,[K_1 \cos \Phi + K_2 \cos \theta] + \cos W_m t\,[K_1 \sin \Phi - K_2 \sin \theta]\right\}$$

The approximate expression for f(t) neglects the even harmonic terms which do not carry information in this system. This approximation is used to calculate the phase shift through the bandpass amplifier in the following section.

Preamplifier: The preamplifier is designed to provide a low-noise, high-input impedance to the infrared detector and a differential output with low-output impedance to the wideband amplifier. The circuit uses four small signal silicon transistors in a feedback amplifier (Appendix, Dr No. 404741). A bootstrap technique is employed to generate the high-input impedance (2 megohms). A differential output is utilized to provide common mode rejection of pickup in the cabling between the preamplifier and the wideband amplifier.

The preamplifier is packaged to provide a magnetic moment of less than 0.25 gamma at 2 inches. This is accomplished by using nonmagnetic components and by minimizing the current loop in the interconnectors. The equivalent transfer function for system considerations: K_2 = 10v/v.

Wideband Amplifier: The wideband amplifier is designed to provide additional gain in the signal path and to compensate for the sensor gain variations resulting from the responsivity variations in the infrared detector. The amplifier has a differential input to accept the preamplifier output. The second harmonic signal component provides the ideal agc reference, since it is effectively independent of error signal dynamics and is directly proportional to the sensor gain $K_1(s)$. The wideband amplifier output is demodulated (half wave rectified) and applied through a resistor to a pair of 1N647 diodes. The gain of the divider network is inversely related to the voltage applied to the control input. The distortion produced at the diodes is small because the signal level is low. To reduce the distortion effects further, the two diodes are used to produce balanced or odd harmonic distortion. The agc characteristics are shown in Figure 6. Equivalent transfer function: K = 30v/v (typical). The nominal gain will be used in the system calculations.

28

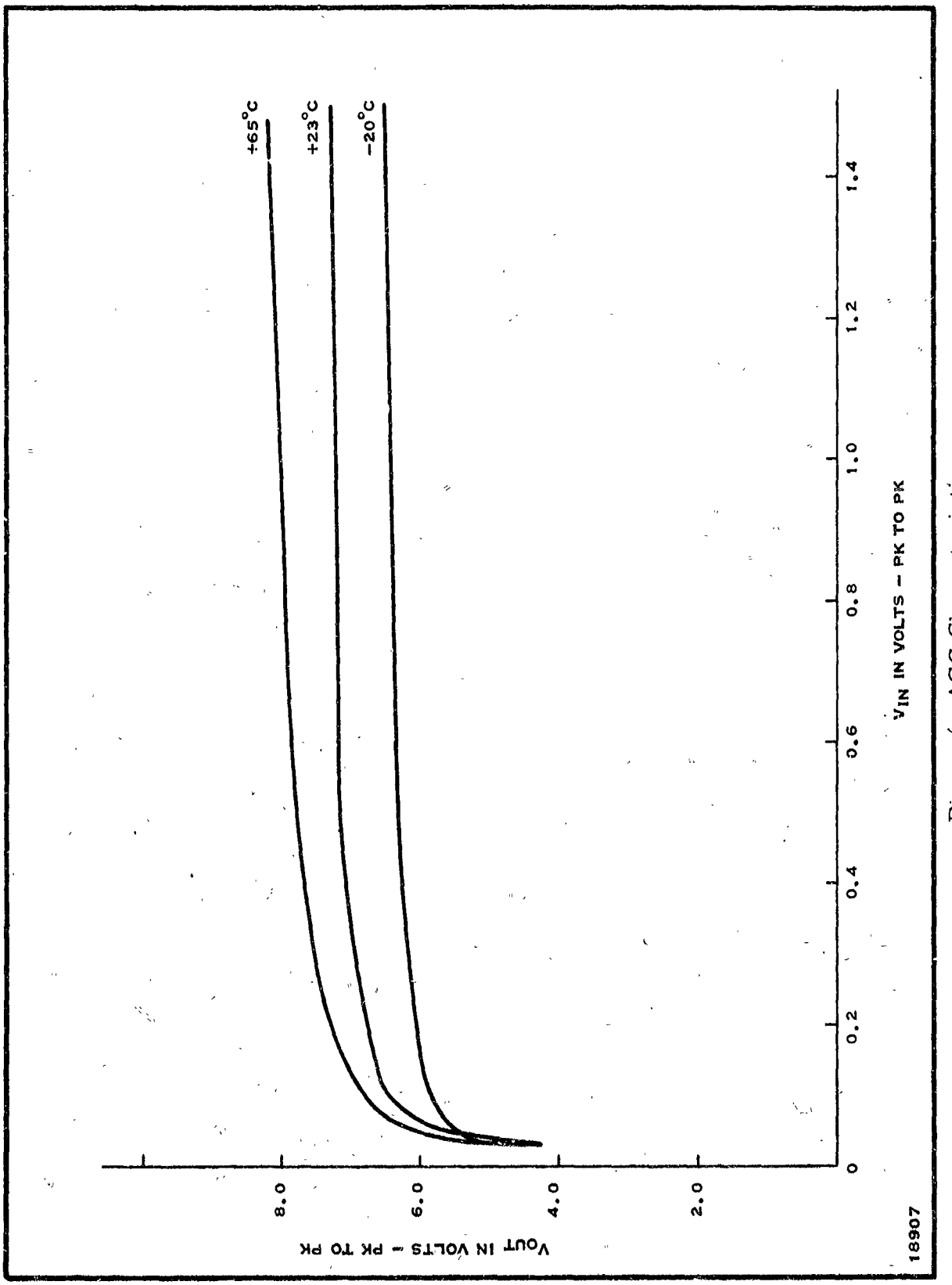

Figure 6. AGC Characteristics

29

The phase characteristics are essentially flat over the signal frequencies of interest, and the agc does not act on the error signal components.

Wideband Amplifier Filter: The wideband amplifier filter is designed to attenuate the second harmonic (2w) signal following the wideband amplifier. Since this filter precedes the decommutation, a minimum phase and amplitude distortion is desired at frequencies other than 2w. A bridged tee notch filter has the best characteristic for this purpose. Refer to Figure 7 for the phase and amplitude characteristics. The effect of the filter on loop performance can be seen by examining the phase and amplitude characteristics in the vicinity of w. In terms of the w component, the filter can be expressed as a gain and a phase angle. Effective gain: K = 1. The effective gain will be valid for loop gain and stability consideration.

Commutator and Bandpass Amplifier: This circuit decommutates the signal separating the X and Y components and performs a bandpass filtering operation centered about w (50 cps). The decommutation process is performed by shorting the signal path to ground during the off periods. The bandpass frequency response illustrated in Figure 8 is generated by placing a twin tee filter in the feedback path of an ac amplifier. Gain stability is achieved at the pass frequencies by individual stage feedback in the amplifier.

The phase-shift-versus-modulation-frequency and amplitude-versus-modulation-frequency plots for the bandpass amplifier illustrate the equivalent low pass characteristics (Figure 9):

$$K_5(s) = \frac{K_5}{ST + 1}$$

$$= \frac{K_5}{S(0.032) + 1} .$$

Demodulator and DC Amplifier: The demodulator and dc amplifier is a medium-gain amplifier ($K_6 \approx 1000$) connected as an integrator to provide a high loop gain and a means for adjusting the system frequency response. The half-wave demodulation is accomplished with a shunt transistor switch. The offset voltage on the transistor is approximately 15×10^{-3} volt. A pair of transistors with balanced h_{fe} and V_{be} are used in a differential input stage to achieve low drift and high gain. The circuit goes single ended to a complementary output emitter follower. The amplifier is connected as a positive integrator in the magnetometer electronics (Figure 10). The transfer function for this circuit can be expressed

$$K_6(s) = \left[\frac{(SC_2Z_2 + 1)}{(SC_1Z_1 + 1)}\right] \left[\frac{K_6}{S(Z_2C_2K_6) + 1}\right] .$$

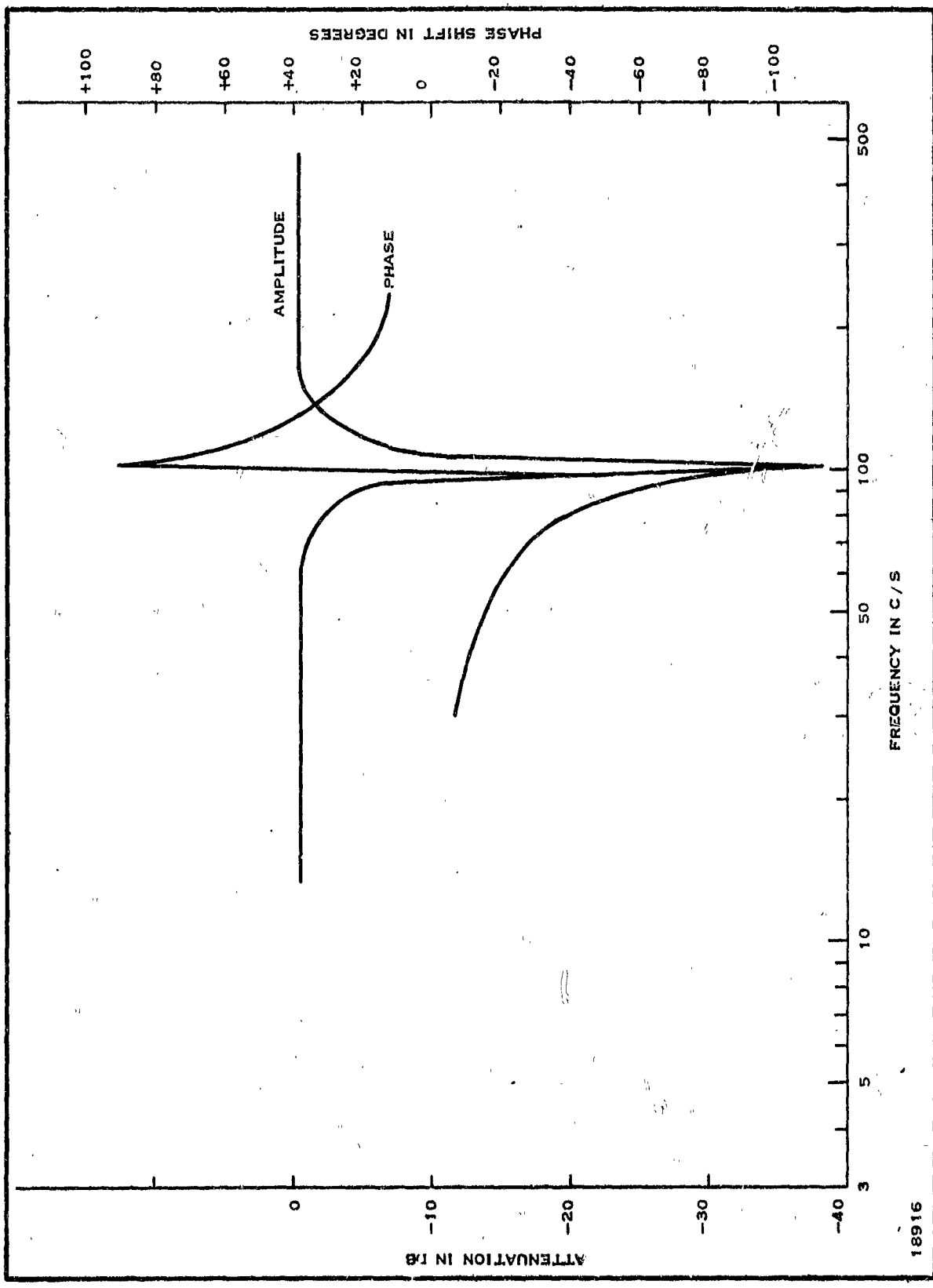

Figure 7. Wideband Amplifier Filter Phase and Amplitude Characteristics

31

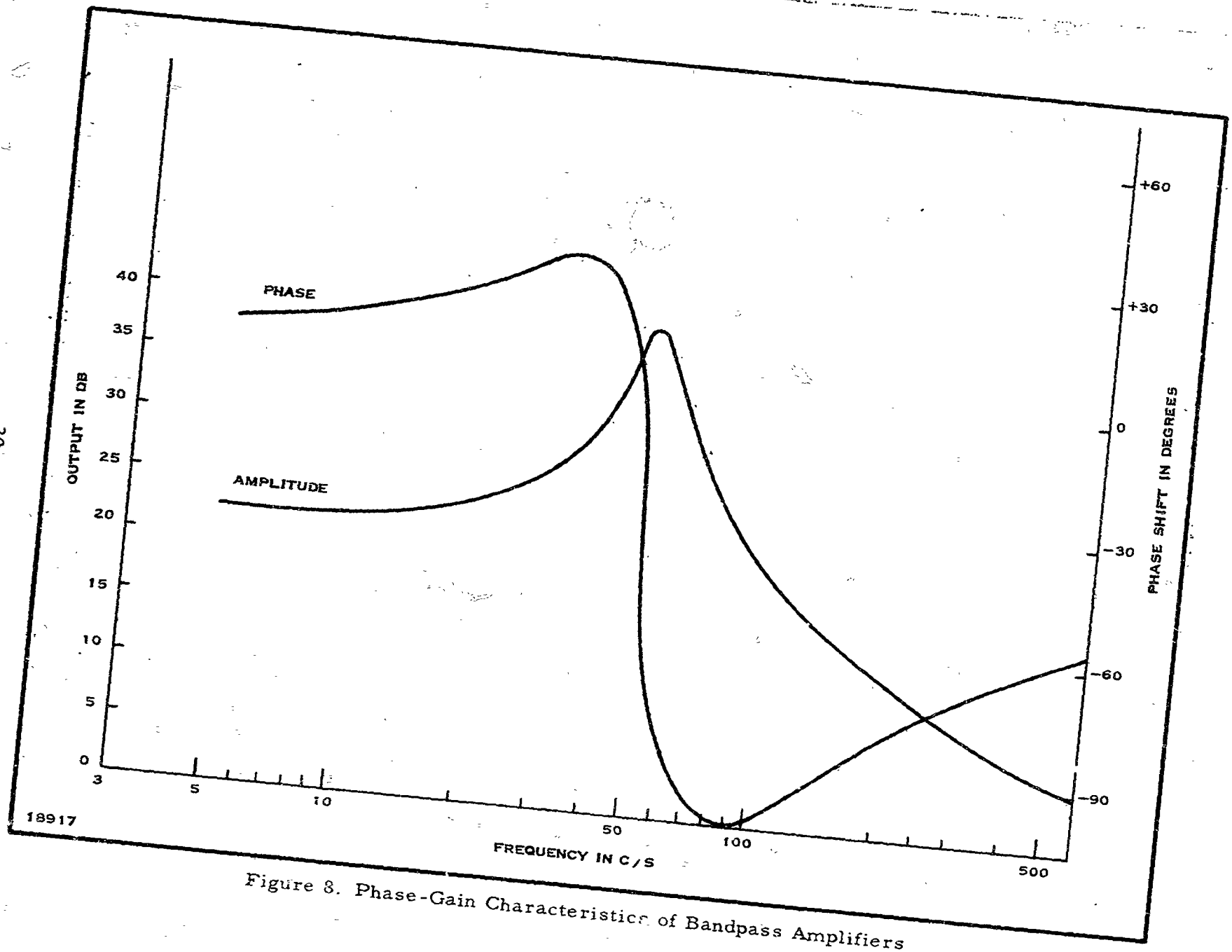

Figure 8. Phase-Gain Characteristics of Bandpass Amplifiers

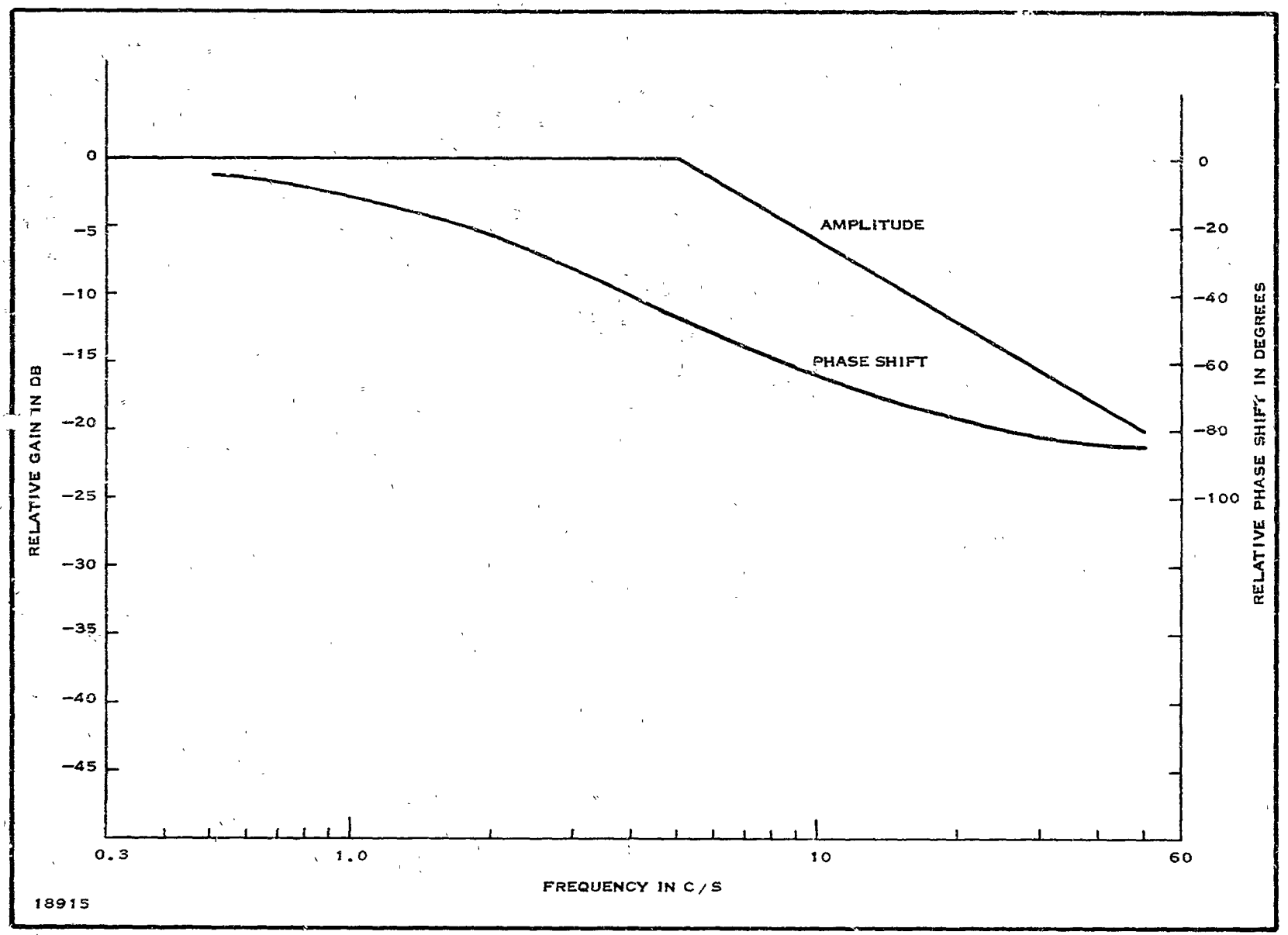

Figure 9. Low Pass Equivalent Phase and Amplitude Characteristics of Bandpass Amplifier

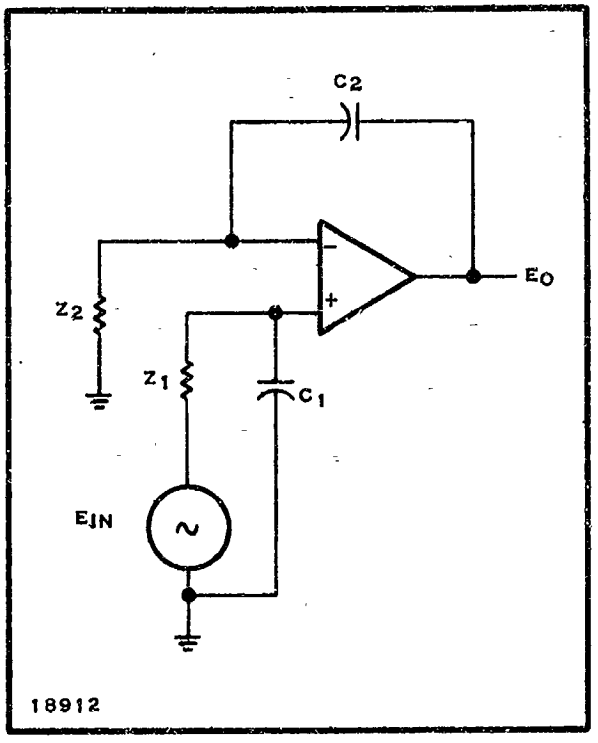

Figure 10. Positive Integrator Diagram

When $C_2Z_2 = C_1Z_1$, we obtain

$$K_6(s) = \frac{K_6}{S(Z_2C_2K_6) + L} .$$

Equivalent transfer function:

$$K_6(s) = \frac{K_6}{S(Z_2C_2K_6) + 1}$$

$$= \frac{1000}{S(1300) + 1}$$

B. Instrument Transfer Function

From the standpoint of stability and dynamic performance, the functional block diagram of the magnetometer will be an effective low pass diagram. The single-axis diagram omits the modulation-demodulation processes and replaces the carrier amplifiers with the equivalent low pass functions. Figure 11 illustrates this block diagram.

h_{x1} = input magnetic field in gamma

h_{xf} = feedback magnetic field in gamma

h_ϵ = magnetic field error in gamma
= $h_{x1} - h_{xf}$

$K_1(s)$ = sensor gain including the infrared detector
= 30×10^{-6} volt for an detector output of 20×10^{-3} volt peak

$K_2(s)$ = preamplifier gain
= 10v/v

$K_3(s)$ = wideband amplifier gain (agc)
= 10 to 200v/v (normal room temperature = 15v/v)

$K_4(s)$ = notch filter to reject the 100-cps second harmonic component
= 1v/v at 50 cps

K_5' = demodulator gain
= 0.318v/v

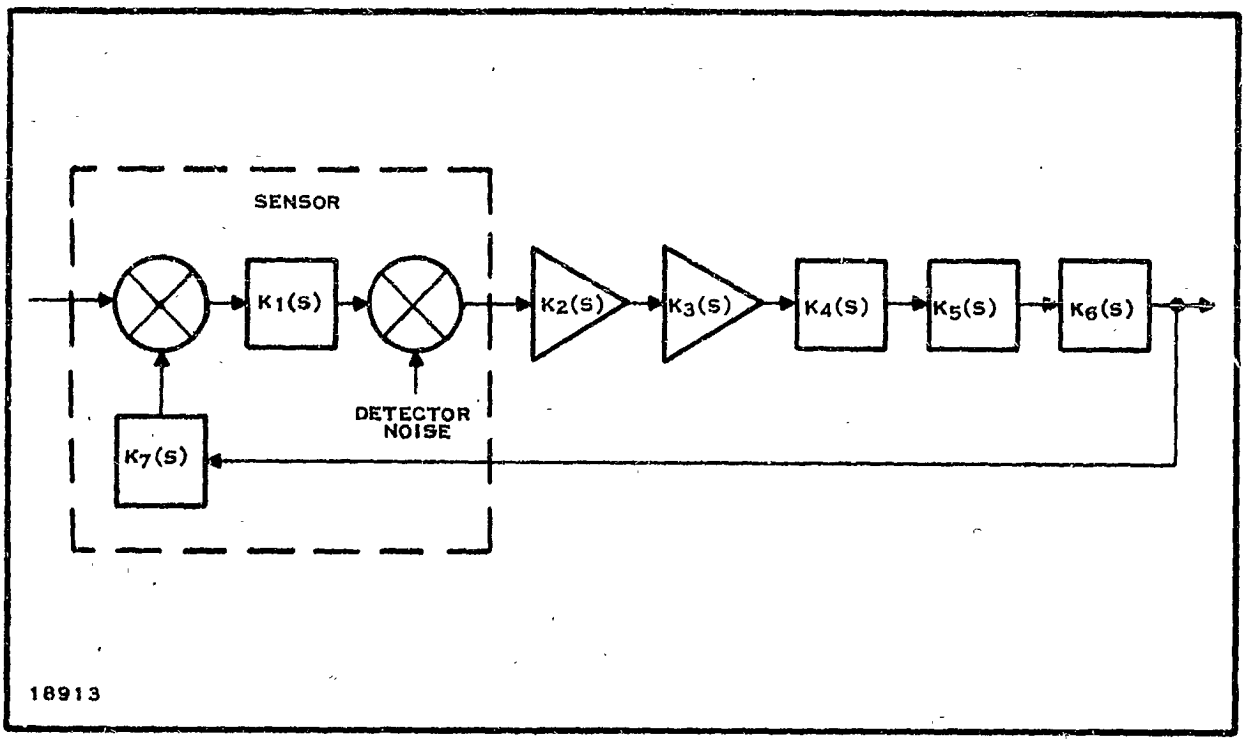

Figure 11. Equivalent Single-Axis Diagram

$K_5(s)$ = bandpass amplifier $\qquad K_5 = 50$
$= K_5/S(0.032) + 1$
$\cong K_5$

$K_6(s)$ = operational amplifier transfer function $\qquad K_6 = 1000$
$= K_6/(S\tau_6 + 1) \qquad \tau_6 = 1300$
$= 1000/(S1300 + 1) \qquad S$ = Laplace operator

K_7 = Helmholtz coil constant on sensor
= 60.6 gamma/volt

$$\frac{E_o}{h_{x1}} \cong \frac{K_1(s)K_2(s)K_3(s)K_4(s)K_5(s)K_6(s)}{1 + K_7(s)K_1(s)K_2(s)K_3(s)K_4(s)K_5(s)K_6(s)}$$

System Closed Loop Transfer Functions:

$$\frac{E_o}{h_x} = \frac{0.0166}{S(0.3) + 1}$$

Bandpass is approximately equal to 0.6 cps.

35

Stability of Magnetometer Loop:

Open loop transfer function equals

$$C(s) = K_1(s)K_2(s)K_3(s)K_4(s)K_5(s)K_5' K_6(s)K_7$$

$$= \frac{K_1 K_2 K_3 K_4 K_5 K_5' K_6 K_7}{(S\tau_5 + 1)(S\tau_6 + 1)}$$

$$= \frac{4340}{[S(0.032) + 1]\ [S(1300) + 1]}$$

Crossover occurs between 0.5 and 1 cps almost one decade before the next significant loop break, which occurs at about 5 cps. The gain margin would be determined by secondary effects encountered beyond the 5-cps lag. The gain margin is greater than 20 db. The phase margin is approximately 90 degrees.

V. SYSTEM ERRORS

A. Error Producing Mechanisms

A number of different causes can produce false outputs on the magnetometer. The important error producing mechanisms discussed in this section are sweep unbalance and the effects of time sharing, phase shift and crosstalk, and dc amplifier drift

Additionally, two other important error sources in the magnetometer should be mentioned: pickup and magnetic moments in the sensor. Pickup has been minimized by a single-point ground, shielding, coaxial transmission to high current loads, and extensive decoupling. Magnetic moments in the sensor have been minimized by selection of nonmagnetic materials and by periodic magnetic checking of the sensor components and assemblies during the assembly process.

B. Signal Processing in the Carrier Section Electronics

The signal processes of time sharing and modulation will be analyzed to provide a theoretical basis for error signals resulting from these operations. The analysis will be limited to errors that produce a false steady-state output signal. Steady-state errors will result if the time-sharing operation generates frequencies equal to 2ω or odd harmonics of 2ω (2ω is the modulation frequency and ω is the time-sharing and gating frequency). The first step of the analysis will consider a perfect system in terms of a flat bandpass. The second step will consider the errors resulting from bandpass limitations in the sensor and the electronics.

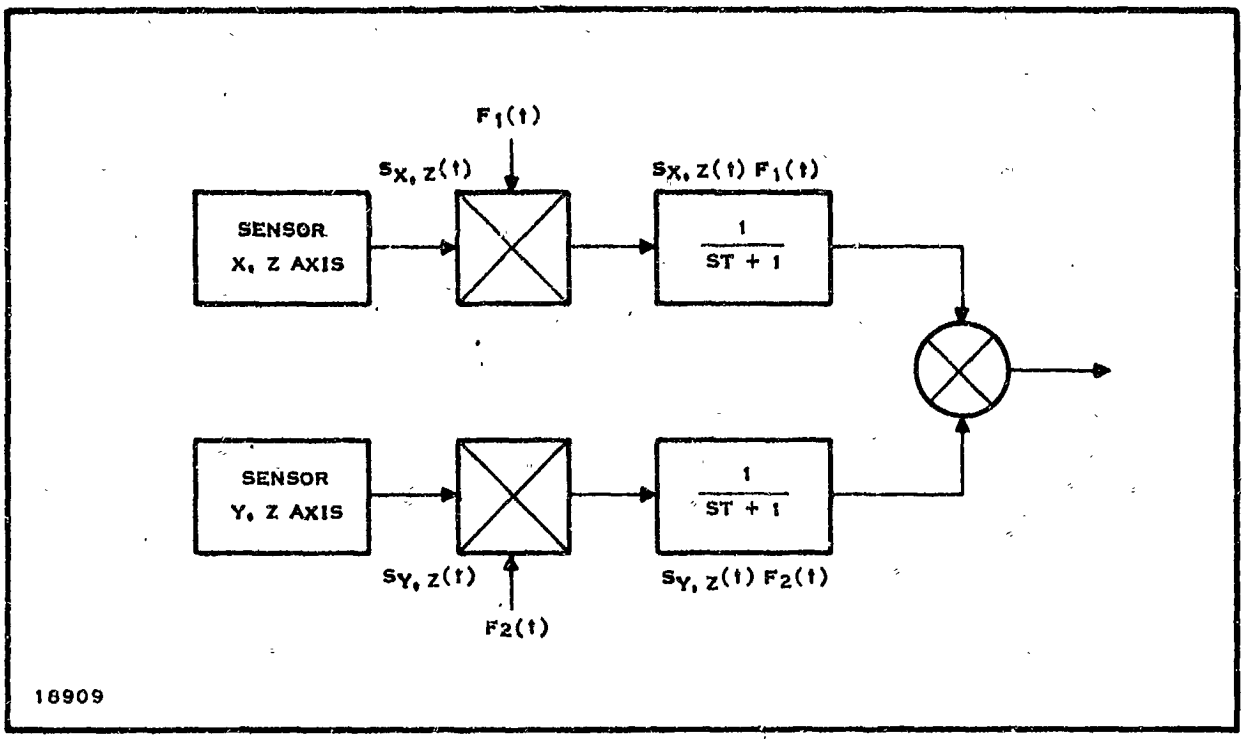

Figure 12. Model of Three-Axis Sensor

The magnetics information is superimposed on the carrier signal by time-sharing and amplitude-suppressed carrier modulation. A model of the sensor for the purposes of this analysis is given in Figure 12. The model supposes two two-axis magnetometers gated by the commutation function $F_1(t)$ and $F_2(t)$ and then added to provide a single output.

$S_{x,z}$ = magnetometer output from two-axis system

$S_{x,z}(t) = A_{x,z} \cos^2 \Phi_{x,z}$

$S_{y,z}$ = magnetometer output from two-axis system

$S_{y,z}(t) = A_{y,z} \cos^2 \Phi_{y,z}$

$F_1(t)$ = gating function for X, Z signal

$F_1(t) = 0.5 + 0.64 \sin \omega t + 0.21 \sin 3\omega t + 0.13 \sin 5\omega t + 0.09 \sin 7\omega t + 0.07 \sin 9\omega t + \ldots$

$F_2(t)$ = gating function for Y, Z signal

$F_2(t) = 0.5 - 0.64 \sin \omega t - 0.21 \sin 3\omega t - 0.13 \sin 5\omega t - 0.09 \sin 7\omega t - 0.07 \sin 9\omega t - \ldots$

ω = commutation frequency

2ω = carrier frequency
$= w$

37

Error signals that can produce steady-state output errors cannot be generated in a composite system where $F_1(t) = 1$ and $F_2(t) = 0$. The signals generated by the sensor are valid and no nonlinear operations are performed in the carrier electronics to generate harmonic or subharmonic frequencies.

The addition of time sharing creates the possibility of generating error signals because of the nonlinear nature of this operation. The commutation (and decommutation) process multiplies the signal by a square wave having the values of 1 and 0. The frequency spectrum of the commutated signals can be evaluated by carrying out the multiplication operation, or the spectrum can be derived directly from the Fourier series. The Fourier series representation of the gated signals will be derived in the following computations.

$$b_m = \frac{1}{T} \int_0^T \left[S_{x,z}(t) F_1(t) \sin m\omega t d(\omega t) \right]$$

$$a_m = \frac{1}{T} \int_0^T \left[S_{x,z}(t) F_1(t) \cos m\omega t d(\omega t) \right]$$

$$S_{x,z}(t) = A_{ox,z} + A_{4(1+n)x,z} \cos 4(1 + n)\omega t$$

$$S_{y,z}(t) = A_{oy,z} + A_{4(1+n)y,z} \cos 4(1 + n)\omega t.$$

The Fourier series expressions are written with the assistance of the graphical representation of the functions $S_{x,z}(t) F_1(t)$ and $S_{y,z}(t) F_2(t)$ given in Figure 13. For $S_{x,z}(t) F_1(t)$, the Fourier series is defined by

$$b_m = \frac{A_{4(1+n)x,z}}{\pi} \left[\int_0^\pi \cos 4(1 + n)u \sin mu du \right] + \frac{A_{ox,z}}{\pi} \int_0^\pi \sin mu du$$

$$= \begin{cases} \dfrac{A_{4(1+n)x,z} \left[m \right] \left[1 - (-1)^{m+4(1+n)} \right]}{\pi \left\{ m - [4(1 + n)]^2 \right\}} & \text{for } m \neq 4(1 + n) \\ 0 & \text{for } m = 4(1 + n) \end{cases}$$

$$+ \begin{cases} \dfrac{2}{\pi} \left[\dfrac{A_{ox,z}}{m} \right] & \text{for } m \text{ even} \\ 0 & \text{for } m \text{ odd} \end{cases}$$

38

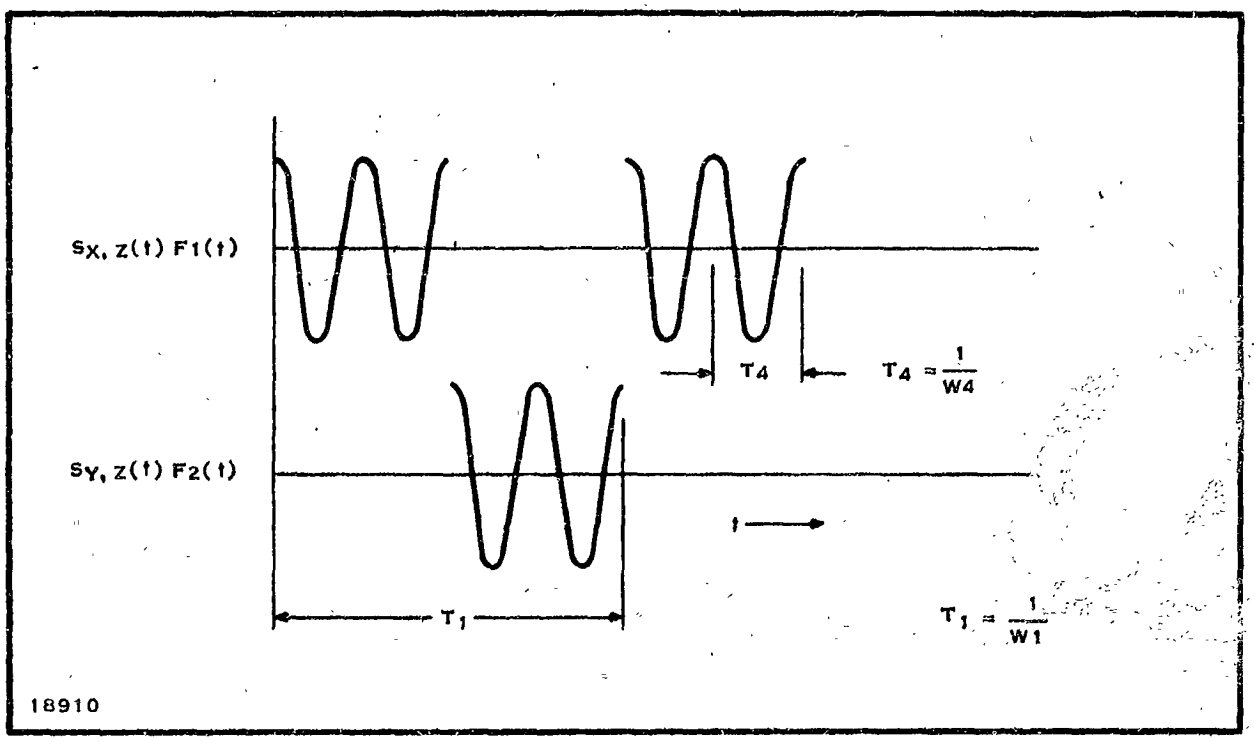

Figure 13. Commutated Waveforms

$$a_m = \frac{A_{4(1+n)x,z}}{\pi} \int_0^{\pi} \cos 4(1+n)u \cos mudu + \frac{A_{ox,z}}{2\pi} \int_0^{\pi} \cos mudu$$

$$= \begin{cases} \frac{A_{4(1+n)x,z}}{2} & \text{for } 4(1+2n) = m \\ 0 & \text{for } m \neq n \end{cases}$$

$$+ \frac{A_{ox,z}}{2} \qquad \text{for } m = 0$$

The Fourier series for $S_{y,z}(t)\,F_2(t)$ is defined by

$$c_m = \frac{1}{T} \int_0^T \left[S_{y,z}(t)\,F_2(t)\right] \sin m\omega t\, d(\omega t)$$

$$d_m = \frac{1}{T} \int_0^T \left[S_{y,z}(t)\,F_2(t)\right] \cos m\omega t\, d(\omega t)$$

$$c_m = \frac{A_{4(1+n)y,z}}{\pi}\left[\int_{\pi}^{2\pi} \cos 4(1+n)u \sin mu\,du + \frac{A_{oy,z}}{\pi}\int_{\pi}^{2\pi} \sin mu\,du\right]$$

$$= \begin{cases} -\dfrac{A_{4(1+n)y,z}\, m\left[1-(-1)^{m+4(1+n)}\right]}{\pi\left\{m^2-[4(1+n)]^2\right\}} & \text{for } m \neq 4(1+n) \\ 0 & \text{for } m = n \end{cases}$$

$$- \begin{cases} \dfrac{2}{\pi}\left(\dfrac{A_{oy,z}}{m}\right) & \text{for } m \text{ odd} \\ 0 & \text{for } m \text{ even} \end{cases}$$

$$d_m = \frac{A_{4(1+n)y,z}}{\pi}\left[\int_{\pi}^{2\pi} \cos 4(1+n)u \cos mu\,du + \frac{A_o}{2\pi}\int_{\pi}^{2\pi} \cos mu\,du\right]$$

$$= \begin{cases} \dfrac{A_{4(1+n)y,z}}{2} & \text{for } 4(1+n) = m \\ 0 & \text{for } 4(1+n) \neq m \end{cases}$$

$$+ \frac{A_{oy,z}}{2} \qquad \text{for } m = 0$$

The series representing the signal output of the sensor is

$$S_{x,z}(t)\,F_1(t) + S_{y,z}(t)\,F_2(t)$$

$$= \frac{1}{2}\left[A_{4(1+n)x,z} + A_{4(1+n)y,z}\right]\cos 4(1+n)\omega t$$

$$+ \frac{2}{\pi m}\left[A_{ox,z} - A_{oy,z}\right]\left[\frac{1-(-1)^m}{2}\right]\sin m\omega t$$

$$+ \begin{cases} \dfrac{m\left[1-(-1)^{m+4(1+n)}\right]}{\pi\left\{m^2-[4(1+n)]^2\right\}}\left[A_{4(1+n)x,z} - A_{4(1+n)y,z}\right]\sin m\omega t \\ 0 \qquad \text{for } 4(1+n) = m \end{cases}$$

$$+ \frac{1}{2}\left[A_{ox,z} + A_{oy,z}\right].$$

H_x, H_y, and H_z have been omitted from the equations $S_{x,z}(t)$ and $S_{y,z}(t)$ because the instrument feedback system maintains these components at less than 0.1 percent of the 4ω component.

For the conditions $S_{x,z}(t) = S_{y,z}(t)$ the Fourier series for the signal is

$$S_{x,z}(t)\,F_1(t) + S_{y,z}(t)\,F_2(t) = A_4 \sin 4\omega t + A_o \ .$$

The decommutation of this expression will reproduce the expressions $S_{x,z}(t)\,F_1(t)$ and $S_{y,z}(t)\,F_2(t)$. Neither of these signals contains a frequency component at the demodulation frequency of 2ω or at odd harmonics of 2ω. Therefore, no error signals will result.

For the condition $S_{x,z}(t) \neq S_{y,z}(t)$ the Fourier series representing $S_{x,z}(t)\,F_1(t) + S_{y,z}(t)\,F_2(t)$ becomes long and complex. The results of time sharing a flat (wideband) system can be seen more directly from the following expressions.

Let

$$F_1(t) = p$$

$$F_2(t) = q$$

From the definition of $F_1(t)$ and $F_2(t)$

$$p' = q$$

or

$$q' = p$$

Using the rules of Boolean algebra, we obtain

$S_{x,z}(t)\,p$ = commutated signal

$S_{x,z}(t)\,p\,p$ = decommutated signal

$S_{x,z}(t)\,p\,p = S_{x,z}(t)\,p$

$S_{x,z}(t)\,p\,p' = 0$

$S_{y,z}(t)\,p'$ = commutated signal

$S_{y,z}(t)\,p'\,p'$ = decommutated signal

$S_{y,z}(t)\,p'\,p' = S_{y,z}(t)\,p'$

$S_{y,z}(t)\,p\,p' = 0$.

As illustrated by these logic equations, no erroneous signals are generated by the time-sharing operations in a flat wideband system.

41

Effects of Band Limiting on Error Signals Resulting From Decommutation

The error signals resulting from the decommutation of the band-limited commutated signals can be determined by evaluating the frequency spectrum at the decommutator output. The Fourier series representing the decommutator inputs are composed of four specific terms:

The $\cos 4(1 + n)\omega t$ frequencies are generated in basic modulation process in the sensor. These signals are present before commutation (or decommutation) is accomplished.

The $[1 - (-1)^m/2] \sin m\omega t$ frequencies result from the commutation of the steady-state term in basic sensor modulation expression. These signals are present only when commutation is used.

The $\sin m\omega t$ frequencies result from the commutation of the $\cos 4(1 + n)\omega t$ terms of the basic sensor modulation expression. These signals are present only when commutated sweeps are used.

The steady-state term composed of $A_{ox,z}$ and $A_{oy,z}$ is a result of the basic modulation process. This component will not be considered in subsequent discussion because it is removed by the ac coupling in the system.

It has been shown that no output errors will result if the transfer function of the system blocks between the commutation and decommutation operation is wide band with constant amplitude characteristics. The actual magnetometer departs from this requirement in the sensor and in the wideband amplifier filter. The important characteristic of these functions will be repeated here.

Sensor: 6-db rolloff corner frequency at 150 cps = 6ω. The frequency sensitivity of the sensor is represented as a lag filter following the commutation point in Figure 12.

Wideband Amplifier Filter Characteristics

Frequency	Att Count	Att Gain	Phase (degrees)
ω	R_1	1.0	10.1
3ω	R_3	0.8	33.4
5ω	R_5	0.5	48.7
7ω	R_7	0.67	19.0

42

The amplitudes of the various signal components will be modified by the sensor and wideband amplifier characteristics before being fed into the decommutator. The decommutation operation will be conducted on each of the signal components.

The decommutation of the cos $4(1 + n)\omega t$ signals will result in the signal frequencies $[4(1 + n) \pm m]\omega t$, $[4(1 + n) \pm 3m]\omega t$, $[4(1 + n) \pm 5m]\omega t$, etc. No signal frequencies of 2ω or odd harmonics of 2ω will result from this operation; therefore, no steady-state error will result.

The decommutation of the signal components having frequency of $[1 - (-1)^m/2] \sin m\omega t$ will result in the signal frequencies of $[m \pm n]\omega t$ for odd values of n and m. This combination will result in signal frequencies of 2ω and odd harmonics of 2ω. The amplitude of the signals will be computed in the following calculations.

k_n = attenuation of sensor and wideband amplifier filter

D_2 = decommutator output as contributed by the second term of the Fourier series

θ_n = phase shift through sensor and wideband amplifier filter

$$D_2 = F_1(t)(A_{ox,z} - A_{oy,z})\left(\frac{2}{\pi}\right)\left[k_1 \sin(\omega t + \theta_1) + \frac{k_3}{3}\sin(3\omega t + \theta_3) + \frac{k_5}{5}\sin(5\omega t + \theta_5) + \frac{k_7}{7}\sin(7\omega t + \theta_7)\right]$$

$$D_2 = F_1(t)(A_{ox,z} - A_{oy,z})\,[0.64 \sin(\omega t - 10.1°) + 0.17 \sin(3\omega t - 33.4°) + 0.064 \sin(5\omega t + 48.7°) + 0.06 \sin(7\omega t + 19.0°)]$$

Performing the indicated operations and simplifying, we obtain

$$D_2 = -(A_{ox,z} - A_{oy,z})[0.074 \sin(\omega t + 68.7°)]$$

Note: The odd harmonics of 2ω have been neglected because of system circuit attenuation at these frequencies. To compensate for a 16.4-degree phase shift at 2ω in the wideband amplifier filter, -16.4 degrees will be added to the D_2 expression, resulting in D_2'.

$$D_2' = -(A_{ox,z} - A_{oy,z})[0.074 \sin(\omega t + 52.3°)]$$

D_3 = decommutator output as contributed by the third term of the Fourier series:

$$D_3 = F_1(t)\left\{\frac{2[A_{4x,z} - A_{4y,z}]}{\pi}\ [-0.067 \sin(\omega t - 10.1°)\right.$$

$$- 0.33 \sin(3\omega t - 33.4°) + 0.28 \sin(5\omega t + 48.7°)$$

$$+ 0.14 \sin(7\omega t + 19°)]$$

$$+ \frac{2[A_{8x,z} - A_{8y,z}]}{\pi}\ [-0.029 \sin(\omega t - 10.1°)$$

$$- 0.087 \sin(3\omega t - 33.4°) - 0.155 \sin(5\omega t + 48.7°)$$

$$\left. + 0.36 \sin(7\omega t + 19°)]\right\}$$

$$D_3(t) = -\frac{2}{\pi}[(A_{4x,z} - A_{4y,z})(0.0431 \cos 2\omega t + 0.056 \sin 2\omega t)$$

$$+ (A_{8x,z} - A_{8y,z})(0.021 \cos 2\omega t + 0.0098 \sin 2\omega t)]$$

$$D_3(t) = -\frac{2}{\pi}[(A_{4x,z} - A_{4y,z})(0.07) \sin(2\omega t + 37.6°)$$

$$+ (A_{8x,z} - A_{8y,z})(0.023) \sin(2\omega t + 65°)]$$

A phase shift of +16.4 degrees occurs at 50 cps in the wideband amplifier filter. The phase sensitive demodulation reference is shifted by −16.4 degrees to compensate for this effect The equivalent operation can be made by subtracting −16.4 degrees from the phase of $D_3(t)$. Let $D_3'(t)$ be the expression corrected for the 16.4-degree phase shift:

$$D_3'(t) = -\frac{2}{\pi}[(A_{4x,z} - A_{4y,z})(0.07) \sin(2\omega t + 21.2°)$$

$$+ (A_{8x,z} - A_{8y,z})(0.023) \sin(2\omega t + 48.6)]$$

The effective error produced as a result of the time sharing is given by the expression V_e.

$$V_e = V[D_2' + D_3'] \cos \alpha$$

where

V = peak voltage output from the sensor at 4ω

α = effective phase angle of $[D_2' + D_3']$

The Z-axis is unaffected by the time sharing, because no decommutation is performed in the Z-axis electronics. (No error signals are produced in the commutation operation.) V_e is the error signal component in phase with the X, Y phase sensitive demodulators and is therefore the effective error component.

The error signal goes to zero for equal sweeps because of the difference terms in D_2' and D_3'. For a sweep unbalance of 10 percent, the computed unbalance is about 1 gamma, and the measured unbalance is about 2 gamma. The polarity of the unbalance agrees with the calculations, and the Z-axis is virtually unaffected.

C. Phase Shift Analysis

The Z signal and the X and Y signals are separated in the magnetometer electronics by the quadrature rejection characteristics of the synchronous demodulators. Theoretically then, the X and Y signals and the X and Y demodulator references are characterized by sin ωt, and the Z signal and the Z demodulator reference are characterized by cos ωt. Any shifts in the relative phases of these components will have a tendency to produce crosstalk and to change the loop gain. A two-axis system will be considered (X and Z) for the purposes of the analysis. The two-axis diagram is presented in Figure 4.

A system model will be devised to aid in computing the effects of phase shifts on crosstalk errors between the X-axis and the Z-axis. The crosstalk signal will be considered as a disturbing signal inserted in the control loop at the input to the operational amplifier.

$K_8 = K_2 K_3 K_4 K_5 K_5'$

$K_1 = 30 \times 10^{-6}$ volts/gamma — Sensor gain

$K_2 = 10$v/v — Preamplifier gain

$K_3 = 15$v/v — Wideband amplifier gain

$K_4 = 1$v/v — Notch filter at 50 cps

$K_5 = 50$v/v — Bandpass amplifier at 50 cps

$K_5' = 0.318$ — Demodulator attenuation

$K_6(5) = 1000/S1300 + 1$ — Operational amplifier

$K_7 = 60.6$ gamma/volt — Coil circuit constant

$K_5'' = \cos \alpha$

α = phase angle between demodulator reference and input signal

V_x = X magnetic field error at the sensor

V_z = Z magnetic field error at the sensor

$90-B$ = phase of E_x with respect to the Z demodulator reference

$90-A$ = phase of E_z with respect to the X demodulator reference

E_{ox} = X-axis output

E_{oz} = Z-axis output

The magnitude and effects of the disturbing signal will be computed from the block diagram in Figure 14. The disturbing signals, S_x and S_z, can be expressed

$$S_x = V_z K_1 K_8 \sin A$$

$$S_z = V_x K_1 K_8 \sin B .$$

The effects of the errors S_x and S_z on the output of the system are

$$\frac{E_{ox}}{S_x} = \frac{1}{K_1 K_8 K_5'' K_7}$$

and

$$\frac{E_{oz}}{S_z} = \frac{1}{K_1 K_8 K_5'' K_7} .$$

Rewriting the preceding expressions as a function of the input on the quadrature axis results in the following crosstalk expressions.

$$\frac{E_{ox}}{h_z} = \frac{\sin A\,[S(1300) + 1]}{(K_5'')^2\ 257 \times 10^3}$$

and

$$\frac{E_{oz}}{h_x} = \frac{\sin B[S(1300) + 1]}{(K_5'')^2\ 257 \times 10^3}$$

D. System Errors Resulting From DC Amplifier Drift

The equivalent input drift of the operational amplifier will produce an erroneous output. The false output, in terms of the equivalent input drift of the dc amplifier S_d, is given by

46

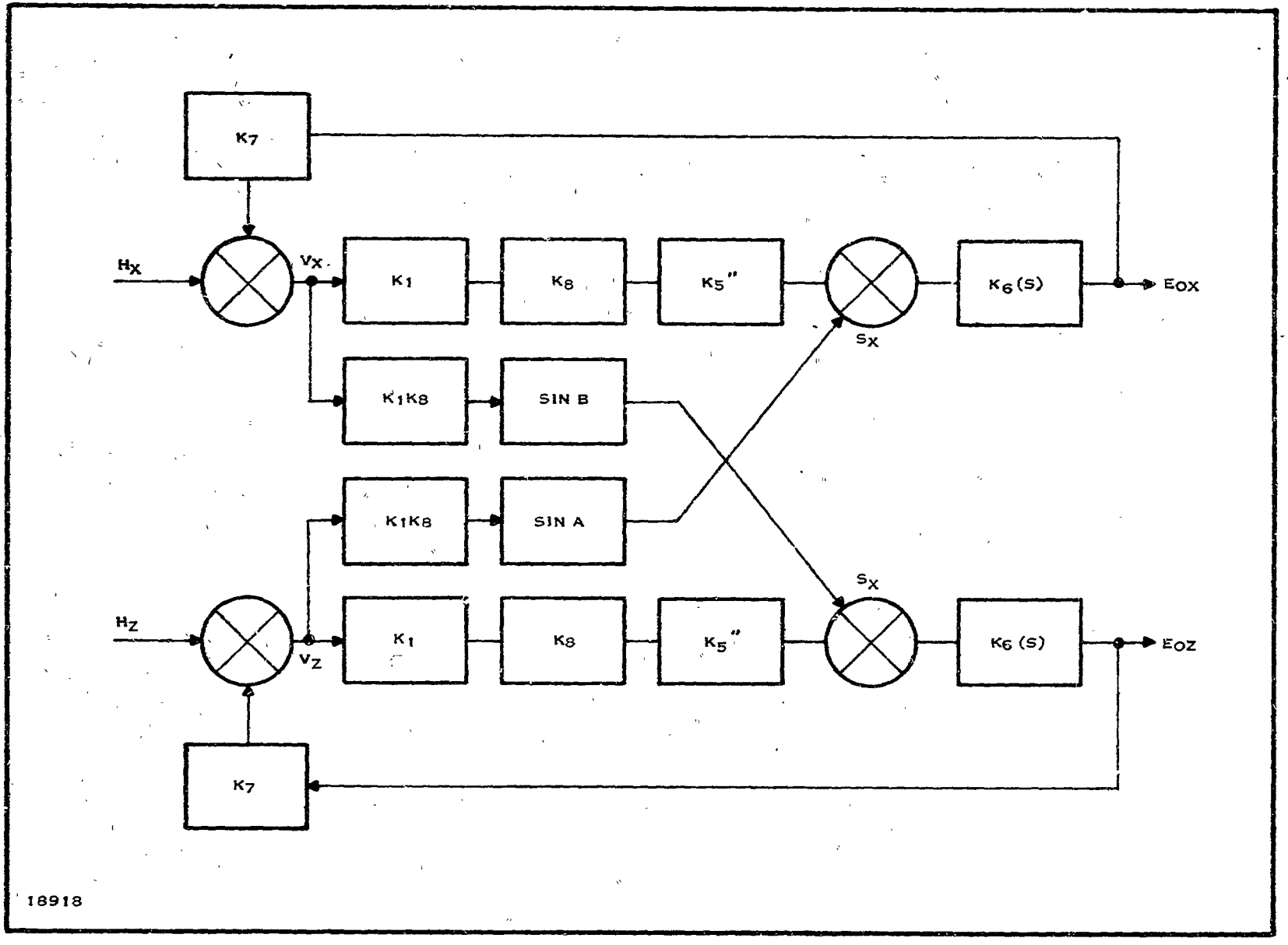

Figure 14. Two-Axis Model Illustrating Crosstalk Mechanism

$$\frac{E_o}{S_d} = \frac{1}{K_1 K_8 K_5 K_7}$$

or

$$\frac{E_o}{S_k} = 0.23 .$$

The typical drift of a dc amplifier over the operating temperature range is approximately 20 millivolts

E. Instrument Noise

The magnetometer is limited by the current generated in the PbS infrared detector used to detect the modulation on the light beam The noise is inserted in the system following the modulation process in the sensor After amplification and filtering, the noise is demodulated by a half-wave phase sensitive demodulator. Two segments of the noise spectrum will appear in the 0- to 0.5-cps passband of the magnetometer:

The spectrum-included 0.5 cps of the carrier frequency

The noise in the 0- to 0 5-cps spectral region.

The noise in the 0- to 0.5-cps bandpass is attenuated to a negligible value by the low frequency rolloff in the ac amplifiers. The remaining region of interest is centered at the carrier frequency of 50 cps. The detector characteristics can be measured by two techniques. (1) by narrow band filtering and (2) by synchronous demodulation and low pass filtering. The synchronous demodulation approach was used to check detectors because of the convenience and accuracy of the method.

A detector noise of approximately 7×10^{-6} volt peak in a 0- to 0 5-cps bandpass was measured with a phase demodulation test apparatus. This is equivalent to a noise level of approximately 0.25 gamma.

APPENDIX

DRAWINGS

Drawing No.	Title
484703	Magnetometer Sensor Outline Dimensions
456469	Igniter Sensor (33A1)
508352	Power Supply Helium Magnetometer (33A2)
456462	Diagram, Electronic Schematic Power Supply (33A2)
484777	Diagram, Electronic Schematic Helium Magnetometer, No 3, Step 1 (33A2)
484756	Diagram, Logic and Block, Helium Magnetometer
484775	Diagram, Electronic Schematic, Helium Magnetometer, No 1, Step 1 (33A3)
484752	Helium Magnetometer, No 1, Step 2 (33A3)
484776	Diagram, Electronic Schematic, Helium Magnetometer, No. 2, Step 1 (33A3)
484796	Helium Magnetometer, No 2, Step 2 (33A3)
456482	Diagram, Electronic Schematic, X- and Y-Axis Sweep Driver
456462	Diagram, Electronic Schematic, Wideband Amplifier Filter
484706	Diagram, Electronic Schematic, Wideband Amplifier
484710	Diagram, Electronic Schematic, Flip-Flop and Clock-Pulse Generator
484728	Diagram, Electronic Schematic, RF Exciter
484733	Diagram, Electronic Schematic, Bandpass Amplifier, Commutated
481736	Diagram, Electronic Schematic, Igniter Sensor
481740	Diagram, Electronic Schematic, Twin Tee Filter
484741	Diagram, Electronic Schematic, Sensor Preamplifier
484744	Diagram, Electronic Schematic, Demodulator, DC Amplifier and Output
484749	Diagram, Electronic Schematic, Oscillator, 50 CPS
484750	Diagram, Electronic Schematic, Bandpass Amplifier Noncommutated

Drawing No	Title
484757	Diagram, Electronic Schematic, Phase Shifter and Demodulator Driver
484772	Diagram, Electronic Schematic, Z-Axis Sweep
484782	Diagram, Electronic Schematic, Ignition Logic
484791	Diagram, Electronic Schematic, Feedback Filter

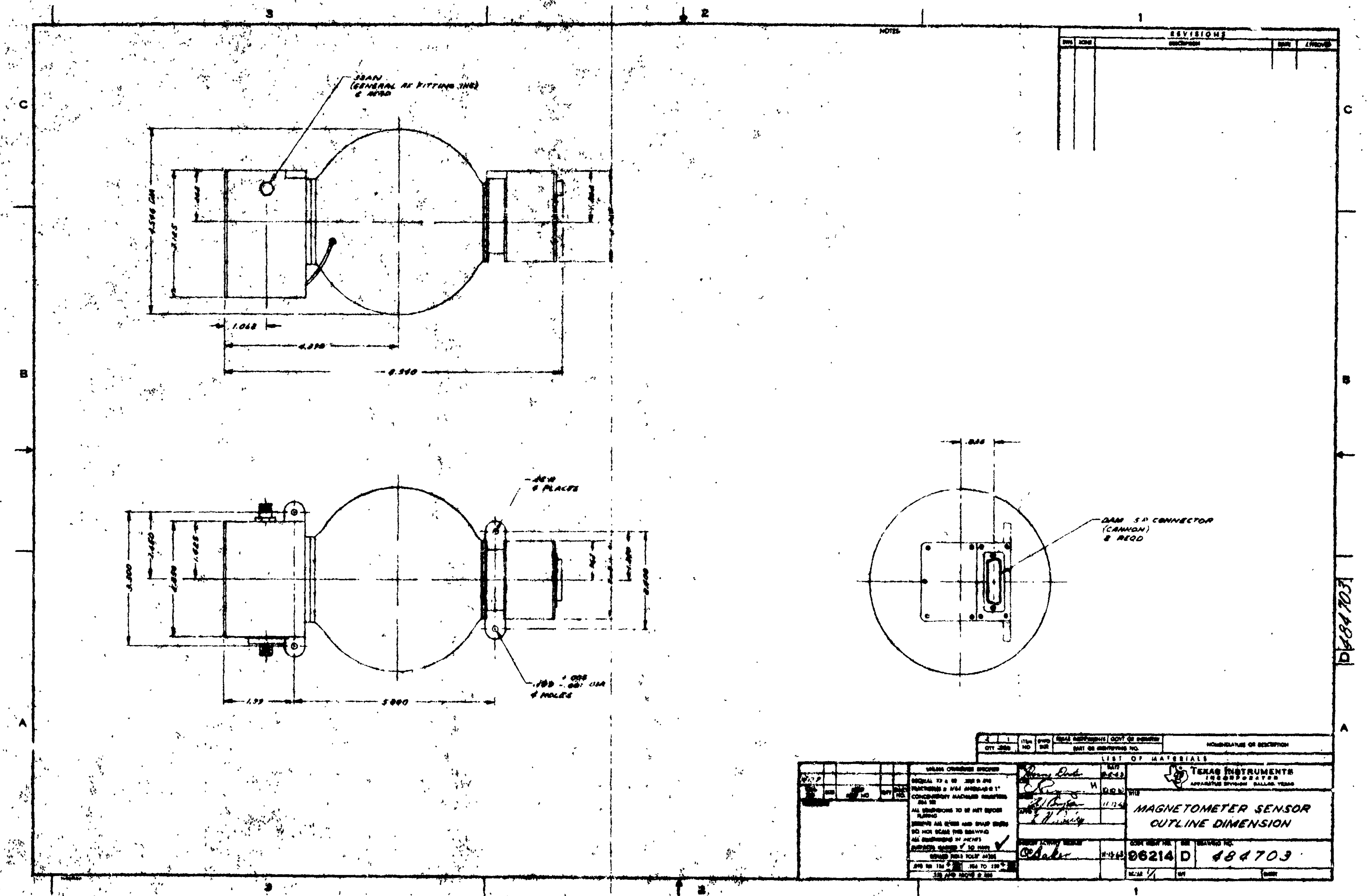

3
2
1
C
B
A
NOTES
REVISIONS
38AN
(GENERAL RF FITTING INC)
2 REQD
1.062
4.290
8.940
1.33
5.880
.169 4 HOLES
DAM 5P CONNECTOR
(CANNON)
2 REQD
LIST OF MATERIALS
NOMENCLATURE OR DESCRIPTION
DO NOT SCALE THIS DRAWING
ALL DIMENSIONS IN INCHES
TEXAS INSTRUMENTS
INCORPORATED
APPARATUS DIVISION DALLAS, TEXAS
MAGNETOMETER SENSOR
OUTLINE DIMENSION
06214
D
484703
D 484703

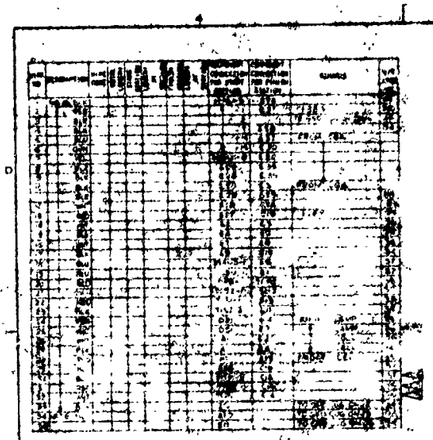

52

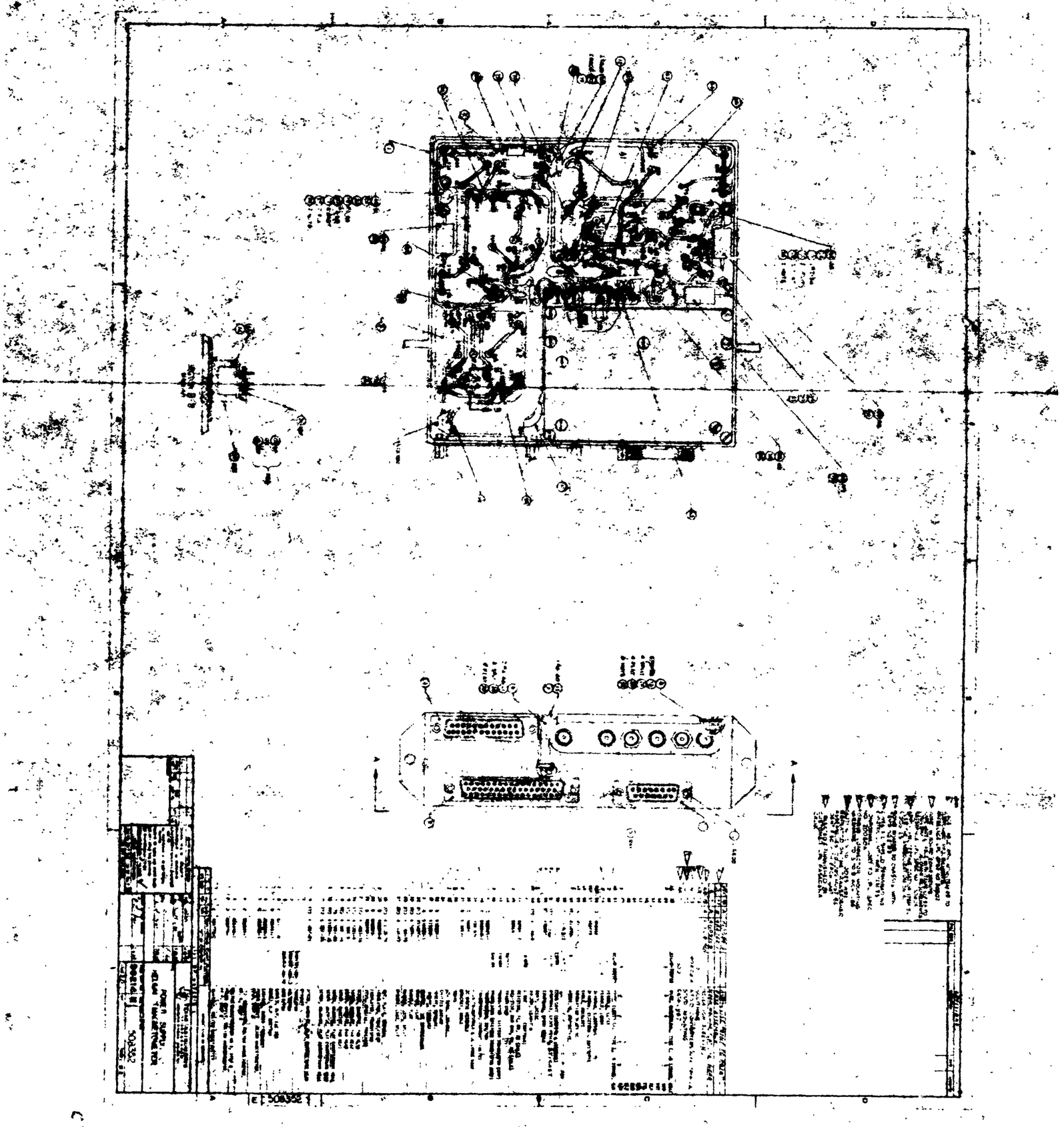

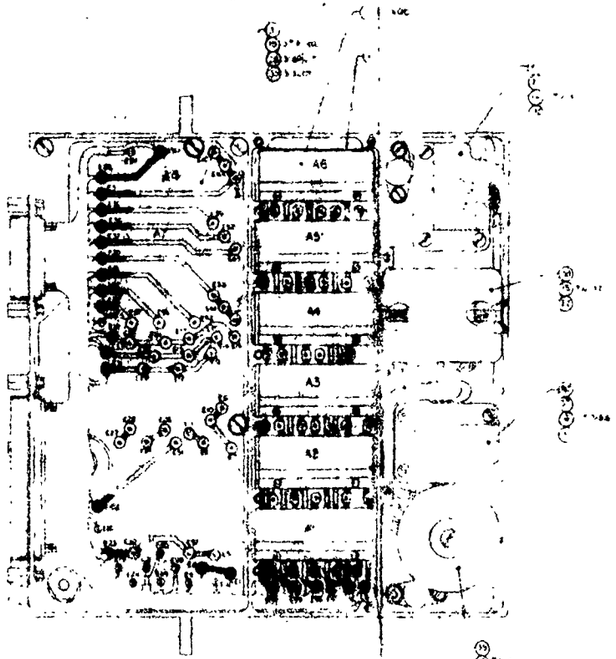

		TEXAS INSTRUMENTS INCORPORATED
		POWER SUPPLY, HELIUM MAGNETOMETER
		86214 E 508352

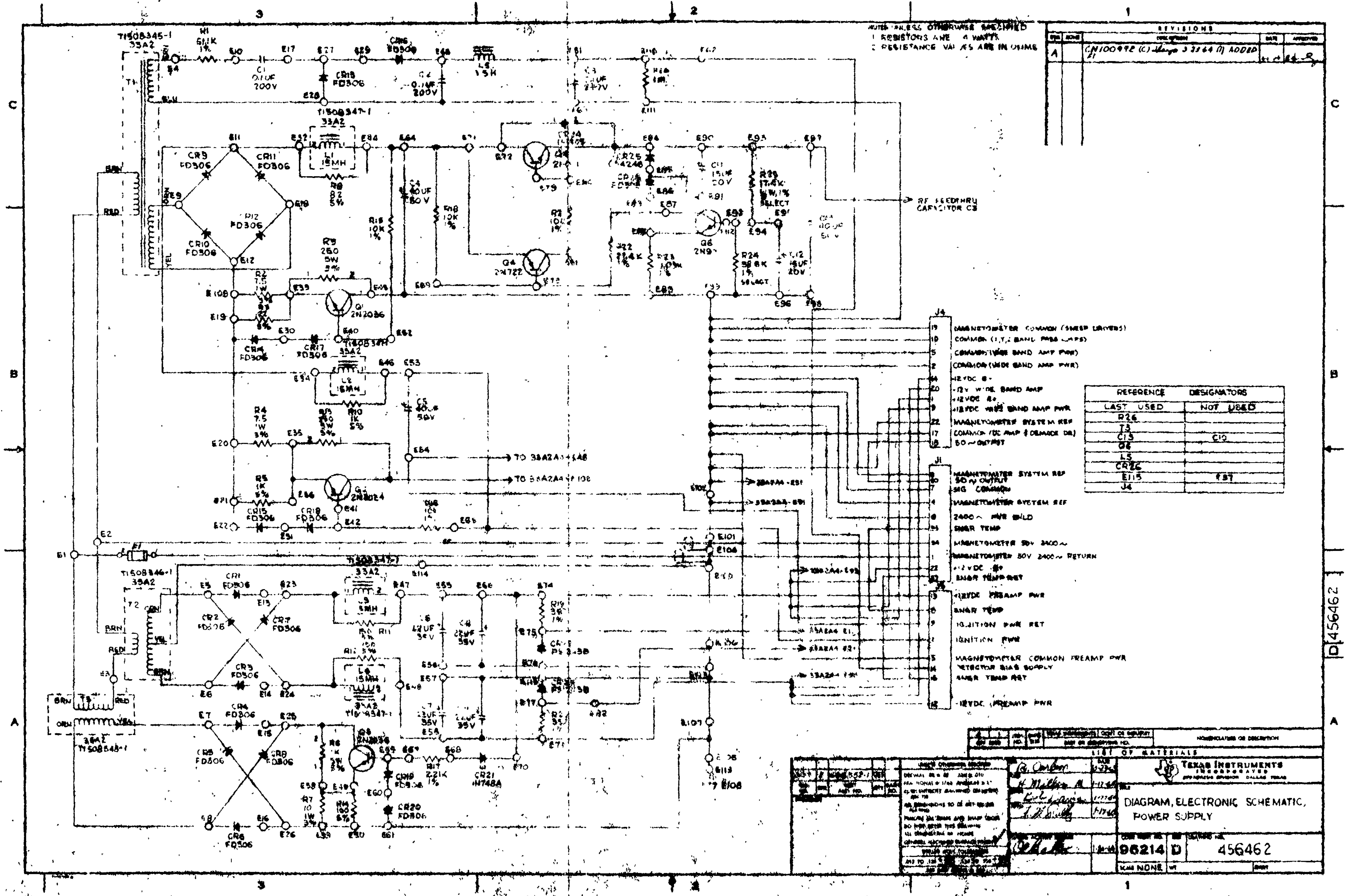
NOTES: UNLESS OTHERWISE SPECIFIED
1 RESISTORS ARE 1/4 WATTS
2 RESISTANCE VALUES ARE IN OHMS
REVISIONS
REFERENCE DESIGNATORS
LAST USED
NOT USED
R26
T3
C13
C10
Q6
L5
CR26
E115
E87
J4
J4
J1
RF FEEDTHRU CAPACITOR C3
TO 33A2A4-E48
TO 33A2A4-E108
MAGNETOMETER COMMON (SWEEP DRIVERS)
COMMON (I.T., BAND PASS AMPS)
COMMON (WIDE BAND AMP PWR)
COMMON (WIDE BAND AMP PWR)
+12VDC B+
-12V WIDE BAND AMP
+12VDC B+
+12VDC WIDE BAND AMP PWR
MAGNETOMETER SYSTEM REF
COMMON (DC AMP & DEMADE DR)
50 ~ OUTPUT
MAGNETOMETER SYSTEM REF
50 ~ OUTPUT
SIG COMMON
MAGNETOMETER SYSTEM REF
2400 ~ PWR SHLD
SNSR TEMP
MAGNETOMETER 50V 2400 ~
MAGNETOMETER 50V 2400 ~ RETURN
+12VDC B+
SNSR TEMP RET
+12VDC PREAMP PWR
SNSR TEMP
IGNITION PWR RET
IGNITION PWR
MAGNETOMETER COMMON PREAMP PWR
DETECTOR BIAS SUPPLY
SNSR TEMP RET
-12VDC PREAMP PWR
LIST OF MATERIALS
TEXAS INSTRUMENTS INCORPORATED
DIAGRAM, ELECTRONIC SCHEMATIC, POWER SUPPLY
96214
D
456462
SCALE NONE

D 456462

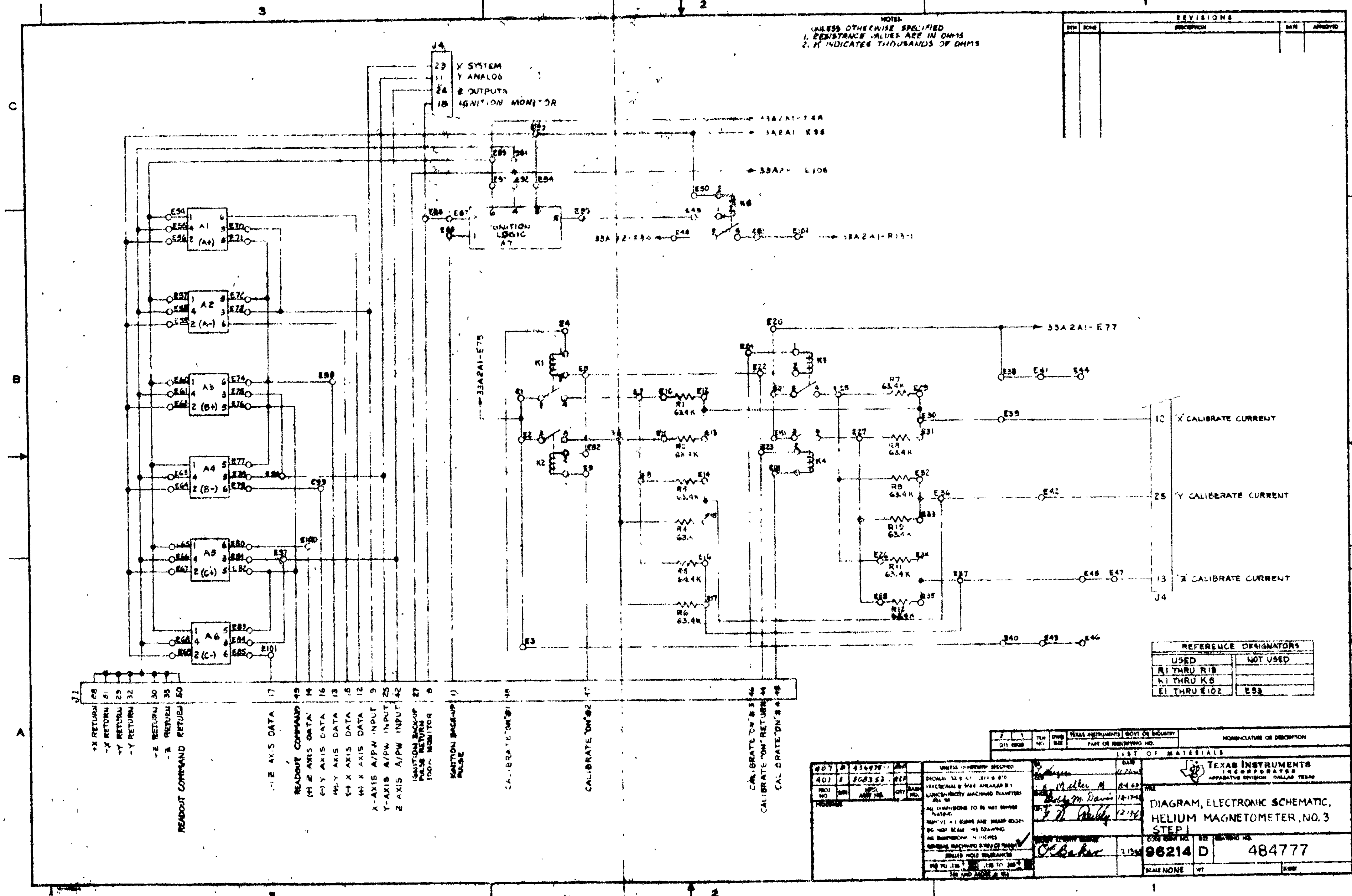
NOTES:
UNLESS OTHERWISE SPECIFIED
1. RESISTANCE VALUES ARE IN OHMS
2. K INDICATES THOUSANDS OF OHMS
REVISIONS
J4
X SYSTEM
Y ANALOG
Z OUTPUTS
IGNITION MONITOR
IGNITION LOGIC A7
33A2A1-E77
'X' CALIBRATE CURRENT
'Y' CALIBRATE CURRENT
'Z' CALIBRATE CURRENT
REFERENCE DESIGNATORS
USED
NOT USED
R1 THRU R18
K1 THRU K8
E1 THRU E102
E83
+X RETURN
-X RETURN
+Y RETURN
-Y RETURN
+Z RETURN
-Z RETURN
READOUT COMMAND RETURN
Z AXIS DATA
READOUT COMMAND
(+) Z AXIS DATA
(-) Y AXIS DATA
(+) Y AXIS DATA
(-) X AXIS DATA
(+) X AXIS DATA
X-AXIS A/PW INPUT
Y-AXIS A/PW INPUT
Z AXIS A/PW INPUT
IGNITION BACKUP PULSE RETURN
100% MONITOR
IGNITION BACK-UP PULSE
CALIBRATE "ON" #1
CALIBRATE "ON" #2
CALIBRATE "ON" #3
CALIBRATE "ON" RETURN
CALIBRATE "ON" #4
LIST OF MATERIALS
TEXAS INSTRUMENTS INCORPORATED
APPARATUS DIVISION DALLAS TEXAS
DIAGRAM, ELECTRONIC SCHEMATIC,
HELIUM MAGNETOMETER, NO. 3
STEP I
96214 D 484777
SCALE NONE
D 484777

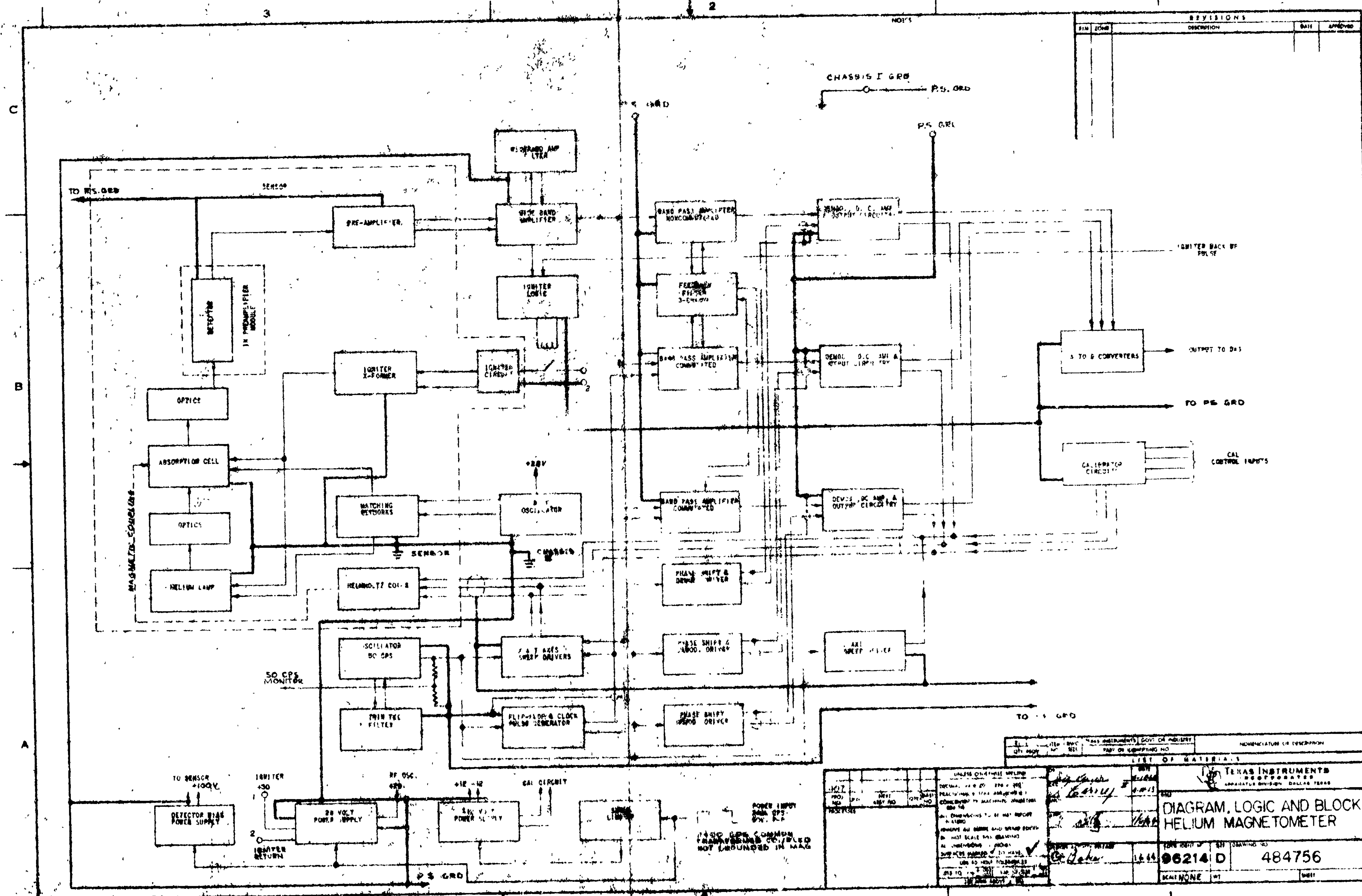

REVISIONS
CHASSIS I GRD
P.S. GRD
TO P.S. GRD
SENSOR
WIDEBAND AMP FILTER
PRE-AMPLIFIER
WIDE BAND AMPLIFIER
IGNITER LOGIC
DETECTOR
IN PHOTOMULTIPLIER MODULE
IGNITER X-FORMER
IGNITER CIRCUIT
OPTICS
ABSORPTION CELL
MAGNETIC SHIELDING
HELIUM LAMP
MATCHING NETWORKS
+28V
RF OSCILLATOR
SENSOR
CHASSIS
HELMHOLTZ COILS
OSCILLATOR 50 CPS
X, Y, Z AXES SWEEP DRIVERS
50 CPS MONITOR
TWIN TEE FILTER
FLIP-FLOP & CLOCK PULSE GENERATOR
BAND PASS AMPLIFIER NONCOMMUTATED
FEEDBACK FILTER 3-CHANNEL
BAND PASS AMPLIFIER COMMUTATED
PHASE SHIFT & DEMOD. DRIVER
PHASE SHIFT & DEMOD. DRIVER
PHASE SHIFT DEMOD DRIVER
DEMOD., D.C. AMP & OUTPUT CIRCUITRY
IGNITER BACK UP PULSE
A TO D CONVERTERS
OUTPUT TO DAS
TO PS GRD
CALIBRATOR CIRCUITRY
CAL CONTROL INPUTS
TO PS GRD
TO SENSOR +100V
DETECTOR BIAS POWER SUPPLY
IGNITER +30
28 VOLT POWER SUPPLY
IGNITER RETURN
RF OSC. +28
+12 -12
POWER SUPPLY
CAL CIRCUIT
POWER INPUT
1400 CPS COMMON TRANSFORMER COUPLED NOT GROUNDED IN MAG
P S GRD
LIST OF MATERIALS
TEXAS INSTRUMENTS INCORPORATED
APPARATUS DIVISION DALLAS TEXAS
DIAGRAM, LOGIC AND BLOCK, HELIUM MAGNETOMETER
96214 D 484756
SCALE NONE
D 484756

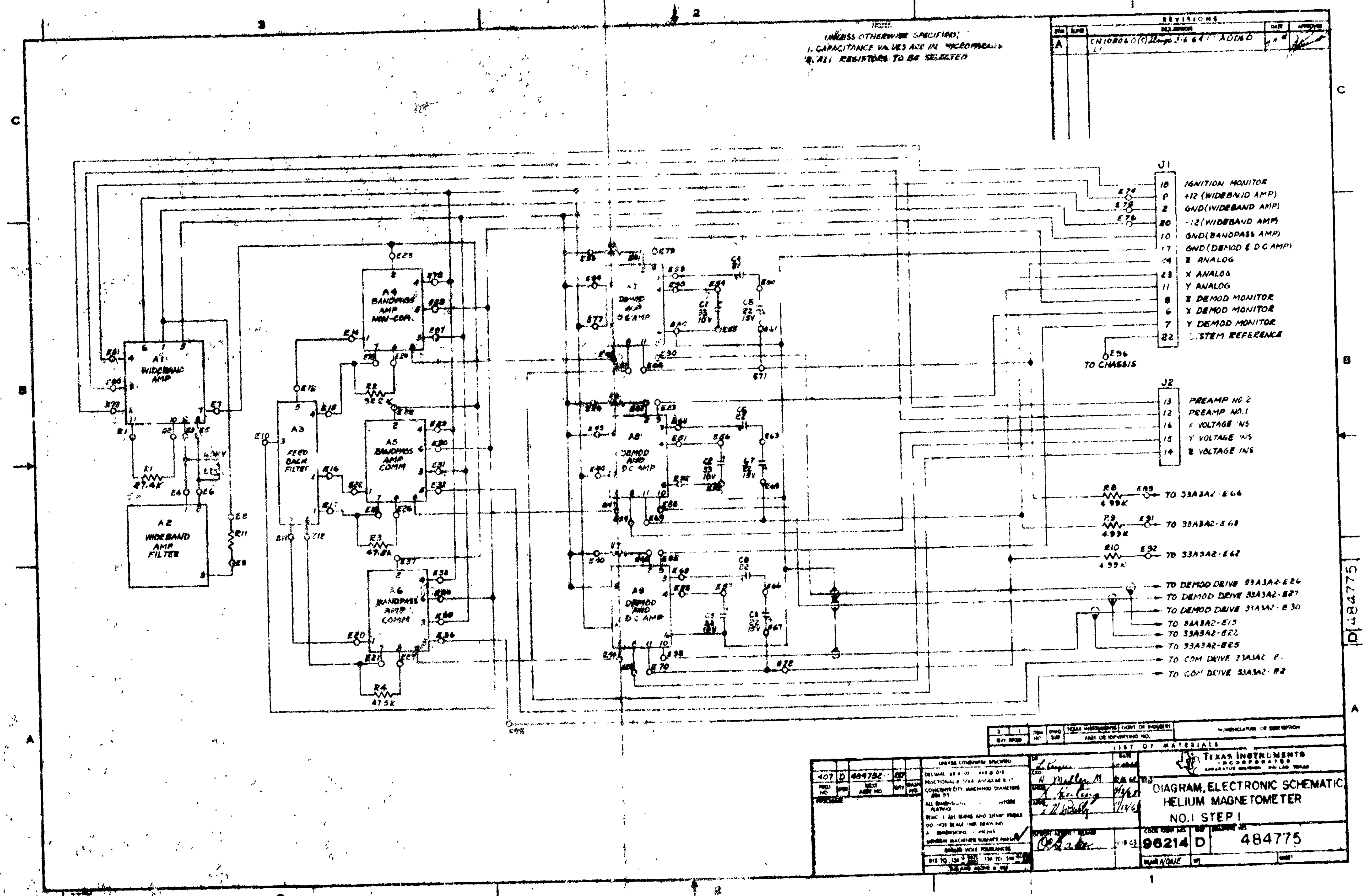
UNLESS OTHERWISE SPECIFIED:
1. CAPACITANCE VALUES ARE IN MICROFARADS
2. ALL RESISTORS TO BE SELECTED
REVISIONS
A1 WIDEBAND AMP
A2 WIDEBAND AMP FILTER
A3 FEED BACK FILTER
A4 BANDPASS AMP NON-COM.
A5 BANDPASS AMP COMM
A6 BANDPASS AMP COMM
A7 DEMOD AND DC AMP
A8 DEMOD AND DC AMP
A9 DEMOD AND DC AMP
J1
IGNITION MONITOR
+12 (WIDEBAND AMP)
GND (WIDEBAND AMP)
-12 (WIDEBAND AMP)
GND (BANDPASS AMP)
GND (DEMOD & DC AMP)
Z ANALOG
X ANALOG
Y ANALOG
Z DEMOD MONITOR
X DEMOD MONITOR
Y DEMOD MONITOR
SYSTEM REFERENCE
TO CHASSIS
J2
PREAMP NO 2
PREAMP NO.1
X VOLTAGE INS
Y VOLTAGE INS
Z VOLTAGE INS
TO 33A3A2-E66
TO 33A3A2-E63
TO 33A3A2-E62
TO DEMOD DRIVE 33A3A2-E26
TO DEMOD DRIVE 33A3A2-E27
TO DEMOD DRIVE 33A3A2-E30
TO 33A3A2-E15
TO 33A3A2-E22
TO 33A3A2-E25
TO COM DRIVE 33A3A2
TO COM DRIVE 33A3A2-E8
TEXAS INSTRUMENTS INCORPORATED
DIAGRAM, ELECTRONIC SCHEMATIC HELIUM MAGNETOMETER NO.1 STEP I
96214 D 484775
D484775

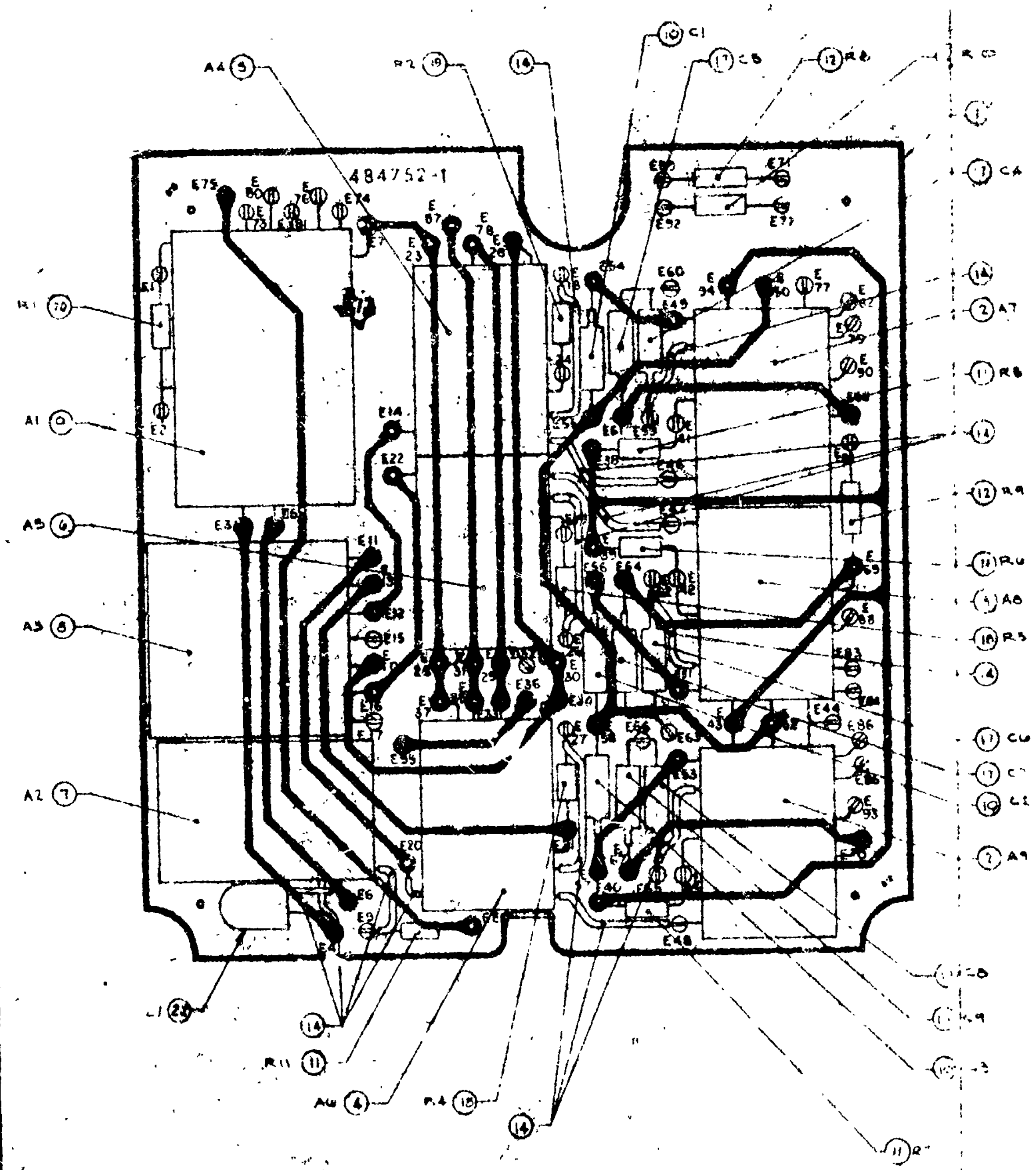

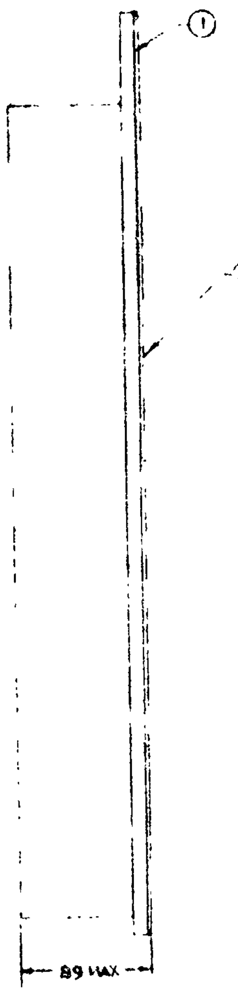

NOTES
1 COMPONENT LEAD BENDS RADII .12 MIN
2 VALUES TO BE SELECTED
3 TERMINAL NUMBERS ARE FOR REF ONLY
4 SECURE ITEM 16 ITEM 21 WITH ITEM 16 TRIM ITEM 21 TO BOARD CONFIGURATION

REVISIONS				
LTR	ZONE	DESCRIPTION	DATE	APPROVED
A		CN 108055 (CH) [illegible] 3-9-64 (1) ADDED ITEM 22 (2) CORRECTED ITEM 7 PICTORIALLY (3) ADDED ITEM 14 TO ITEM 22	[illegible]	[illegible]

QTY REQD	ITEM NO	DWG SIZE	TEXAS INSTRUMENTS PART OR IDENTIFYING NO	GOV'T OR INDUSTRY PART OR IDENTIFYING NO	NOMENCLATURE OR DESCRIPTION
1	22			UTC-M110	CHOKE, AUDIO (UTC CO)
AR	21	STD	411324-56		PLASTIC SHEET
1	20	A	413381-147		RESISTOR, FIXED, 1/8W 27.4K
1	19	A	413387-109		RESISTOR, FIXED, 1/8W 82.5K
2	18	A	413387-145		RESISTOR, FIXED, 1/8 W, 47.5K
2	17	STD	419054-226		CAPACITOR FIXED 22 UF 10V
AR	16	STD	411980-1		COMPOUND, EPOXY
REF	15	D	484775		DIAGRAM, ELECTRONIC SCHEMATIC
AR	14	STD	410499-609		INSULATION SLEEVING, ELECTRICAL
AR	13		411140-3		SOLDER, LEAD TIN ALLOY
3	12				RESISTOR FIXED [illegible] CEA
4	11				RESISTOR, FIXED
3	10	STD	419054-336		CAPACITOR FIXED 33UF 10V
	9	D	484709-1		WIDE BAND AMPLIFIER
	8	D	484794-1		FEED BACK FILTER
1	7	D	484798		WIDE BAND AMPL FILTER
	6	D	484735-1		BANDPASS AMPL, COMMUTATED
	5	D	484748-1		BANDPASS AMPL, NONCOMMUTATED
	4	D	484735-2		BANDPASS AMPL, COMMUTATED
1	3	D	484746-2		DEMODULATOR & DC AMPL OUTPUT CKT
2	2	D	484746-1		DEMODULATOR & DC AMPL OUTPUT CKT
1	1	D	484751-2		PRINTED CIRCUIT BOARD

LIST OF MATERIALS

FINSH NO	QTY	NEXT ASSY NO	QTY	DASH NO
407		50R349	1	1

APPLICATION

UNLESS OTHERWISE SPECIFIED
DECIMAL [illegible]
FRACTIONAL [illegible] ANGULAR [illegible]
CONCENTRICITY MACHINED DIAMETERS [illegible]
ALL DIMENSIONS TO BE MET BEFORE PLATING
REMOVE ALL BURRS AND SHARP EDGES
DO NOT SCALE THIS DRAWING
ALL DIMENSIONS IN INCHES
SURFACES MARKED ✓ TO HAVE ✓
DRILLED HOLE TOLERANCES
[illegible]
.250 AND ABOVE [illegible]

DR [signature] DATE 10-10-63
CHK [signature]
PROJ [signature]
APPD [signature]
DESIGN ACTIVITY RELEASE [signature] 11-4-63

TEXAS INSTRUMENTS INCORPORATED
APPARATUS DIVISION DALLAS TEXAS

TITLE
HELIUM MAGNETOMETER, NO 1, STEP 2

CODE IDENT NO 96214 SIZE D DRAWING NO 484752
SCALE 2/1 WT SHEET

D 484752

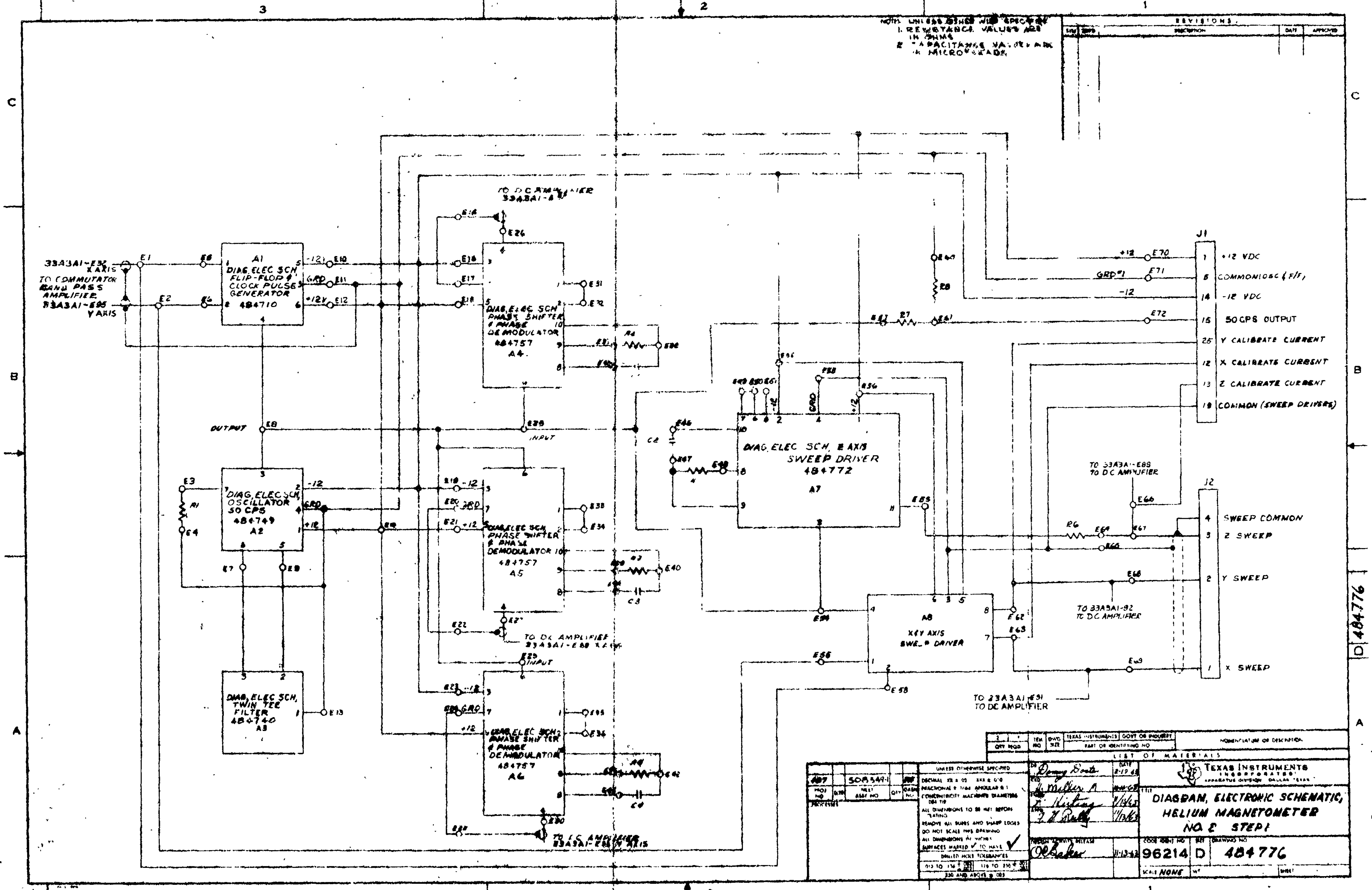

NOTES: UNLESS OTHERWISE SPECIFIED
1. RESISTANCE VALUES ARE IN OHMS
2. CAPACITANCE VALUES ARE IN MICROFARADS
REVISIONS
33A3A1-E32 X AXIS
TO COMMUTATOR BAND PASS AMPLIFIER
33A3A1-E95 Y AXIS
A1 DIAG. ELEC SCH. FLIP-FLOP & CLOCK PULSE GENERATOR 484710
DIAG. ELEC SCH. OSCILLATOR 50 CPS 484749 A2
DIAG. ELEC SCH. TWIN TEE FILTER 484740 A3
DIAG. ELEC SCH. PHASE SHIFTER & PHASE DEMODULATOR 484757 A4
DIAG. ELEC SCH. PHASE SHIFTER & PHASE DEMODULATOR 484757 A5
DIAG. ELEC SCH. PHASE SHIFTER & PHASE DEMODULATOR 484757 A6
DIAG. ELEC SCH. Z AXIS SWEEP DRIVER 484772 A7
A8 X & Y AXIS SWEEP DRIVER
OUTPUT
INPUT
TO DC AMPLIFIER 33A3A1-E
TO DC AMPLIFIER 33A3A1-E88 X AXIS
TO DC AMPLIFIER 33A3A1-E87 Y AXIS
TO 33A3A1-E85 TO DC AMPLIFIER
TO 33A3A1-92 TO DC AMPLIFIER
TO 33A3A1-E51 TO DC AMPLIFIER
J1
+12 VDC
COMMON DC (F/F)
-12 VDC
50 CPS OUTPUT
Y CALIBRATE CURRENT
X CALIBRATE CURRENT
Z CALIBRATE CURRENT
COMMON (SWEEP DRIVERS)
J2
SWEEP COMMON
Z SWEEP
Y SWEEP
X SWEEP
LIST OF MATERIALS
TEXAS INSTRUMENTS INCORPORATED APPARATUS DIVISION DALLAS TEXAS
DIAGRAM, ELECTRONIC SCHEMATIC, HELIUM MAGNETOMETER NO. 2 STEP 1
96214 D 484776
SCALE NONE

NOTES:
1. COMPONENT LEAD BEND RADIUS (.17 MIN)
2. VALUES TO BE SELECTED
3. SECURE ITEM 1 & ITEM 18 WITH ITEM 17 TRIM ITEM 18 TO BOARD CONFIGURATION
4. TERMINAL NUMBERS ARE FOR REFERENCE ONLY

REVISIONS				
SYM	ZONE	DESCRIPTION	DATE	APPROVED

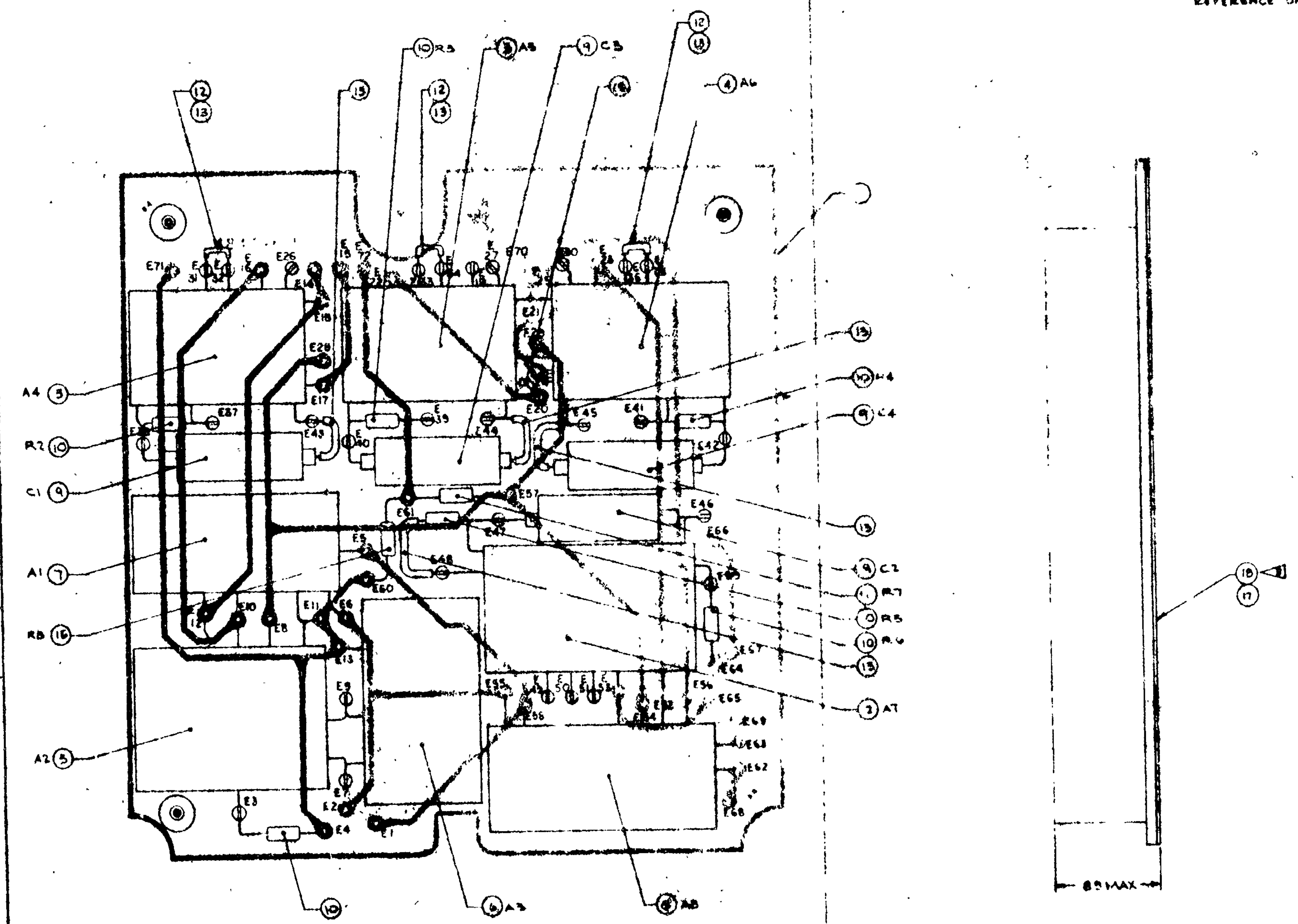

QTY REQD		ITEM NO	DWG SIZE	TEXAS INSTRUMENTS PART OR IDENTIFYING NO	GOVT OR INDUSTRY PART OR IDENTIFYING NO	NOMENCLATURE OR DESCRIPTION
AR		18	STD	411329-08		PLASTIC SHEET
AR		17	STD	415980-1		COMPOUND EPOXY
1		16	A	413387-9		RESISTOR, FIXED 1/8W 2.55K
REF		15	D	484776		DIAGRAM, ELECT, SCHEMATIC
AR		14	STD	411140-3		SOLDER, LEAD-TIN, ALLOY
AR		13		410499-609		INSULATION SLEEVING, ELECTRICAL
AR		12		411490-24		WIRE, ELECTRICAL
1		11	STD	416448-300		RESISTOR, FIXED 1/8W 100K
6		10	A	413387-80		RESISTOR, FIXED
4		9			EG1-4740-16	CAPACITOR, FIXED ELECTRON PRODUCTS ATUR EPOXY
1		8	D	456484-1		X & Y AXIS SWEEP DRIVER
1		7		484715-1		FLIP-FLOP & CLOCK PULSE GEN
1		6		484759-1		TWIN TEE FILTER
1		5		484754-1		50 CPS OSCILLATOR
1		4		484789-2		PHASE SHIFTER & DEMOD DRIVER
2		3		484789-1		PHASE SHIFTER & DEMOD DRIVER
1		2		484774-1		Z AXIS SWEEP DRIVER
1		1	D	484798-1		PRINTED CIRCUIT BOARD
-7	-1					

LIST OF MATERIALS

PROJ NO	SIZE	NEXT ASSY NO	QTY	DASH NO
401	E	508349-1	1	1

REVISIONS

UNLESS OTHERWISE SPECIFIED
DECIMAL .XX ± .02 .XXX ± .010
FRACTIONAL ± 1/64 ANGULAR ± 1°
CONCENTRICITY MACHINED DIAMETERS .005 TIR
ALL DIMENSIONS TO BE MET BEFORE FINISHING
REMOVE ALL BURRS AND SHARP EDGES
DO NOT SCALE THIS DRAWING
ALL DIMENSIONS IN INCHES
SURFACES MARKED ✓ TO HAVE ✓
DRILLED HOLE TOLERANCES
.013 TO .125 +.003 -.001 | .126 TO .750 +.004 -.001
.751 AND ABOVE ± .005

DR [signature] DATE 10-10-63
CHK [signature]
ENGR [signature] 11/1/63
APPD [signature]
DESIGN ACTIVITY RELEASE [signature] 11/4/63

TEXAS INSTRUMENTS INCORPORATED
APPARATUS DIVISION DALLAS TEXAS

TITLE: HELIUM MAGNETOMETER, NO 2 STEP 2

CODE IDENT NO	SIZE	DRAWING NO
96214	D	484796

SCALE 2/1 | WT | SHEET

D 484796

NOTES: UNLESS OTHERWISE SPECIFIED
1. RESISTANCE VALUES ARE IN OHMS
2. K INDICATES THOUSANDS OF OHMS
3. ALL RESISTORS ARE 1/8 W
4. CAPACITANCE VALUES ARE IN MICROFARADS
5. PARTIAL REFERENCE DESIGNATIONS ARE SHOWN FOR COMPLETE DESIGNATION PREFIX WITH THE UNIT NUMBER OR ASSEMBLY DESIGNATION(S)

REVISIONS				
SYM	ZONE	DESCRIPTION	DATE	APPROVED

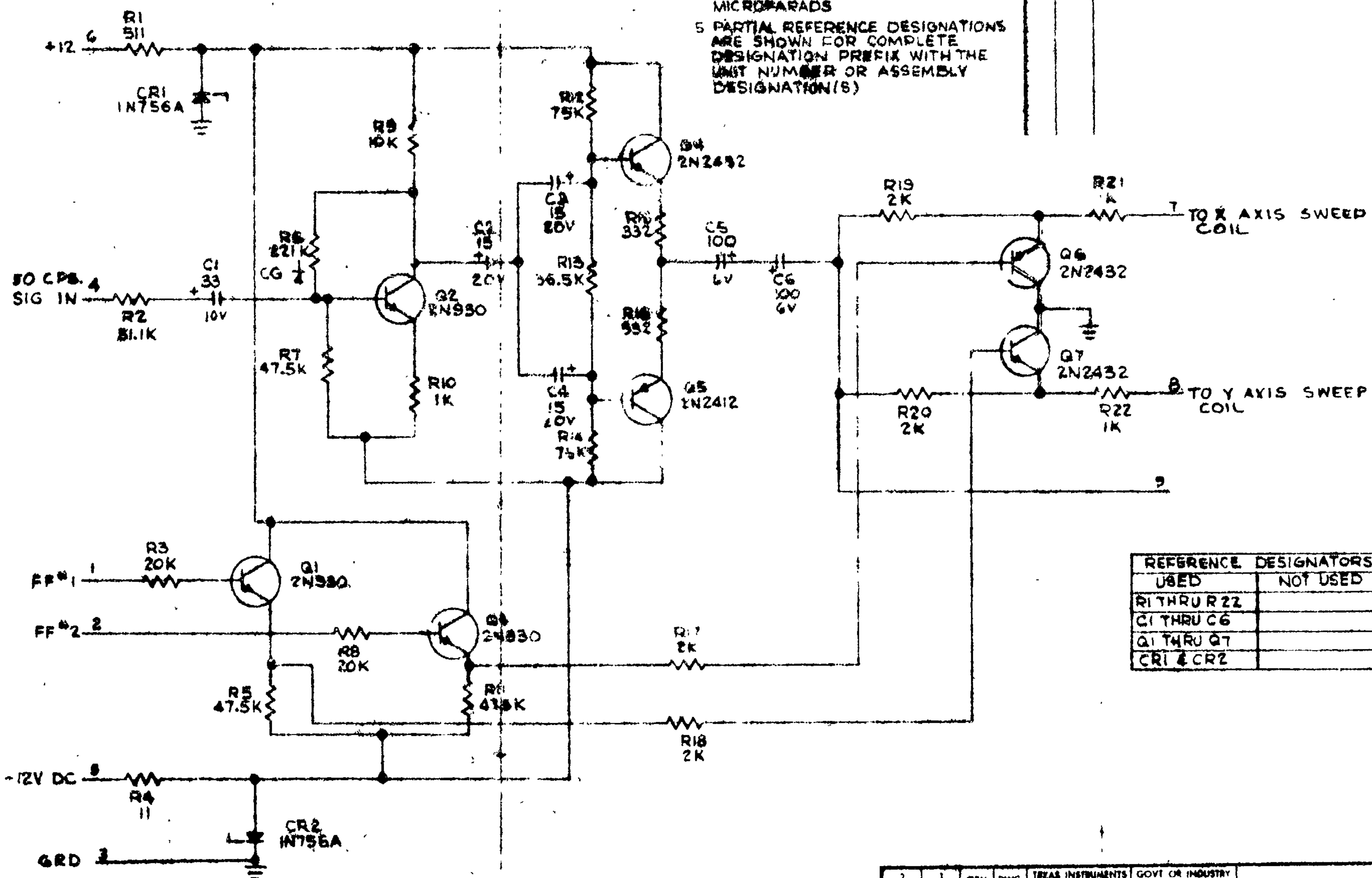

REFERENCE DESIGNATORS	
USED	NOT USED
R1 THRU R22	
C1 THRU C6	
Q1 THRU Q7	
CR1 & CR2	

2	1	ITEM NO	DWG SIZE	TEXAS INSTRUMENTS / GOVT OR INDUSTRY PART OR IDENTIFYING NO.	NOMENCLATURE OR DESCRIPTION
QTY REQD					

LIST OF MATERIALS

USED ON	SIZE	NEXT ASSY NO	QTY	DASH NO.
407	D	456484-1	REF	

UNLESS OTHERWISE SPECIFIED
DECIMAL .XX ± .02 .XXX ± .010
FRACTIONAL ± 1/64 ANGULAR ± 1°
CONCENTRICITY MACHINED DIAMETERS .004 TIR
ALL DIMENSIONS TO BE MET BEFORE PLATING
REMOVE ALL BURRS AND SHARP EDGES
DO NOT SCALE THIS DRAWING
ALL DIMENSIONS IN INCHES
SURFACES MARKED ✓ TO HAVE ✓
DRILLED HOLE TOLERANCES
.013 TO .125 +.003/-.001 .126 TO .250 +.004/-.001
.250 AND ABOVE ± .005

DR B. Carlson 9-16-63
CKD A. Miller II 9-26-63
ENGR L. Hutting 11/29/63
APPD F. N. Reilly 11/29/63
DESIGN ACTIVITY RELEASE O. Baker 11-29-63

TEXAS INSTRUMENTS INCORPORATED
APPARATUS DIVISION DALLAS TEXAS

TITLE
DIAGRAM, ELECTRONIC SCHEMATIC, X & Y AXIS SWEEP DRIVER

CODE IDENT NO. 96214 | SIZE C | DRAWING NO. 456482
SCALE NONE | WT | SHEET

C 456482

62

B 456464

NOTES:
1. REFERENCE DESIGNATIONS ARE ABBREVIATED. PREFIX WITH UNIT OR ASSEMBLY DESIGNATION OR BOTH
2. CAPACITANCE VALUES ARE IN MICROFARADS
3. VALUES TO BE SELECTED

REVISIONS				
SYM	ZONE	DESCRIPTION	DATE	APPROVED
A		CN100977 (C) 3-6-64 (1) REMOVED L1, 60NY BETWEEN INPUT 1 & OUTPUT 2		

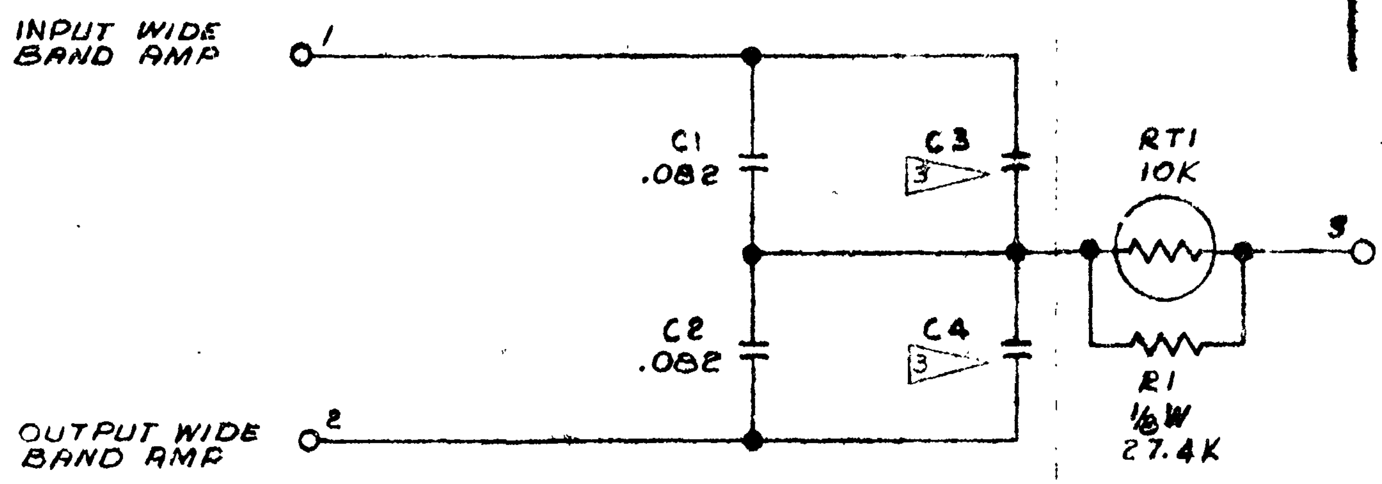

-2	-1	ITEM NO	DWG SIZE	TEXAS INSTRUMENTS PART OR IDENTIFYING NO	GOVT OR INDUSTRY	NOMENCLATURE OR DESCRIPTION
QTY REQD						

LIST OF MATERIALS

PROJ NO.	SIZE	NEXT ASSY NO.	QTY	DASH NO.
407	D	484798-1	REF	

PROCESSES

UNLESS OTHERWISE SPECIFIED
DECIMAL .XX ± .02 .XXX ± .010
FRACTIONAL ± 1/64 ANGULAR ± 1°
CONCENTRICITY MACHINED DIAMETERS .004 TIR
ALL DIMENSIONS TO BE MET BEFORE PLATING
REMOVE ALL BURRS AND SHARP EDGES
DO NOT SCALE THIS DRAWING
ALL DIMENSIONS IN INCHES
SURFACES MARKED ✓ TO HAVE ✓
DRILLED HOLE TOLERANCES
.013 TO .136 +.003/−.002 .136 TO .250 +.004/−.002
.250 AND ABOVE ± .005

		DATE
DR		3-27-63
CKD		
ENGR		10/3/63
APPD		11/1/63
DESIGN ACTIVITY RELEASE		11-1-63

TEXAS INSTRUMENTS INCORPORATED
APPARATUS DIVISION DALLAS, TEXAS

TITLE
DIAGRAM, ELECTRONIC SCHEMATIC, WIDE BAND AMPLIFIER FILTER

CODE IDENT NO	SIZE	DRAWING NO.
96214	B	456464

SCALE NONE WT SHEET

NOTES: UNLESS OTHERWISE SPECIFIED:
1. ALL TRANSISTORS ARE 2N930
2. ALL CAPACITORS .5 UF @ 20V
3. ALL CAPACITANCE VALUES ARE IN MICROFARADS
4. RESISTANCE VALUES ARE IN OHMS
5. ALL RESISTORS ARE 1/8W
6. UF INDICATES MICROFARADS.

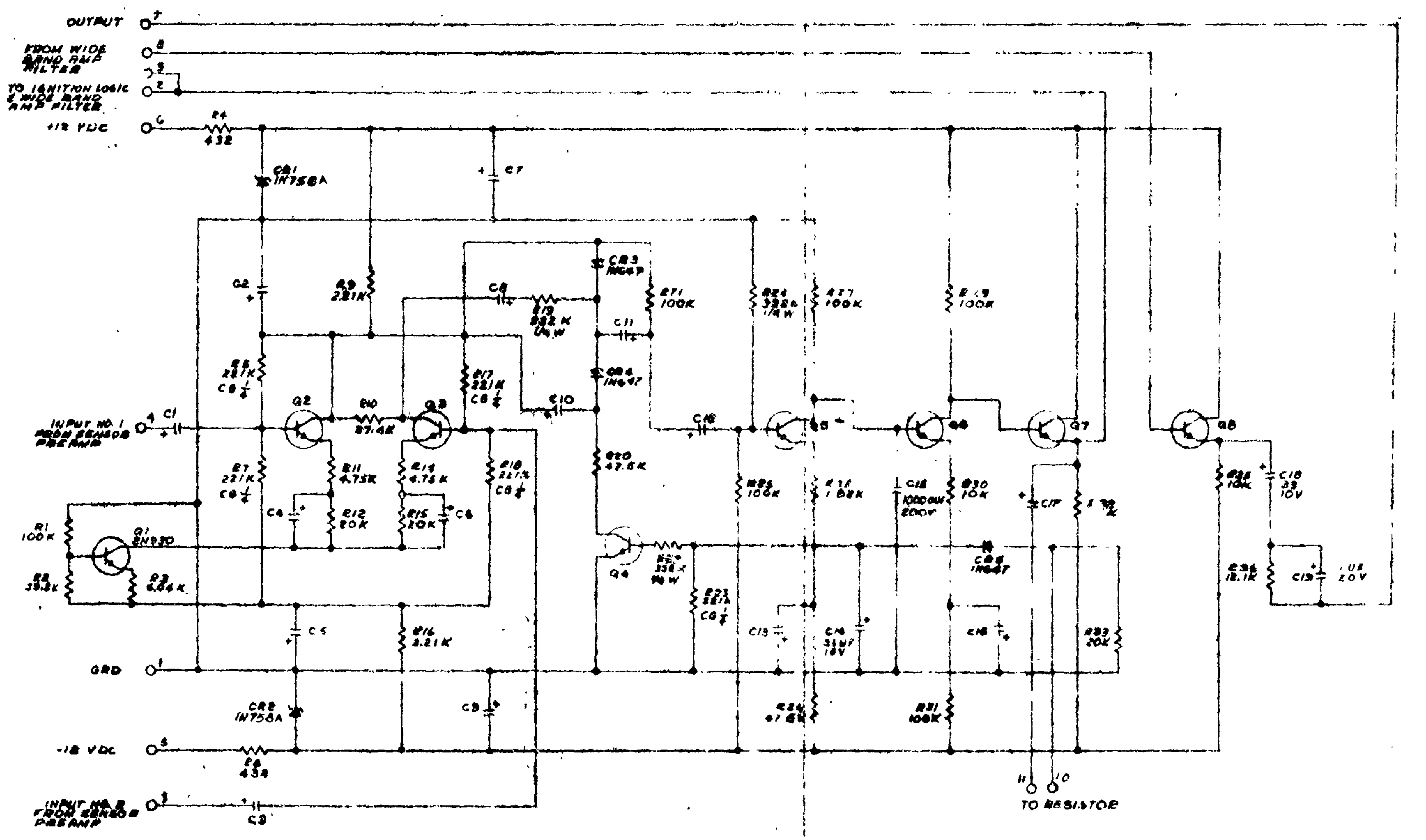

OUTPUT
FROM WIDE BAND AMP FILTER
TO IGNITION LOGIC & WIDE BAND AMP FILTER
+12 VDC
R4 432
CR1 1N758A
C7
Q2
R9 2.21K
C8
R13 332K 1/4W
CR3 1N647
R71 100K
C11
R24 332K 1/4W
R27 100K
R29 100K
R5 221K
C8 1/4
R10 27.4K
R17 221K
C10
CR4 1N647
INPUT NO. 1 FROM SENSOR PREAMP
C1
Q3
C16
Q5
Q6
Q7
Q8
R7 221K
R11 4.75K
R14 4.75K
R18 221K
C4
R12 20K
R15 20K
C6
R20 47.5K
R25 100K
R31 1.82K
C18 1000UF 20V
R30 10K
C17
R35 10K
C18 35 10V
R1 100K
Q1 2N930
R2 39.2K
R3 6.04K
Q4
CR5 1N647
R22 221K
C13
C14 35UF 16V
C15
R33 20K
R36 12.1K
C19 1UF 20V
C5
R16 3.21K
GRD
CR2 1N758A
C9
R26 47.5K
R31 100K
-12 VDC
R6 432
TO RESISTOR
INPUT NO. 2 FROM SENSOR PREAMP
C3

REFERENCE DESIGNATORS	
USED	NOT USED
R1 THRU R36	R2, R19, C36
C1 THRU C19	
CR1 THRU CR5	
Q1 THRU Q8	
R71	

LIST OF MATERIALS

407 | 484709 1 | NEXT ASSY NO. | USED ON

UNLESS OTHERWISE SPECIFIED

TEXAS INSTRUMENTS INCORPORATED
APPARATUS DIVISION DALLAS TEXAS

DIAGRAM, ELECTRONIC SCHEMATIC, WIDE BAND AMPLIFIER

96214 D 484706

SCALE NONE

64

NOTES: UNLESS OTHERWISE SPECIFIED
1. RESISTANCE VALUES ARE IN OHMS
2. ALL RESISTORS ARE 1/8 WATT, ± 1%
3. CAPACITANCE VALUES ARE IN MICROMICROFARADS
4. K INDICATES THOUSANDS OF OHMS

REVISIONS

SYM	ZONE	DESCRIPTION	DATE	APPROVED

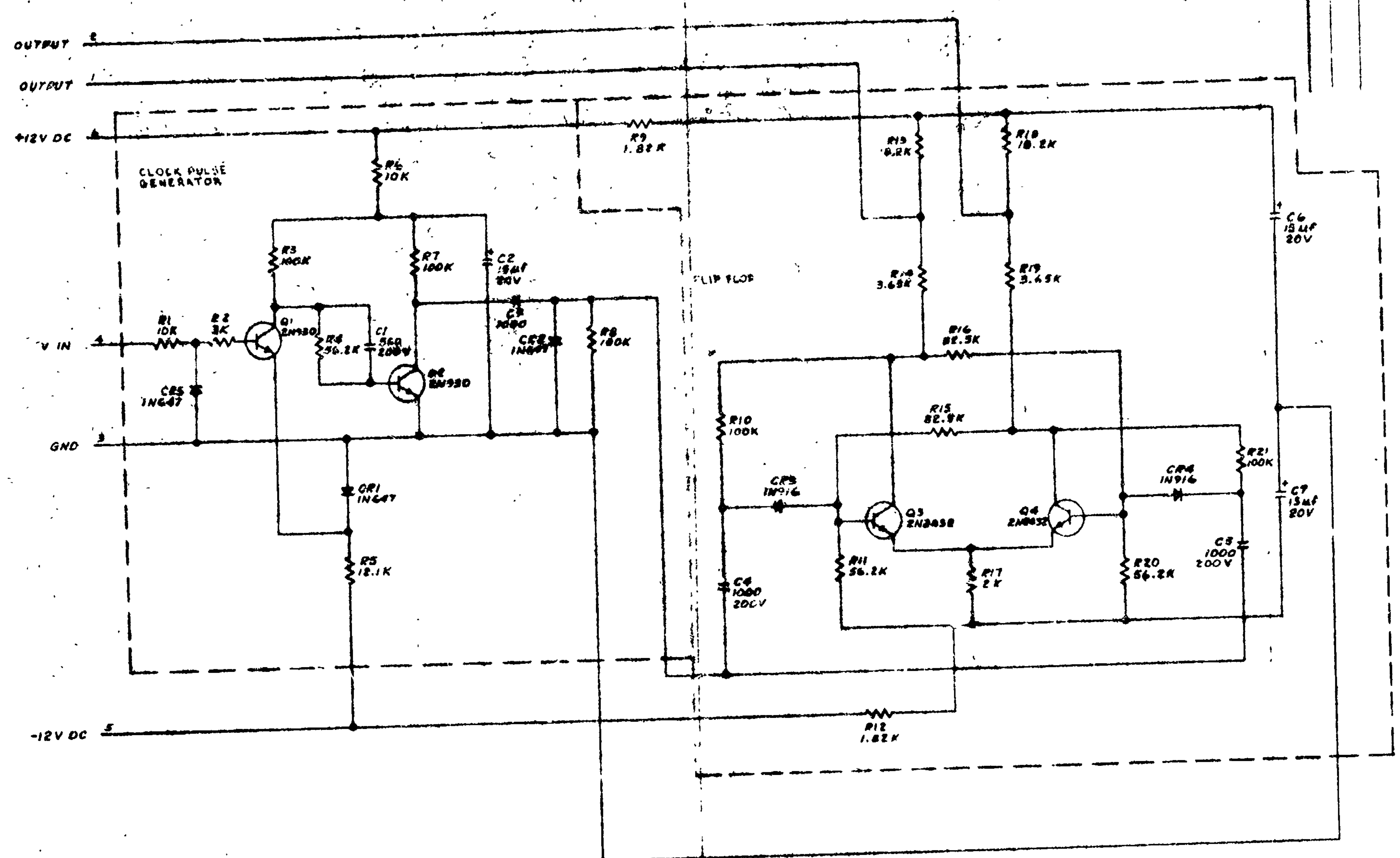

407	D	484715-1	A/F	
PROJ NO.	SIZE	NEXT ASSY NO	QTY	DASH NO.

LIST OF MATERIALS

QTY REQD	ITEM NO	DWG SIZE	TEXAS INSTRUMENTS / GOVT OR INDUSTRY PART OR IDENTIFYING NO	NOMENCLATURE OR DESCRIPTION

UNLESS OTHERWISE SPECIFIED
DECIMAL ± .02 ... ± .010
FRACTIONAL ± 1/64 ANGULAR ± 1°
CONCENTRICITY MACHINED DIAMETERS .004 TIR
ALL DIMENSIONS TO BE MET BEFORE PLATING
REMOVE ALL BURRS AND SHARP EDGES
DO NOT SCALE THIS DRAWING
ALL DIMENSIONS IN INCHES
SURFACES MARKED √ TO HAVE √
DRILLED HOLE TOLERANCES
.015 TO .136 ... .136 TO .750 ...
.750 AND ABOVE ± .003

TEXAS INSTRUMENTS INCORPORATED
APPARATUS DIVISION DALLAS TEXAS

TITLE: DIAGRAM, ELECTRONIC SCHEMATIC, FLIP-FLOP & CLOCK PULSE GENERATOR

CODE IDENT NO 96214 | SIZE D | DRAWING NO 484710

SCALE NONE

D 484710

65

NOTES UNLESS OTHERWISE SPECIFIED
1. RESISTANCE VALUES ARE IN OHMS
2. K INDICATES THOUSANDS OF OHMS.
3. CAPACITANCE VALUES ARE IN MICROMICROFARADS
4. INDUCTANCE VALUES ARE IN MICROHENRIES
5. MC INDICATES MEGACYCLES
6. TO BE SELECTED
7. ALL RESISTORS ARE 1/8 WATT

REVISIONS				
SYM	ZONE	DESCRIPTION	DATE	APPROVED
A		CN 10E067 ... 2-17-64 (1) VALUES OF C15 & C20 WERE 47 & 56 (2) ADDED ... C15 & C20		
B		CN 14718 ... 4-18-64 (1) REPLACED L4, 1.0 WITH R8, 200		

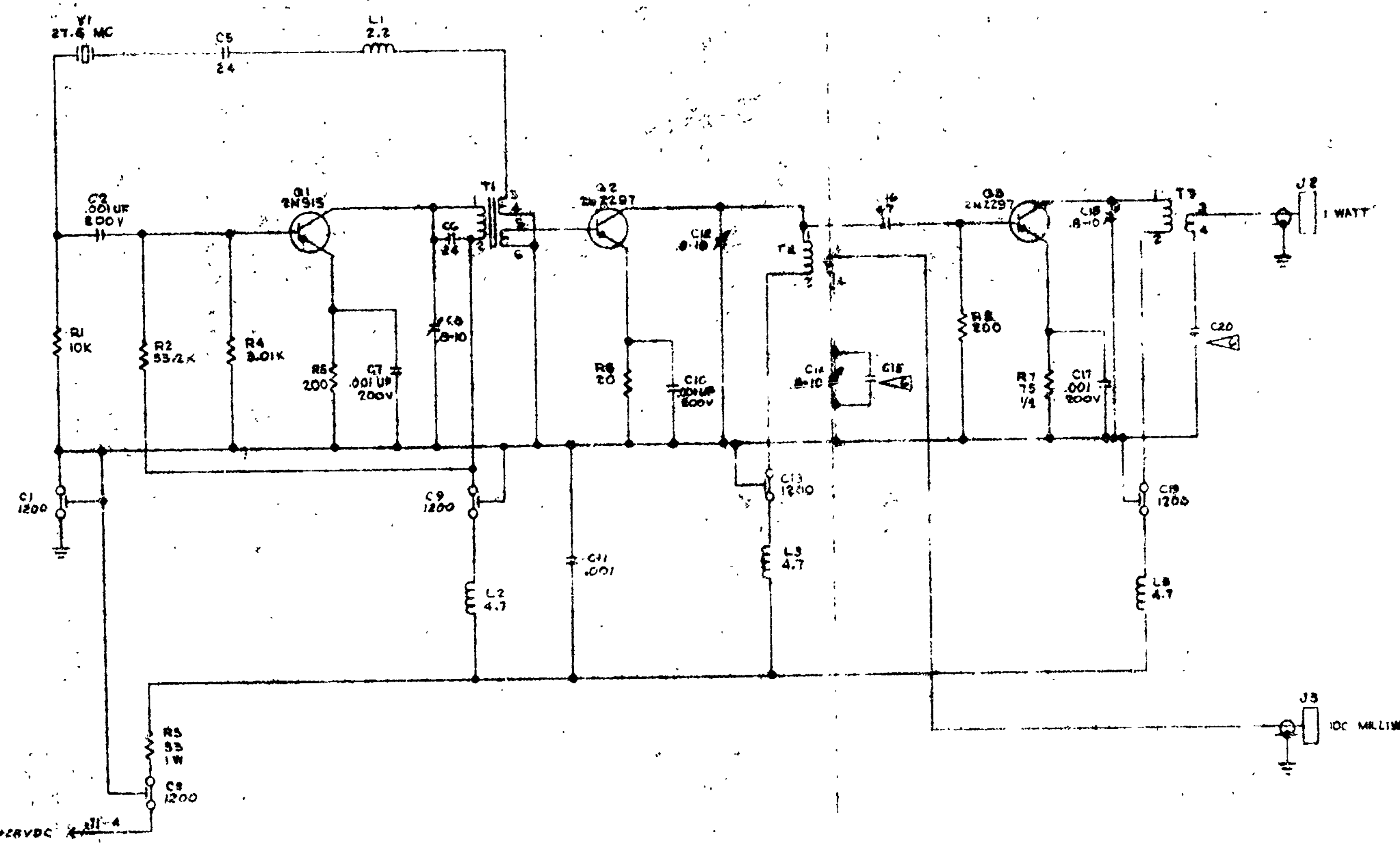

REFERENCE DESIGNATIONS	
USED	NOT USED
R1 THRU R8	
C1 THRU C20	C4
Q1 THRU Q3	
L1 THRU L5	L4
T1 THRU T3	
Y1	

LIST OF MATERIALS

UNLESS OTHERWISE SPECIFIED

TEXAS INSTRUMENTS INCORPORATED
APPARATUS DIVISION DALLAS TEXAS

DIAGRAM, ELECTRONIC SCHEMATIC, RF EXCITER

CODE IDENT NO 96214 SIZE D DRAWING NO. 484728

SCALE NONE

D 484728

NOTE: UNLESS OTHERWISE SPECIFIED:
1. RESISTANCE VALUES ARE IN OHMS
2. K INDICATES THOUSANDS OF OHMS
3. CAPACITANCE VALUES ARE IN MICROFARADS
4. PF INDICATES PICOFARADS
5. ALL RESISTORS ARE

REVISIONS

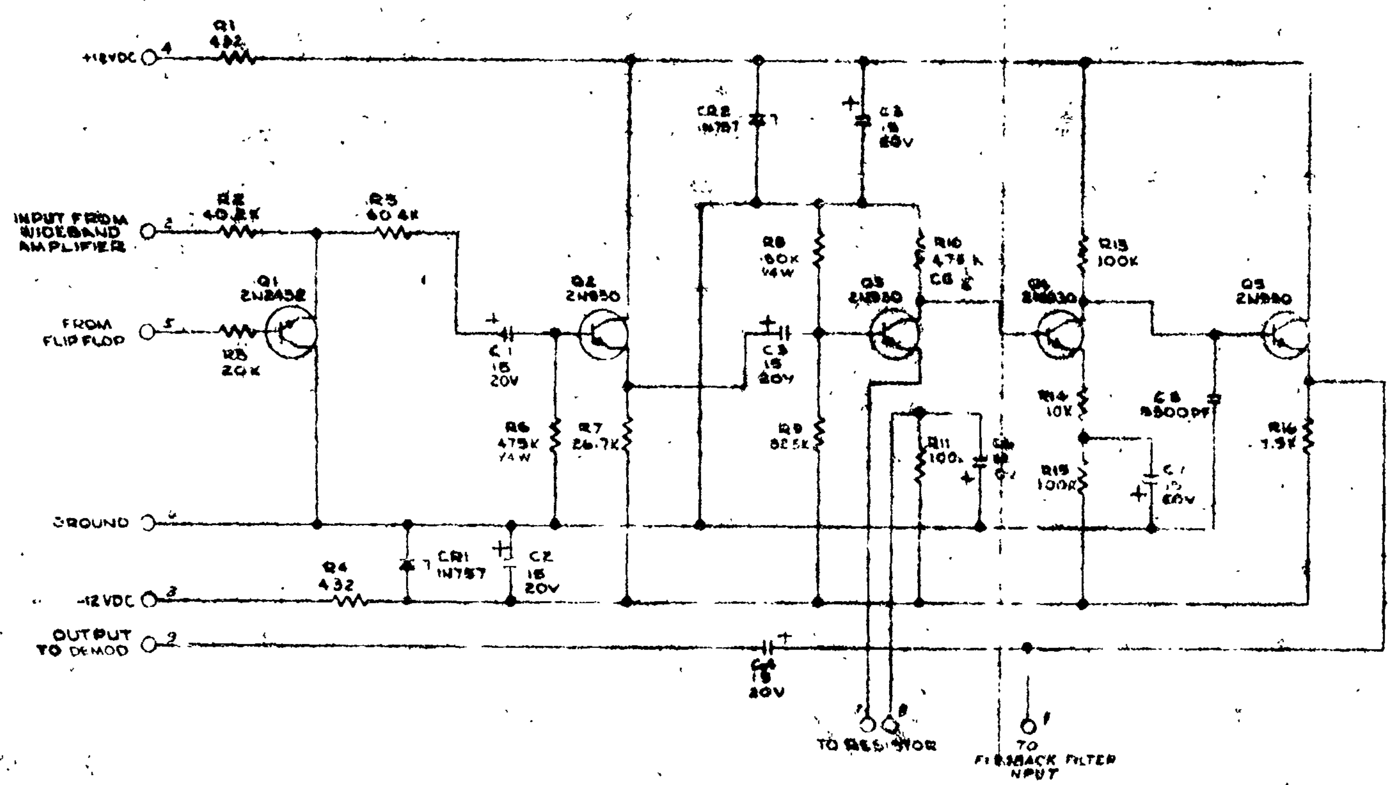

REFERENCE DESIGNATORS	
USED	NOT USED
R1 THRU R16	R12
C1 THRU C8	
Q1 THRU Q5	
CR1 CR2	

LIST OF MATERIALS

TEXAS INSTRUMENTS INCORPORATED
APPARATUS DIVISION DALLAS TEXAS

DIAGRAM, ELECTRONIC SCHEMATIC, BANDPASS AMPLIFIER, COMMUTATED

CODE IDENT NO 86214 | SIZE D | DRAWING NO. 484733

SCALE NONE

D 484733

NOTES:
UNLESS OTHERWISE SPECIFIED:
1. CAPACITANCE VALUES ARE IN PICOFARADS
2. INDUCTANCE VALUES ARE IN MICROHENRIES
3. RESISTANCE VALUES ARE IN OHMS
4. VALUES TO BE SELECTED

REVISIONS				
SYM	ZONE	DESCRIPTION	DATE	APPROVED
A		EN 100981 (C)(1) REVISED CIRCUITRY	[illegible]	[illegible]

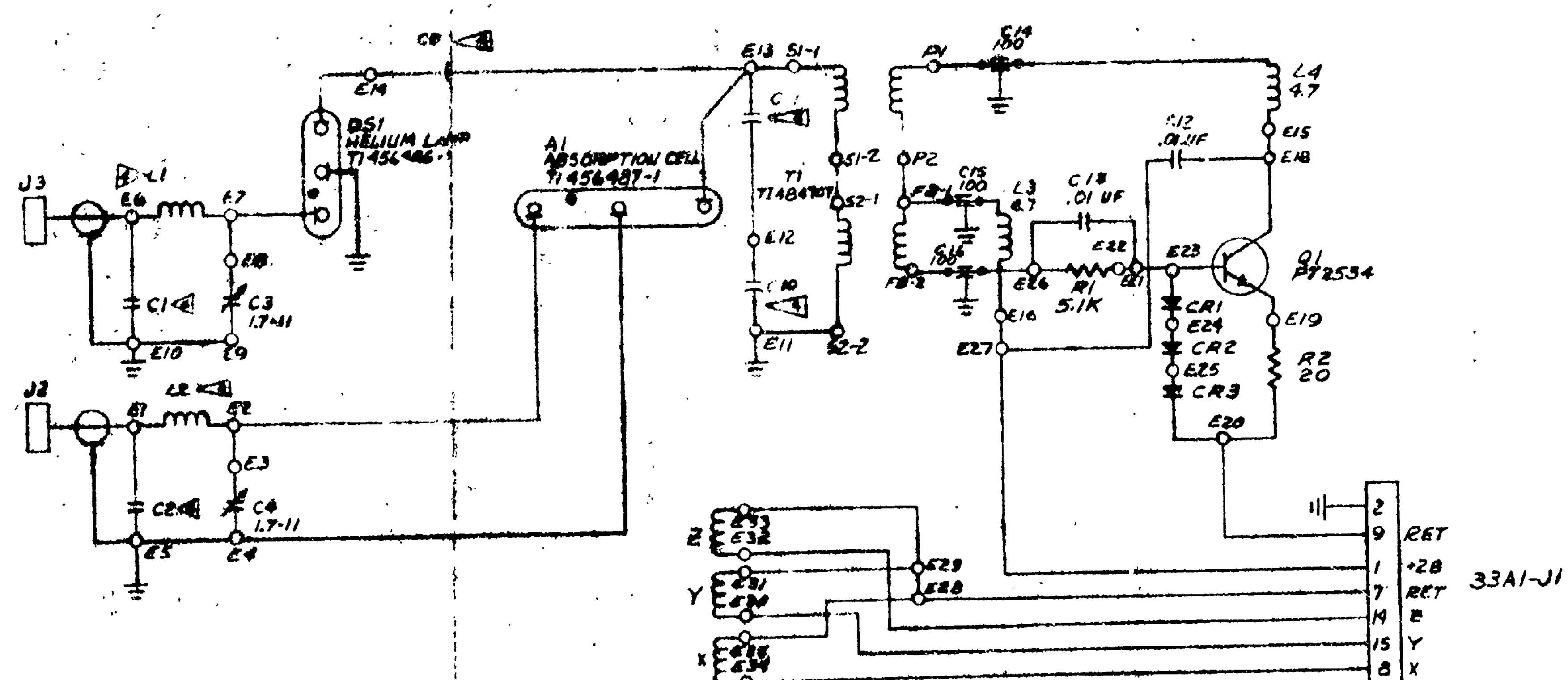

2	1	ITEM NO	DWG SIZE	TEXAS INSTRUMENTS / GOVT OR INDUSTRY PART OR IDENTIFYING NO	NOMENCLATURE OR DESCRIPTION
QTY REQD					

LIST OF MATERIALS

407	C	456491-1	REF		
407	A	456489-1	REF		
PROJ NO.	SIZE	NEXT ASSY NO	QTY	DASH NO	

UNLESS OTHERWISE SPECIFIED
DECIMAL XX ±.03 XXX ±.010
FRACTIONAL ± 1/64 ANGULAR ±1°
CONCENTRICITY MACHINED DIAMETERS .005 TIR
ALL DIMENSIONS TO BE MET BEFORE PLATING
REMOVE ALL BURRS AND SHARP EDGES
DO NOT SCALE THIS DRAWING
ALL DIMENSIONS IN INCHES
SURFACES MARKED ✓ TO HAVE ✓
DRILLED HOLE TOLERANCES
.010 TO .136 +.003/-.002 .136 TO .250 +.004/-.001
.250 AND ABOVE ±.005

DR L. Kasper [illegible]
CKD H. Miller M 10-7-63
ENGR J. R. [illegible] 12/[illegible]/63
APPD F. [illegible] 12/[illegible]/63
DESIGN ACTIVITY RELEASE O. Baker 12-11-63

TEXAS INSTRUMENTS INCORPORATED
APPARATUS DIVISION DALLAS, TEXAS

TITLE
DIAGRAM, ELECTRONIC SCHEMATIC, IGNITOR, SENSOR

CODE IDENT NO 96214 SIZE C DRAWING NO 484736
SCALE NONE WT SHEET

C 484736

NOTES:

1. RESISTANCE VALUES ARE IN OHMS.
2. CAPACITOR VALUES ARE IN MICROFARADS

REVISIONS				
SYM	ZONE	DESCRIPTION	DATE	APPROVED
A		CN100979(C) P. Lankford 1-3-64 (1) INPUT TERMINAL WAS 3 (2) GRD TERMINAL WAS 1	1-6-64	F. Cobb

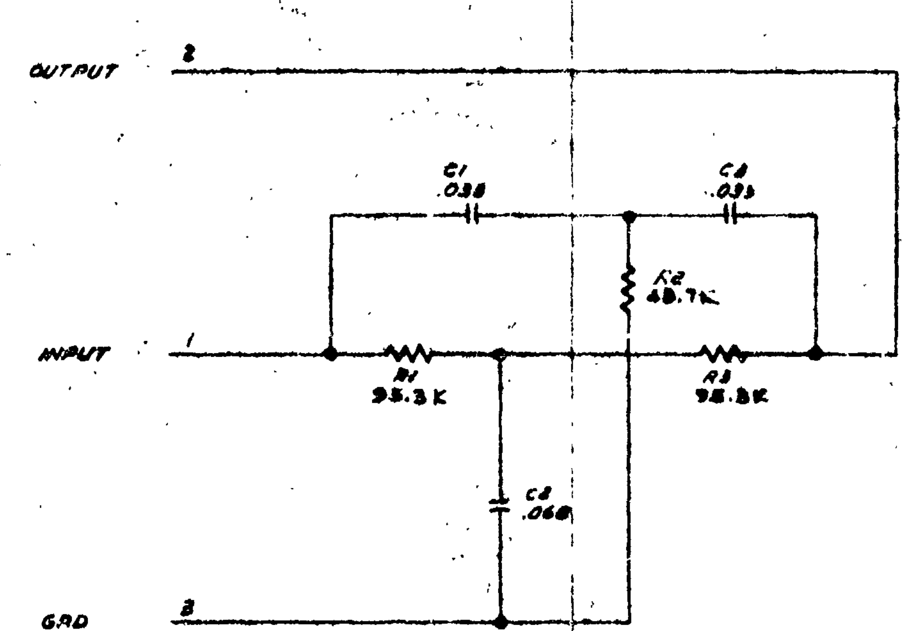

-2	1				
QTY REQD		ITEM NO.	DWG SIZE	TEXAS INSTRUMENTS GOVT OR INDUSTRY PART OR IDENTIFYING NO	NOMENCLATURE OR DESCRIPTION

LIST OF MATERIALS

407	D	484739-1		
PROJ NO.	SIZE	NEXT ASSY NO	QTY	DASH NO.

PROCESSING

UNLESS OTHERWISE SPECIFIED
DECIMAL .XX ± .03 .XXX ± .010
FRACTIONAL ± 1/64 ANGULAR ± 1°
CONCENTRICITY MACHINED DIAMETERS .004 TIR
ALL DIMENSIONS TO BE MET BEFORE PLATING
REMOVE ALL BURRS AND SHARP EDGES
DO NOT SCALE THIS DRAWING
ALL DIMENSIONS IN INCHES
SURFACES MARKED ✓ TO HAVE ✓
DRILLED HOLE TOLERANCES
.013 TO .136 + .003 / - .001 | .136 TO .250 + .004 / - .001
.250 AND ABOVE ± .005

DR Donny Drake | DATE 11-63
CKD Bob J. May II
PROJ R. Hinting
APPD F. H. Smith | 11/4/63
DESIGN ACTIVITY RELEASE O. Baker | 11-1-63

TEXAS INSTRUMENTS INCORPORATED
APPARATUS DIVISION DALLAS, TEXAS

TITLE: DIAGRAM, ELECTRONIC SCHEMATIC, TWIN TEE FILTER

CODE IDENT NO.	SIZE	DRAWING NO
96214	C	484740

SCALE NONE | WT | SHEET

C 484740

NOTES:
UNLESS OTHERWISE SPECIFIED
1. RESISTANCE VALUES ARE IN OHMS
2. K INDICATES THOUSANDS OF OHMS
3. MEG INDICATES MILLIONS OF OHMS
4. CAPACITANCE VALUES ARE IN MICROFARADS
5. PF INDICATES PICOFARADS
6. ALL TRANSISTORS ARE SP8488
7. ALL RESISTORS ARE 1/4 WATT

REVISIONS				
SYM	ZONE	DESCRIPTION	DATE	APPROVED
A		CN100987 ... 1-14-64 (1) 261 K WAS 270K, 499K WAS 511K (2) DELETED E6, E9, E12 (3) ADDED E22, E23, E24 (4) RELOCATED E18 & E19	1-17-64	

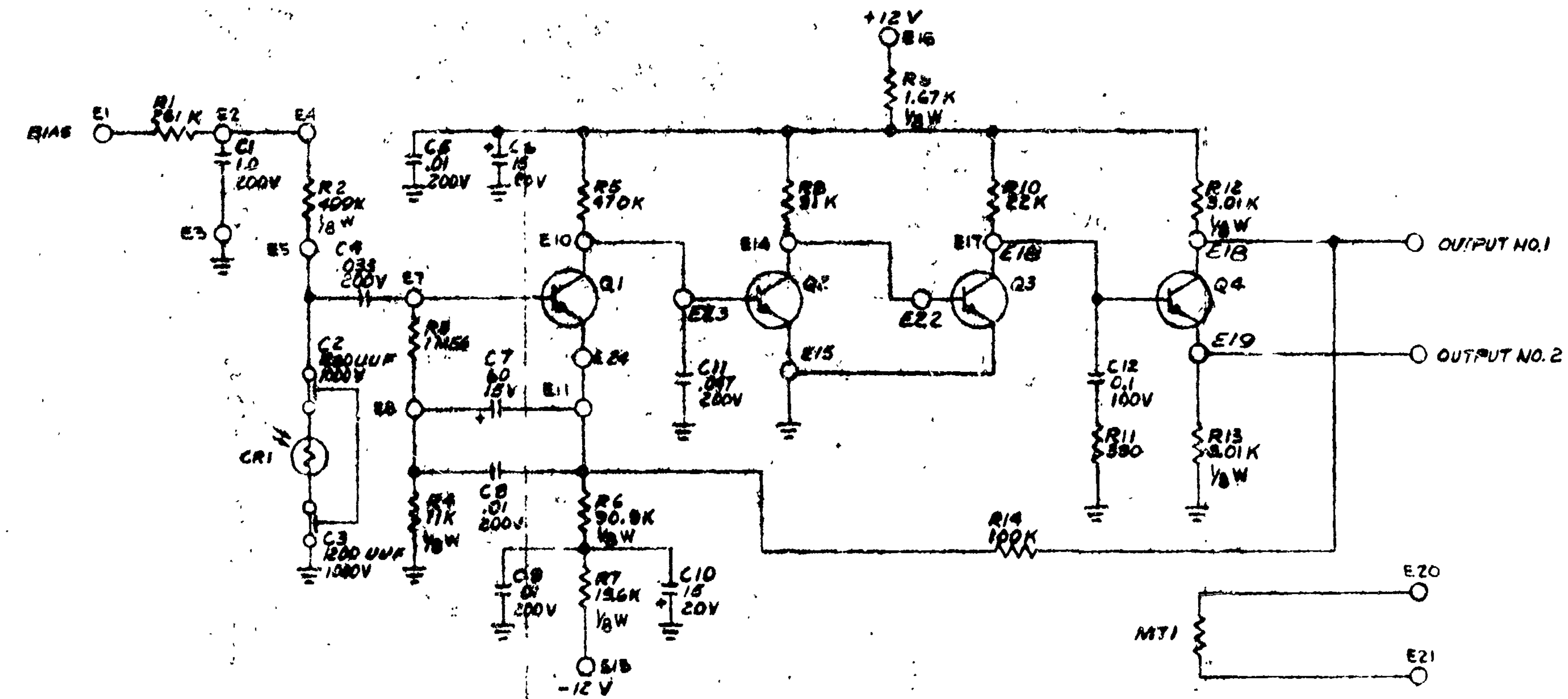

2	1			TEXAS INSTRUMENTS	GOVT OR INDUSTRY	
QTY REQD		ITEM NO	DWG SIZE	PART OR IDENTIFYING NO		NOMENCLATURE OR DESCRIPTION

LIST OF MATERIALS

407	D	SC1935...		
USED ON	SIZE	NEXT ASSY NO.	QTY	

PROCESS

UNLESS OTHERWISE SPECIFIED
DECIMAL ±.XX OF .XXX ±.010
FRACTIONAL ±1/64 ANGULAR ±1°
CONCENTRICITY MACHINED DIAMETERS .006 TIR
ALL DIMENSIONS TO BE MET BEFORE PLATING
REMOVE ALL BURRS AND SHARP EDGES
DO NOT SCALE THIS DRAWING
ALL DIMENSIONS IN INCHES
SURFACE MARKING ✓ TO HAVE ✓
DRILLED HOLE TOLERANCES
.013 TO .125 ... .126 TO .220 ...
.220 AND ABOVE ±.006

DR L. Kruger — DATE ...
CKD H. Miller — ...
... Drummond — 11/12/63
... R. Daly — 11/4/6...
DESIGN ACTIVITY RELEASE O. Baker — ...

TEXAS INSTRUMENTS INCORPORATED
APPARATUS DIVISION DALLAS TEXAS

TITLE
DIAGRAM, ELECTRONIC SCHEMATIC, SENSOR PREAMPLIFIER

CODE IDENT NO	SIZE	DRAWING NO.
96214	C	4847-11

SCALE NONE WT SHEET

C 484741

NOTES: UNLESS OTHERWISE SPECIFIED
1. ALL RESISTANCE VALUES ARE IN OHMS
2. K INDICATES THOUSANDS OF OHMS
3. UF INDICATES MICROFARAD
4. ALL RESISTORS ARE 1/8 W

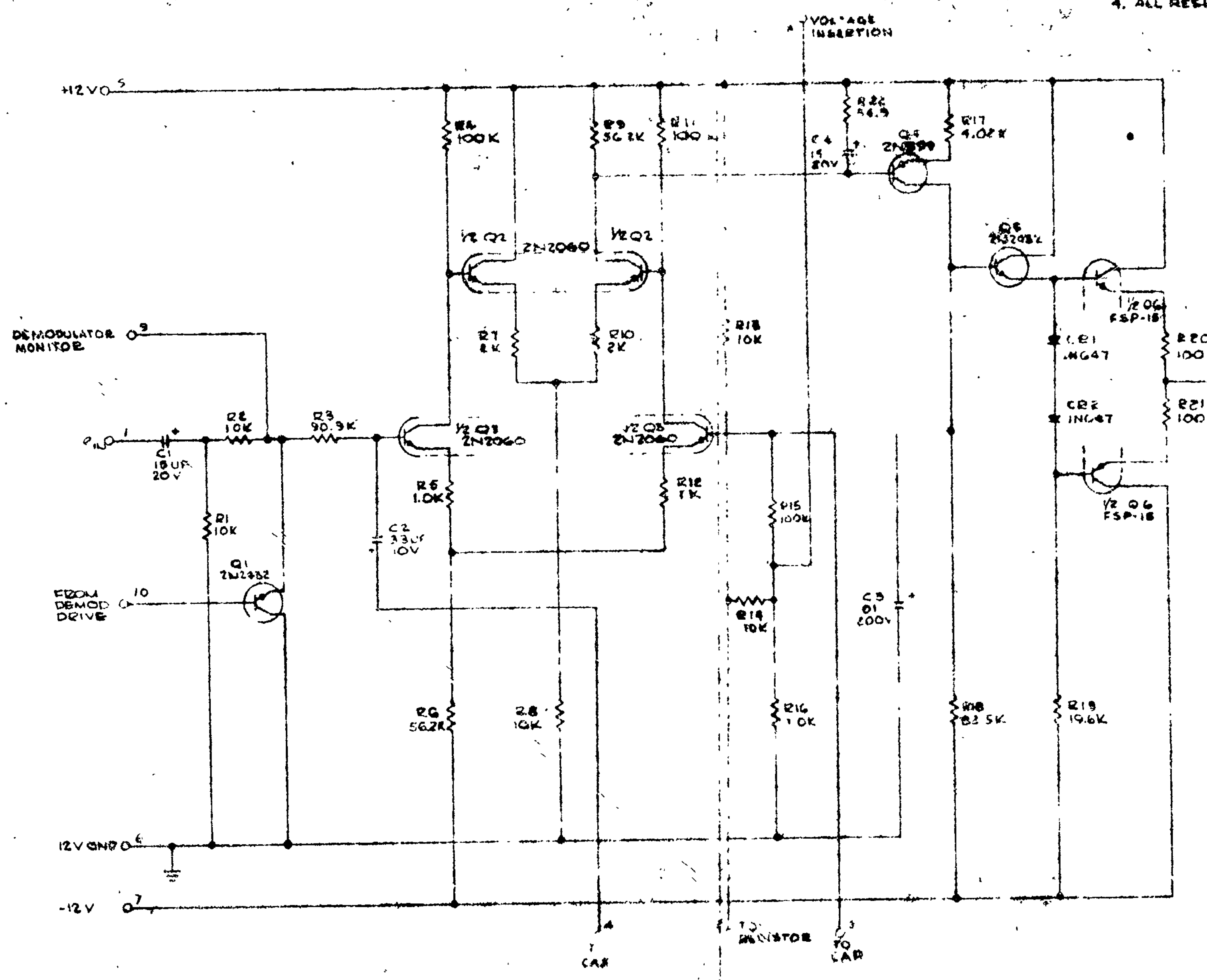

REFERENCE DESIGNATORS	
USED	NOT USED
C1, C2, C3, C4	
R1 THRU R21	
Q1 THRU Q6	
CR1, CR2	

LIST OF MATERIALS

TEXAS INSTRUMENTS INCORPORATED

DIAGRAM, ELECTRONIC SCHEMATIC, DEMODULATOR D.C. AMPLIFIER & OUTPUT

96214 | D | 484744

D 484744

71

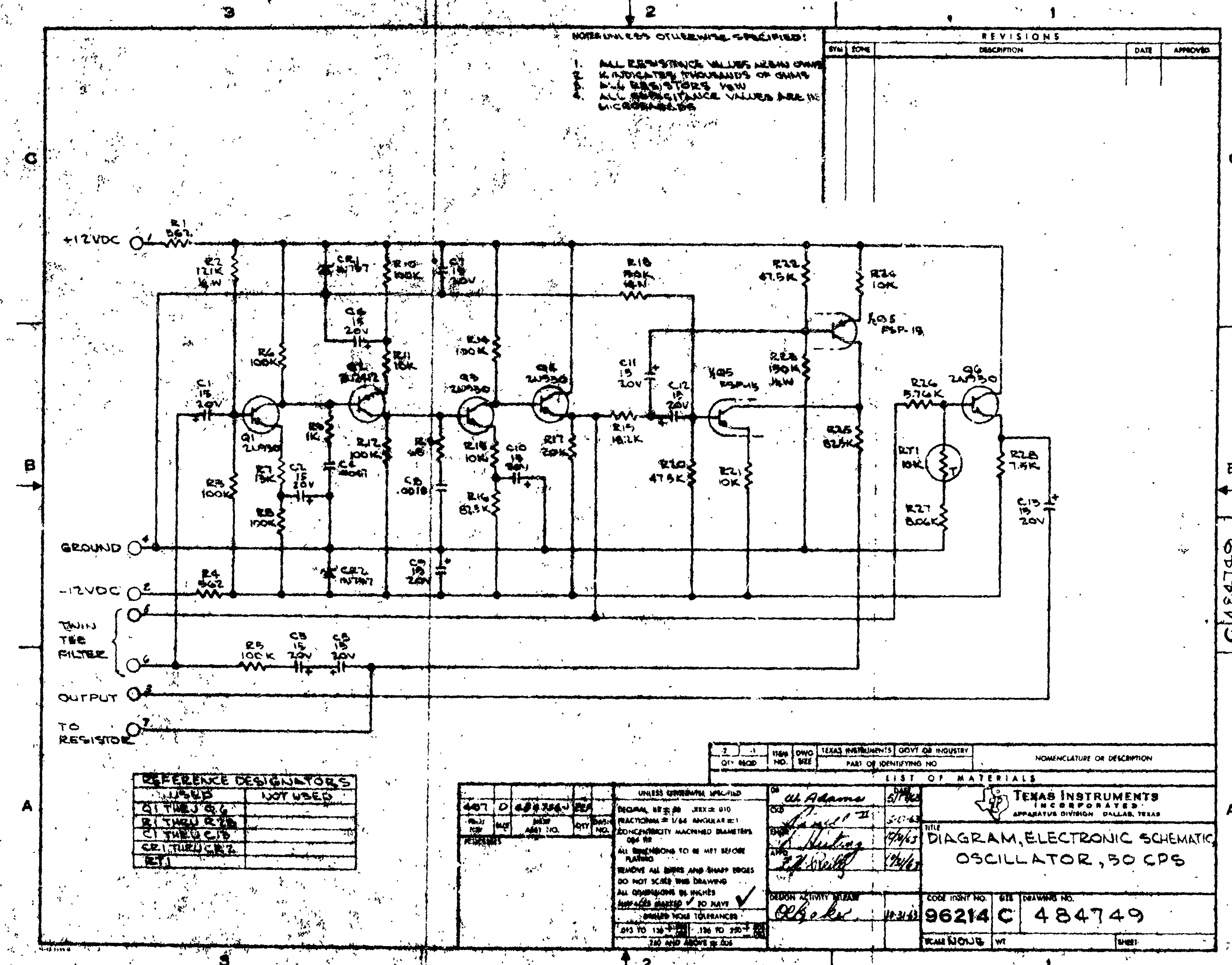
NOTES: UNLESS OTHERWISE SPECIFIED:
1. ALL RESISTANCE VALUES ARE IN OHMS
2. K INDICATES THOUSANDS OF OHMS
3. ALL RESISTORS ¼W
4. ALL CAPACITANCE VALUES ARE IN MICROFARADS
REVISIONS
+12VDC
GROUND
-12VDC
TWIN TEE FILTER
OUTPUT
TO RESISTOR
REFERENCE DESIGNATORS
USED
NOT USED
Q1 THRU Q6
R1 THRU R28
C1 THRU C13
CR1 THRU CR2
RT1
UNLESS OTHERWISE SPECIFIED
DO NOT SCALE THIS DRAWING
ALL DIMENSIONS IN INCHES
LIST OF MATERIALS
NOMENCLATURE OR DESCRIPTION
TEXAS INSTRUMENTS INCORPORATED
APPARATUS DIVISION DALLAS, TEXAS
DIAGRAM, ELECTRONIC SCHEMATIC
OSCILLATOR, 50 CPS
CODE IDENT NO. 96214
SIZE C
DRAWING NO. 484749
SCALE NONE
C 484749

NOTE: UNLESS OTHERWISE SPECIFIED
1 RESISTANCE VALUES ARE IN OHMS
2 K INDICATES THOUSANDS OF OHMS
3 CAPACITANCE VALUES ARE IN MICROFARADS
4. PF INDICATES PICOFARADS
5 ALL RESISTORS ARE 1/8W

REVISIONS				
SYM	ZONE	DESCRIPTION	DATE	APPROVED

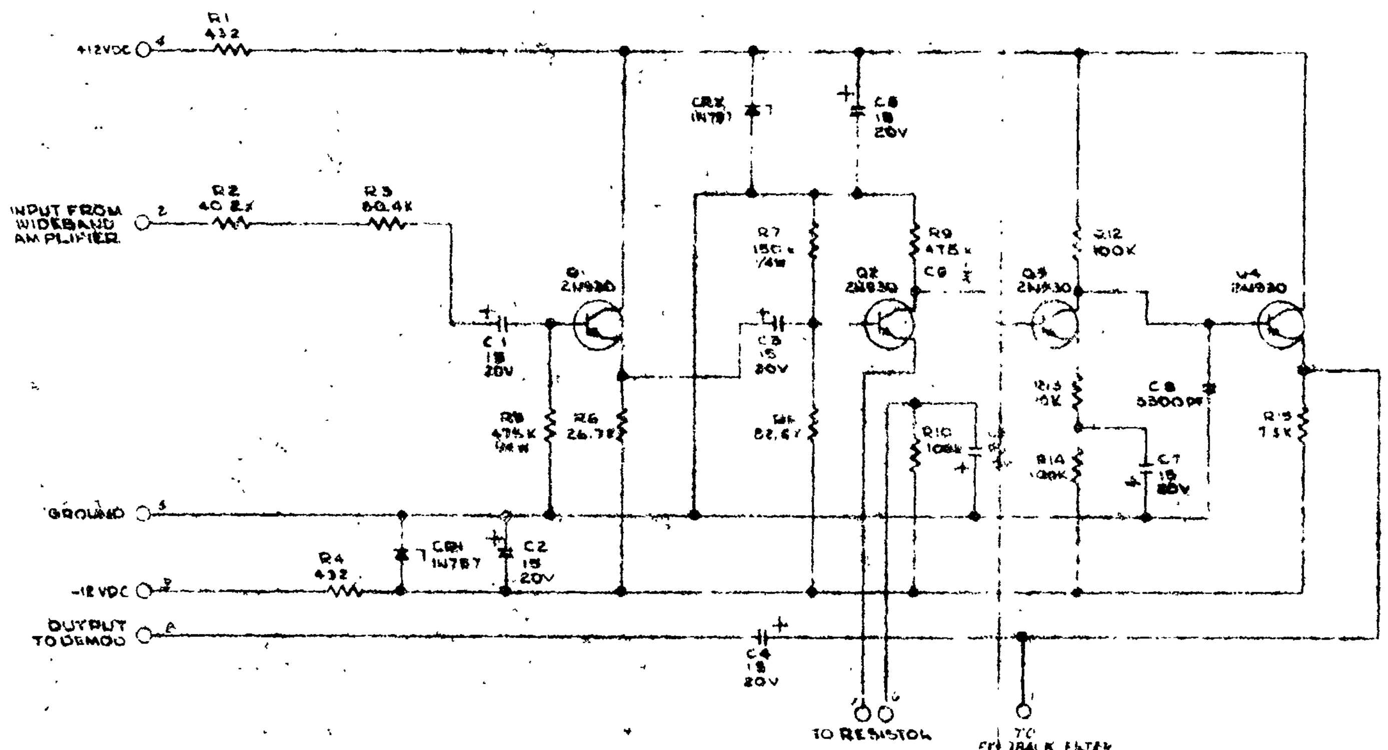

REFERENCE DESIGNATORS	
USED	NOT USED
R1 THRU R15	R11
C1 THRU C8	
Q1 THRU Q4	
CR1, CR2	

LIST OF MATERIALS

QTY REQD	ITEM NO	DWG SIZE	TEXAS INSTRUMENTS / GOVT OR INDUSTRY PART OR IDENTIFYING NO	NOMENCLATURE OR DESCRIPTION

PROJ NO	DASH	NEXT ASSY NO	QTY	DASH NO
607		484748	REF	

UNLESS OTHERWISE SPECIFIED
DECIMAL .XX ± .02 .XXX ± .010
FRACTIONAL ± 1/64 ANGULAR ± 1°
CONCENTRICITY MACHINED DIAMETERS .004 TIR
ALL DIMENSIONS TO BE MET BEFORE PLATING
REMOVE ALL BURRS AND SHARP EDGES
DO NOT SCALE THIS DRAWING
ALL DIMENSIONS IN INCHES
SURFACES MARKED ✓ 125 RMS
DRILLED HOLE TOLERANCES
.013 TO .126 .126 TO .250
.250 AND ABOVE ± .006

TEXAS INSTRUMENTS INCORPORATED
APPARATUS DIVISION DALLAS TEXAS

DIAGRAM, ELECTRONIC SCHEMATIC, BANDPASS AMPLIFIER, NONCOMMUTATED

CODE IDENT NO 96214 | SIZE D | DRAWING NO 484750

SCALE NONE | WT | SHEET

D 484750

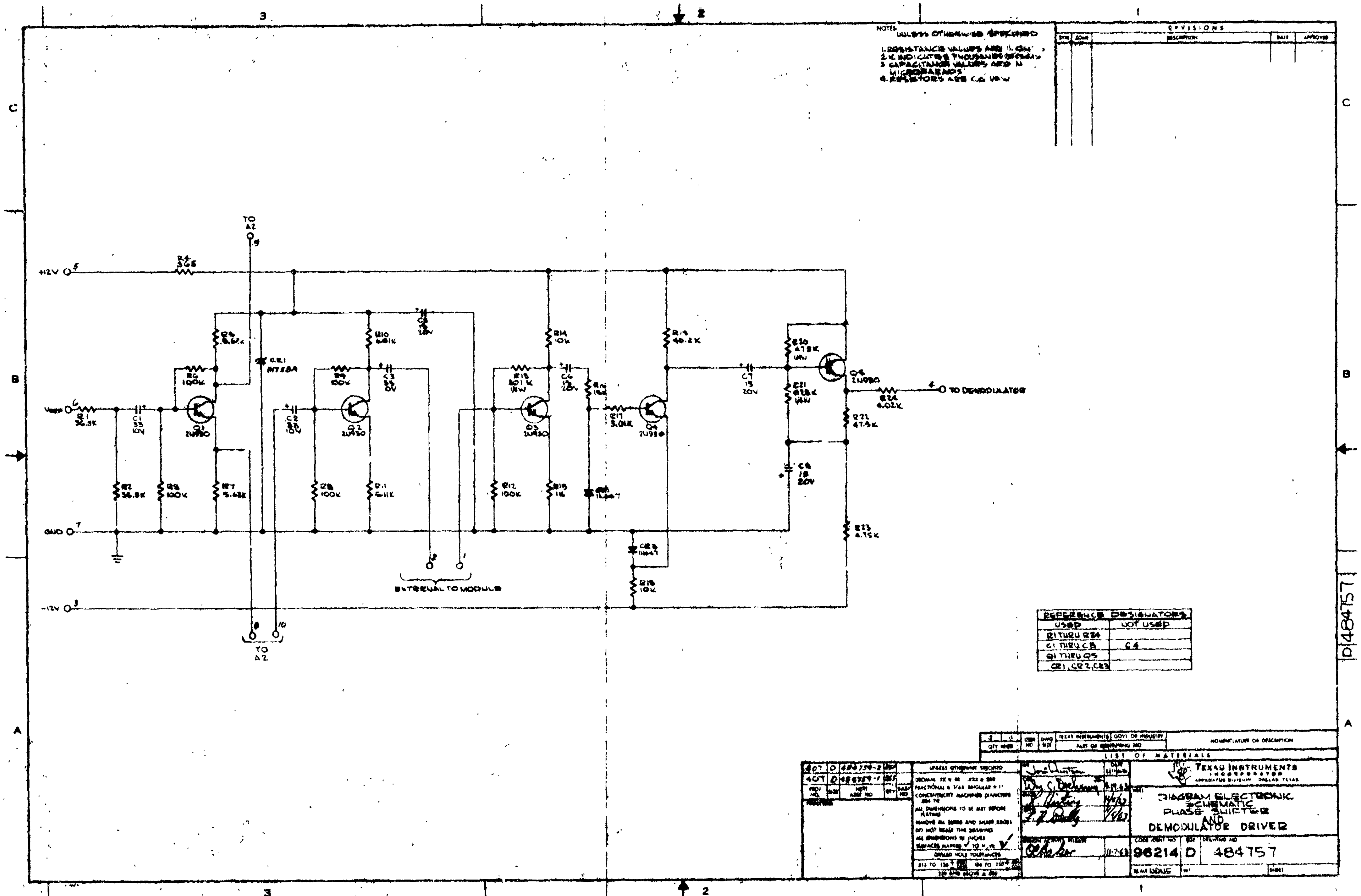
NOTES:
UNLESS OTHERWISE SPECIFIED
1. RESISTANCE VALUES ARE IN OHMS
2. K INDICATES THOUSANDS OF OHMS
3. CAPACITANCE VALUES ARE IN MICROFARADS
4. RESISTORS ARE C.C. 1/4W
REVISIONS
+12V
-12V
GND
TO A2
TO DEMODULATOR
EXTERNAL TO MODULE
REFERENCE DESIGNATORS
USED
NOT USED
R1 THRU R24
C1 THRU C8
C4
Q1 THRU Q5
CR1, CR2, CR3
LIST OF MATERIALS
UNLESS OTHERWISE SPECIFIED
TEXAS INSTRUMENTS INCORPORATED
APPARATUS DIVISION DALLAS TEXAS
DIAGRAM ELECTRONIC SCHEMATIC
PHASE SHIFTER AND DEMODULATOR DRIVER
96214
D
484757
D 484757

NOTES UNLESS OTHERWISE SPECIFIED:

1. ALL RESISTANCE VALUES ARE IN OHMS
2. K INDICATES THOUSANDS OF OHMS
3. ALL RESISTORS 1/2W
4. ALL CAPACITANCE VALUES ARE IN MICROFARADS
5. ALL CAPACITORS 20V

REVISIONS				
SYM	ZONE	DESCRIPTION	DATE	APPROVED

+12VDC 1
V IN 3
GROUND 4
10
8
9
7
5
6
-12 VDC 2
V1 OUT 11

R9 511
R10 5.62K
R14 6.81K
CR1 1N756A
R13 100K
R18 221K 1/4W
R19 10K
C6 15
C7 15
R23 39.2K
R24 150K 1/4W
Q5 2N2432
R8 100K
Q3 2N930
C5 33 10V
R12 100K
C8 15
Q4 2N930
R21 39.2K
R25 511
C8 100 6V
C9 100 6V
R4 36.5K
C1 33 10V
Q2 2N930
R16 47.5K
R20 1K
R26 511
R8 51.1K
R7 100K
R11 5.11K
C4 33 10V
R15 5.11K
CR2 1N756A
Q6 2N2412
R22 150K 1/4W
R17 511

REFERENCE DESIGNATORS	
USED	NOT USED
Q1 THRU Q6	Q7
R1 THRU R26	R7, R8, R6, R8
C1 THRU C9	C2
CR1, CR2	

ITEM NO.	QTY REQD	DWG SIZE	TEXAS INSTRUMENTS PART OR IDENTIFYING NO	GOVT OR INDUSTRY	NOMENCLATURE OR DESCRIPTION
1	2				

LIST OF MATERIALS

PROJ NO.	REV	NEXT ASSY NO.	QTY	DASH NO.
407	D	484779-1		

APPLICATIONS

UNLESS OTHERWISE SPECIFIED
DECIMAL XX ± .02 XXX ± .010
FRACTIONAL ± 1/64 ANGULAR ± 1°
CONCENTRICITY MACHINED DIAMETERS .004 TIR
ALL DIMENSIONS TO BE MET BEFORE PLATING
REMOVE ALL BURRS AND SHARP EDGES
DO NOT SCALE THIS DRAWING
ALL DIMENSIONS IN INCHES
SURFACES MARKED ✓ TO HAVE ✓
DRILLED HOLE TOLERANCES
.013 TO 136 +.003 -.002
136 TO 250 +.005 -.002
250 AND ABOVE ± .005

DR	W. Adams	DATE 5/1/63
CKD		
ENGR		11/1/63
APPD		11/1/63

DESIGN ACTIVITY RELEASE O.O. Baker 11-1-63

TEXAS INSTRUMENTS INCORPORATED
APPARATUS DIVISION DALLAS TEXAS

TITLE
DIAGRAM, ELECTRONIC SCHEMATIC,
Z AXIS
SWEEP DRIVER

CODE IDENT NO	SIZE	DRAWING NO
96214	C	484772

SCALE NONE WT SHEET

C 484772

75

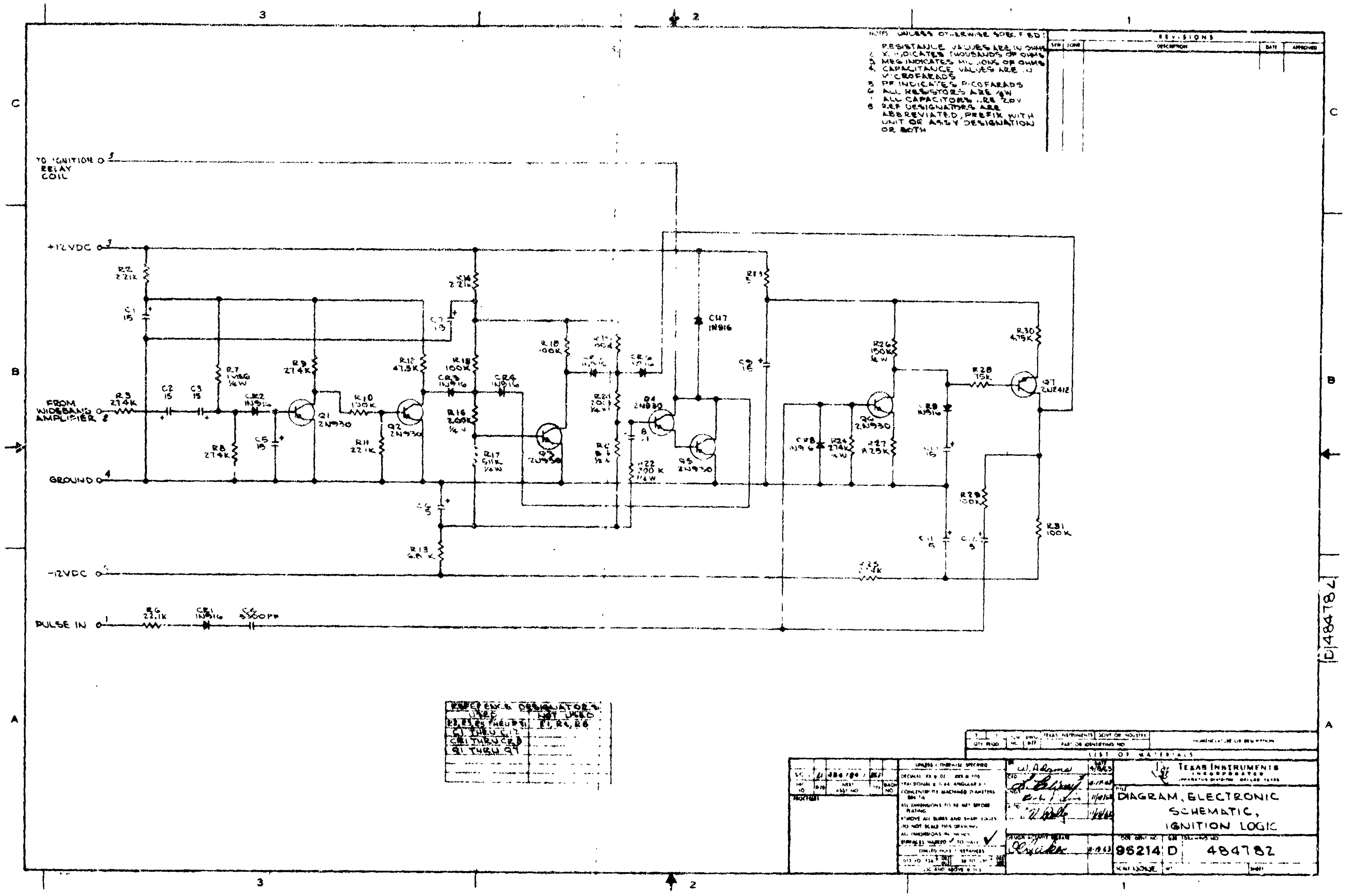
NOTES UNLESS OTHERWISE SPECIFIED:
RESISTANCE VALUES ARE IN OHMS
2 K INDICATES THOUSANDS OF OHMS
3 MEG INDICATES MILLIONS OF OHMS
4 CAPACITANCE VALUES ARE IN MICROFARADS
5 PF INDICATES PICOFARADS
6 ALL RESISTORS ARE 1/8W
ALL CAPACITORS ARE 20V
8 REF DESIGNATIONS ARE ABBREVIATED, PREFIX WITH UNIT OR ASSY DESIGNATION OR BOTH
REVISIONS
TO IGNITION RELAY COIL
+12VDC
FROM WIDEBAND AMPLIFIER
GROUND
-12VDC
PULSE IN
Q1 2N930
Q2 2N930
Q3 2N930
Q4 2N930
Q5 2N930
Q6 2N930
Q7 2N2412
CR7 IN916
C6 3300PF
LIST OF MATERIALS
TEXAS INSTRUMENTS INCORPORATED
DIAGRAM, ELECTRONIC SCHEMATIC, IGNITION LOGIC
96214 D 484782
SCALE NONE
D 484782

76

NOTES
UNLESS OTHERWISE SPECIFIED:
1. RESISTANCE VALUES ARE IN OHMS
2. K INDICATES THOUSANDS OF OHMS
3. CAPACITANCE VALUES ARE IN MICROFARADS
4. ALL CAPACITORS ARE .01 MF, 50 V (GOODALL 627G)
5. 332K AND 165K RESISTORS ARE CG 1/4
27.4K RESISTORS ARE CG 1/8

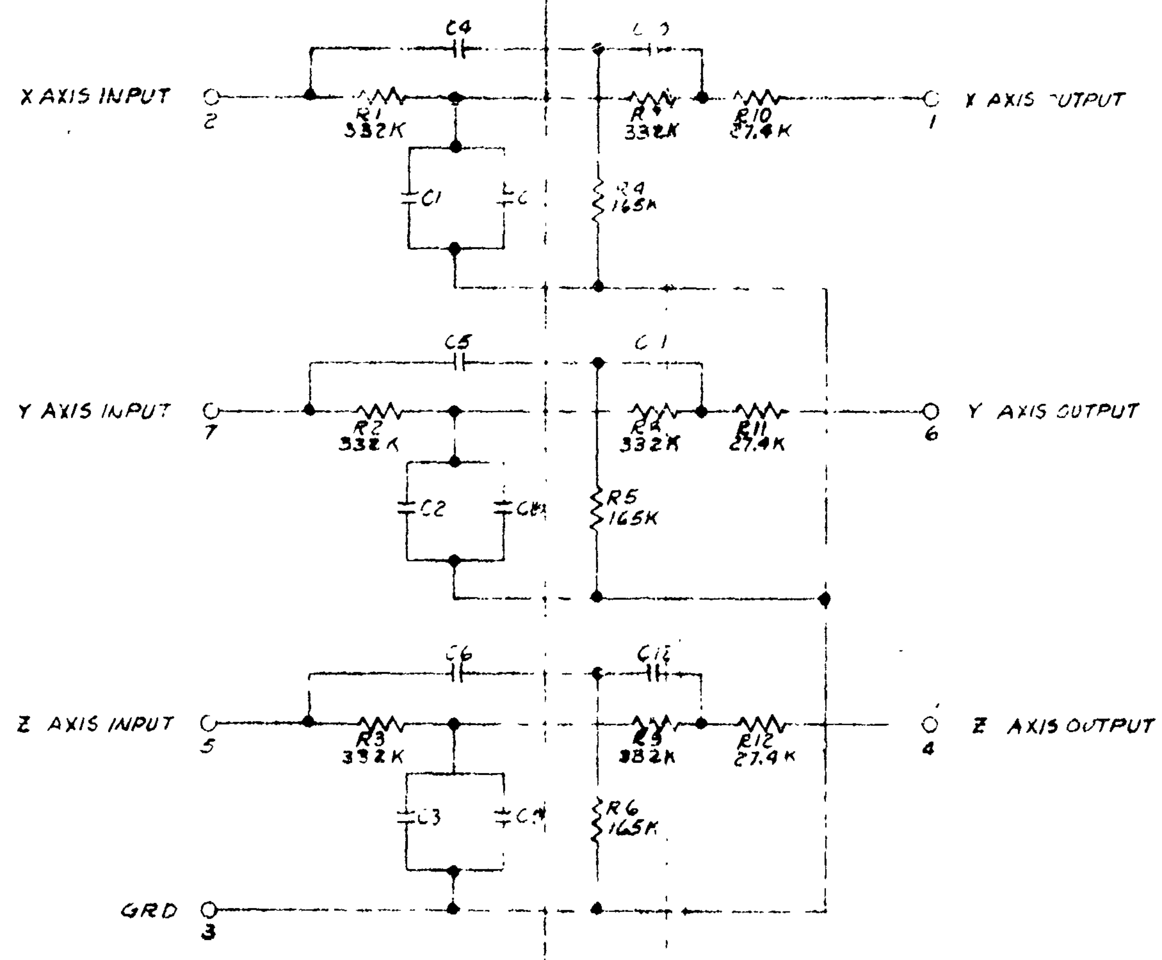

REVISIONS

SYM	ZONE	DESCRIPTION	DATE	APPROVED

LIST OF MATERIALS

407 | D | 484794 | REF
PROJ NO | NEXT ASSY NO

UNLESS OTHERWISE SPECIFIED
DRAWN 8-23-63
CHECKED 10-5-63
ENGR 10/4/63
APPD 11/1/63
DESIGN ACTIVITY RELEASE 11-1-63

TEXAS INSTRUMENTS INCORPORATED
APPARATUS DIVISION DALLAS TEXAS

DIAGRAM, ELECTRONIC SCHEMATIC, FEED BACK FILTER

CODE IDENT NO 96214 | SIZE C | DRAWING NO 484791

SCALE NONE

C 484791